Hunter, Central and Lower North Coast Regional Climate Change Project 2008

REPORT 2

Climate Variability of the Hunter, Lower North Coast and Central Coast Region of NSW

An initiative of the Hunter & Central Coast Regional Environmental Management Strategy

The Hunter & Central Coast Regional Environmental Management Strategy – a program of the Environment Division of Hunter Councils

Authors: Karen L. Blackmore (Earth Sciences, School of Environmental and Life Sciences, University of Newcastle) and Ian D. Goodwin (Climate Risk CORE, Macquarie University)

Publisher
HCCREMS (Hunter Councils Inc. as legal agent)
PO Box 137
THORNTON NSW 2322
Phone: 02 4978 4020
Fax: 4966 2188
Email: envirodirector@huntercouncils.com.au

ISBN: 978-1-920859-38-1

Suggested Bibliographic Citation:
Blackmore. K.L. & Goodwin, I.D (2008). Report 2: Climate Variability of the Hunter, Lower North Coast and Central Coast Region of NSW. A report prepared for the Hunter and Central Coast Regional Environmental Management Strategy, NSW.

Acknowledgements

New South Wales Government

Funding has been provided by the New South Wales Government through its Climate Action Grants Program; Valuable support & assistance have been provided by the Tom Farrell Institute & Newcastle Innovation (The University of Newcastle) and Climate Risk CORE (Macquarie University)
Cover photograph: Hugh Cross

Executive Summary

This report presents the results of the second stage of a research project, "Regional Climate Change Study", which focuses on the identification of key climate change variables and impacts for the Hunter, Lower North Coast and Central Coast regions. The project partners are Newcastle Innovation and the Tom Farrell Institute for the Environment (University of Newcastle) and the Hunter and Central Coast Regional Environmental Strategy (HCCREMS). The project comprises four stages: (1) Identification of the key synoptic patterns relevant to the study region; (2) analysis of how the synoptic patterns drive climate and climate-related variability in the region; (3) downscaling CSIRO global climate model (GCM) predictions for New South Wales (NSW) to the study region; and, (4) determination of the potential climate change impacts on the region based on the statistical downscaling.

Review of Stage 1

Stage 1 focused on the identification and collation of regionally specific climate data for use in Stages 2 and 4 of the project. The study region encompasses 14 local government areas of the Hunter, Central and Lower North Coast region of NSW. A detailed quality assurance procedure was implemented to identify data sets that are of a suitable nature for use in the project. The data includes: Australian daily precipitation; Australian daily maximum and minimum temperatures; Australian hourly temperature, humidity and pressure; Australian daily evaporation; Australian daily wind data; Australian hourly wind data; Daily cloudiness, visibility and sunshine hours data for Bureau of Meteorology (BOM) districts 60, 61 and 62; Six minute pluvial data for districts 60, 61 and 62, NSW monthly ocean wave height, period and direction data, and monthly ocean tide gauge data on sea-level.

An important component of Stage 1 of the project was to define the key synoptic patterns that drive the climate variability of the region for use in the downscaling of the Global Climate Model (GCM) output to a regional scale. A process known as self-organising mapping (SOM) was selected to derive the key synoptic types (STs) from monthly sea level pressure (SLP) data from January 1948 to December 2007. An initial 35 key STs were selected during Stage 1 of the project. These STs and the selected key climate data sets provided input to the analysis conducted in Stage 2 of the project.

Results from Stage 2

Stage 2 of the project provides an analysis climate variability, and of how synoptic patterns drive climate and climate-related variability in the region. The key outcome of Stage 2 is a comprehensive analysis of sub-regional climate distributions, including seasonal, interannual and interdecadal variability of key climate variables and extreme events. Additionally, the drivers of climate variability in the region are analysed. This incorporates an analysis of key synoptic patterns and their influence on sub-regional climate distributions.

Synoptic Typing

The 35 STs, derived using the SOM process in Stage 1, were evaluated as drivers of climate variability in the region. Analysis revealed that the large number of types made isolating specific type "signatures", in terms of unique climate characteristics, difficult. As such, the SOM process was repeated to derive 6, 9, 12, 15 and 20 types. These STs were then evaluated for their ability to explain climate variability in the region. A SOM consisting of 12 STs (3x4) was found to be optimal.

Monthly SLP data from National Centers for Environmental Protection (US) /National Center for Atmospheric Research (US) (NCEP/NCAR) for the period from January 1948 to December 2007 was used as input data to the SOM process to derive the STs. Of key interest however are the variations from the mean conditions that produce different climate conditions in the region. Thus the SOM process was also completed using SLP anomalies. These anomalies are created by subtracting the mean SLP value for the period from January 1968 to December 1996 for a given grid point from the actual value for the grid point. The anomaly data is then used as the input to the SOM process. The resulting anomaly types correspond to the SLP types, however they provide an improved visualisation. In this report, the SLP STs and corresponding anomaly STs are shown in Chapter 4 and a profile of each type is provided in Appendix C of the Stage 2 report.

Regional Climate Variability

The analysis of sub-regional climate distributions includes annual and seasonal variability, interannual and interdecadal variability, and extreme events. In addition to the key climate variables identified in Stage 1, sea surface temperature (SST), sea level rise (SLR), extreme sea levels and wave climate are included in the analysis.

The analysis of regional climate variables highlights the need to use sub regional data in the data analysis to avoid over smoothing of sub-regional trends and variability. For example, average annual precipitation ranges from 630mm to 1900mm across the region. If analysing at a regional level, information on this variability is lost. Additionally, trends in key climate variables were found to differ at a sub-regional level (i.e. minimum temperatures in some areas decreased between 1948 to 2007 whereas increases were found to occur in others). To address this issue, the region has been divided into 3 distinct climate zones (coastal, central and western) using a statistical technique for climate zonation based on seasonal precipitation and temperature, and elevation.

Interannual and interdecadal variability included the analysis of trends over time in key climate variables. At the regional level, a decrease of 3.3mm per annum in precipitation is evident. This equates to approximately 200mm over the period from January 1948 to December 2007. Seasonal analysis of individual stations and climate zones reveals that this

decrease is not uniform across the region. Statistically significant increases in precipitation were found to have occurred in summer and spring in Murrurundi and other centres within the western climate zone. Importantly, corresponding changes in STs were also identified.

A statistically significant increase in maximum temperature for the region is also evident. This increase of approximately 0.03°C per annum equates to 1°C over the period from January 1970 to December 2007. This trend is generally consistent both seasonally and across the region, however stronger increases are evident in the coastal zone.

Average wind speed shows a slight decrease across the region of 2.4km/hr for the period from Jan 1970 to Dec 2007. While not large, this decrease is statistically significant. Sub-regional analysis of trends shows a decrease in average wind speed in the central and western parts of the region. Only the decrease in the central part of the region of 6.5km/hr over the 38 year time period is statistically significant.

Annual average sea surface temperatures off the study region have increased by ~0.5° C in the past few decades. Tide gauge measurements at Fort Denison in Sydney indicate that relative sea-level has risen by 1.2 mm/year over the past century (White et al., 2005), with an acceleration to ~3 mm/yr in the past decade. Mean annual sea level along the Central, Hunter and Lower North Coast NSW can vary by as much as 0.150 m between years, without any long-term trend in sea level Extreme water levels have been found to have increased in frequency by a factor of 2-3 since 1950.

Regionally, extreme precipitation events are less likely to occur during late winter to early spring. Extreme precipitation events occur more frequently along the coast during January, February and March. In Newcastle, this period extends through April and May, and peaks in June. Of the stations analysed, high temperature events occur most frequently at Jerry's Plains, which is in the central sub-region. A slight increase in the frequency of high temperature events from 1970 to 2007 is evident at Taree, Jerry's Plains and Murrurundi. Trends in the frequency of temperature events below or equal to 0°C have also been analysed. Coastal influences result in no recorded events at Newcastle from 1970 to 2007. Murrurundi, the most westerly of the recording stations analysed, shows an increasing trend.

Discussion and Recommendations for Stages 3 and 4

Key findings from Stage 2 of the project include the identification of sub-regional temporal trends in key climate variables such precipitation and minimum and maximum temperature. Analysis at the level of climate zone and individual BOM recording station highlights the spatial variability in these key climate variables that is evident in the region. Furthermore, analysis of synoptic pattern variability between 1948 to 1976 and 1977 to 2007 has resulted in the identification of synoptic patterns responsible for the distinct weather patterns

prevalent in these two periods. These results provide the basis for analysis of sub-regional climate change through to 2100AD using projected data from global climate models (GCMs). This analysis forms Stage 3 of the project.

Due to the spatial variability of key climate variables evident in the region, Stage 3 analysis will be focused on the identified coastal, central and western zones with some analysis also occurring at the individual BOM station level. Additionally, the synoptic typing process undertaken during Stage 2 indicates that the use of ST anomalies will be most useful for the analysis of sub-regional climate change to be conducted in Stage 3 using the output from GCMs.

Table of Contents

List of Figures

Section 5

List of Tables

List of Acronyms

BOM	*Bureau of Meteorology*
DEM	*Digital Elevation Model*
ENSO	*El Niño-Southern Oscillation*
GCM	*Global Climate Model*
ICOADS	*International Comprehensive Ocean-Atmosphere Data Set*
IPO	*Interdecadal Pacific Oscillation*
MLC	*Maximum Likelihood Classification*
MWD	*mean wave direction*
NCEP	*National Centers for Environmental Protection (US)*
NCAR	*National Center for Atmospheric Research (US)*
NOAA	*National Oceanic & Atmospheric Administration*
PCA	*principal components analysis*
PSA	*Pacific-South American*
SOI	*Southern Oscillation Index*
SLP	*sea level pressure*
SLR	*sea level rise*
SAM	*Southern Annular Mode*
SOM	*self-organising map*
SST	*sea surface temperature*
ST	*synoptic type*

1 Introduction

The Hunter and Central Coast Regional Environmental Management Strategy (HCCREMS) are currently implementing a Regional Climate Change Project. This project aims to identify possible impacts of climate change in the Hunter, Central and Lower North Coast and raise awareness and understanding by local governments, industry and community in the region. In order to implement these goals, HCCREMS has commissioned the University of Newcastle (via Newcastle Innovation) to conduct the scientific research required for this study. This report forms the second stage of this project and provides an analysis of the climate variability of the region.

The study region extends from above Taree in the north (31°16'54."S) to below Gosford in the south (33°34'48.97"S), and from a most easterly point on the coast (152°48'13.5"E) to inland of Cassils in the west (149°40'8.49"E). In total, an area of 39,021.58 sq/km is considered in this study. Elevation varies throughout the region, with the highest point at Brumlow Top (1586 meters) on the Barrington Tops and the lowest at sea level on the coast (Figure 1.1).

The region encompasses 14 local government areas (LGAs) of the Hunter, Central and Lower North Coast region of New South Wales (see Figure 2.1). The LGAs comprising the region are Greater Taree, Great Lakes, Gloucester, Upper Hunter, Dungog, Port Stephens, Maitland, Newcastle, Singleton, Muswellbrook, Cessnock, Lake Macquarie, Wyong, Gosford. Also included are parts of the Hastings, Walcha and Tamworth Regional areas.

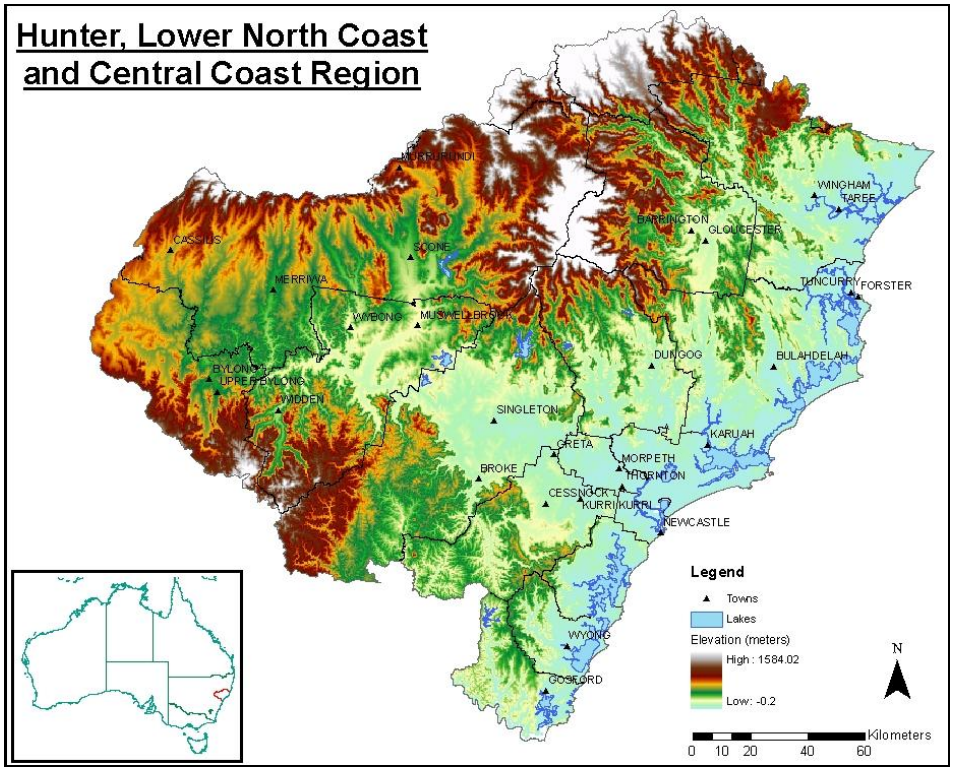

Figure 1.1. Digital Elevation Model (DEM) of the study region

The analysis of regional climate variability presented in this report is conducted using two principle data sources. Firstly, climate data for the region encompassing 13 key climate variables is obtained from instrumental climate data obtained from the Australian Bureau of Meteorology (BOM). A discussion of each of the variables and the results of analysis to select suitable stations is presented in Section 2.1 of this report. Global reanalysis climate data forms the second major data source for the analysis. These data are used to identify key synoptic type patterns influencing the region and are discussed in Section 2.2.

Section 3 of the report describes the methodology adopted to interpolate BOM station data to gridded surfaces and to cluster the synoptic types to key features. Section 4 provides an analysis and discussion of synoptic climate types and climate variability. This section includes a discussion of large scale atmospheric circulation, Pacific basin variability, the two Inter-decadal Pacific Oscillation (IPO) periods and the key synoptic types as mechanisms. Sub-regional climate distributions are discussed in Section 5. This also includes an analysis of interannual and interdecadal variability of the key climate variables. Finally, the results and key findings are discussed and summarised in Section 6 of the report.

2 Climate Data for the Region

2.1 Bureau of Meteorology Instrumental Climate data

Instrumental climate data sets have been obtained from the National Climate Centre of the Australian Bureau of Meteorology (BOM) for use in the project. These data represent the recordings from ground stations within the region, from the beginning of collection for the station to 31 December 2007. These data sets form the primary source of information used to study climate variability (contained in this report) and for the future study of climate change impacts for the region. The variables acquired are listed in Table 2.1.

Key Climate Variable	**Units**
Australian daily precipitation	Millimeters (mm)
Australian daily maximum and minimum temperatures	Degrees Celsius (°C)
Australian hourly temperature	Degrees Celsius (°C)
Australian hourly humidity	Percent (%)
Australian daily evaporation	Millimeters (mm)
Australian daily wind data	Kilometers per hour (km/hr)
Australian hourly wind gust data	Kilometers per hour (km/hr)
Daily cloudiness, visibility and sunshine hours data for BOM districts 60,61 and 62	Eighths, Kilometers(km), and Hours (hrs)
Six minute pluvial data for districts 60, 61 and 62	Millimeters (mm)

Table 2.1. Key climate variables and their units of measure

For the purpose of data selection only, a buffer of 50 km was placed around the study region shown in Figure 1.1. This buffer region ensures that appropriate stations (i.e. those just outside the study region) are included in the analysis to facilitate the interpolation of point based climate data to a grid based format. The study region and 50 km buffer zone used for data selection is shown in Figure 2.1.

Figure 2.1. Study region and buffer zone used in climate data selection

In addition to the buffer zone, selection criteria were used to insure that the data sets used in this study are of a sufficient length, cover a common time span and are reasonably complete. The first stage of the data selection process was to filter the available data to obtain a subset of data that included only those stations that have observations spanning a consistent time period. The second stage of the data selection process determined the completeness of each of the records within the given time period. A threshold of 90% complete was used in this stage. The selection criteria used, the number of stations considered, and the time period covered by each climate variable is summarised in Table 2.2.

Key Climate Variable	Selection Criteria	Total Stations in Region	No. Stations Meeting Selection Criteria	Start Date	End Date
Australian daily precipitation	> 90% complete; time period equivalent to NCEP/NCAR data; stations in the Sydney region filtered to key stations	2000	80	1/01/1948	31/12/2007
Australian daily maximum and minimum temperatures	> 90% complete	91	17	1/01/1970	31/12/2007
Australian hourly temperature	> 90% complete	91	18	1/01/1970	30/04/2007
Australian hourly humidity	> 90% complete	91	11	1/01/1970	30/04/2007
Australian daily wind data	> 90% complete	96	14	1/01/1970	31/12/2007
Australian hourly wind gust data	> 90% complete	26	1	1/01/1970	31/12/2007
Australian daily evaporation	> 90% complete	30	7	1/01/1974	31/12/2007

Table 2.2. Key climate variable selection criteria

In some instances weather stations have been decommissioned and relocated within a short distance from the original position (e.g. the monitoring station may have been moved from a post office to the new airport within the town) and in most cases the BOM assigns a new station number for this station gauge. Therefore, in order to maximise spatial coverage, stations that have been discontinued and replaced by a secondary gauge at a nearby location were also considered for inclusion in the final data set. To maintain quality assurance, only those gauges with a period of overlap existing for the two data sets were considered. The station time series during the simultaneous time period were then compared to determine if the two gauges could suitably be merged to represent one continuous record. The results of these analysis are presented in Appendix A.

2.1.1 Daily Precipitation

Daily precipitation data is available for approximately 17300 sites across Australia. Of these, approximately 2000 are within the study region and 50 km buffer zone. The record length and continuity of the data varies from station to station, with some stations recording daily precipitation for more than 100 years, while others may have been operational for only a short period of time (e.g. less than one year). The locations of all stations that have recorded daily precipitation for the study region and buffer zone are shown in Figure 2.2(a).

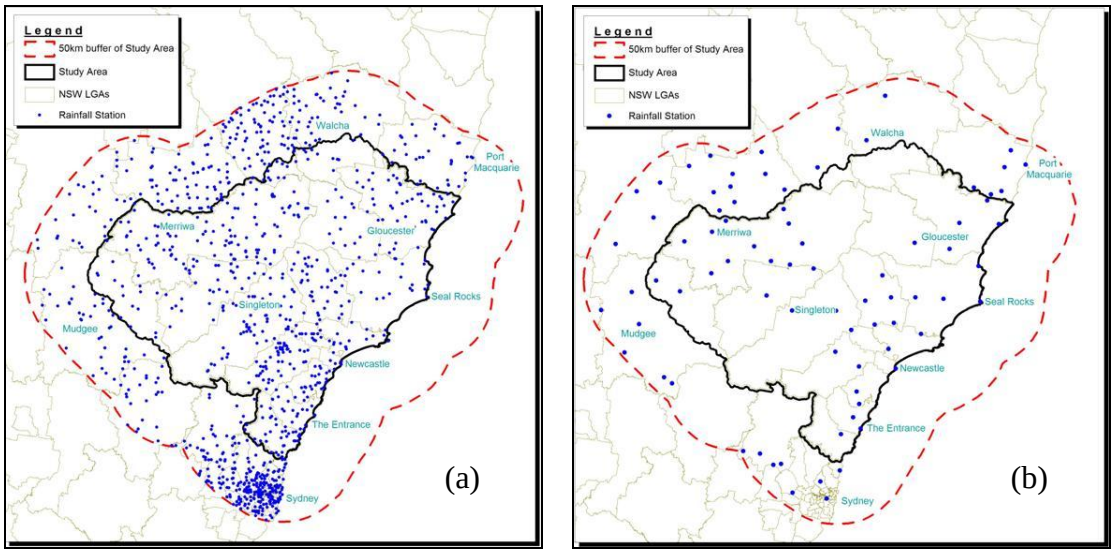

Figure 2.2. Potential (a) and final (b) precipitation stations

The available data shown in Figure 2.2(a) was filtered to obtain a subset of data that included only those stations that have rainfall observations spanning the 1948 through to 2007 epoch (59 years). The year 1948 was chosen as the lower bound as this corresponds to the first year for which the atmospheric data is available in the NCEP/NCAR Reanalysis dataset (see Section 2.2). Further filtering to the 90% complete threshold was undertaken. A high number of stations are clustered around the Sydney region. As this area is outside the primary study boundary only a selection of key Sydney based stations were chosen for use in future analysis involving the interpolation of point source data to gridded data for the study region.

A total of 80 stations were found to satisfy the selection criteria. The location of the rainfall stations that satisfied the selection criteria adopted is shown in Figure 2.2(b). The final stations chosen provide suitable spatial coverage for a regional climate study with at least one gauge located in each LGA (and in many cases more than one). The coastal region is well represented, along with the in Upper Hunter. Stations recording rainfall in the Singleton, Dungog and Gloucester regions are not as dense; however it appears that sufficient data exist within the study boundary and buffer zone to interpolate precipitation surfaces in these regions.

2.1.2 Daily Maximum and Minimum Temperature

Daily maximum and minimum temperature data are available for 1700 sites across Australia. Of these, 91 are located within the study region and buffer zone, as shown in Figure 4(a). The record length and continuity of the data also varies from station to station. Generally, temperature records are much shorter than those available for rainfall, with fewer stations measuring this element.

The data set shown in Figure 2.3(a) was filtered to include only those stations with measured maximum and minimum temperatures from at least 1970 through to 2007 (37 years). Many weather stations were opened just prior to 1970, therefore this date threshold was found to provide the longest data set with the greatest spatial coverage.

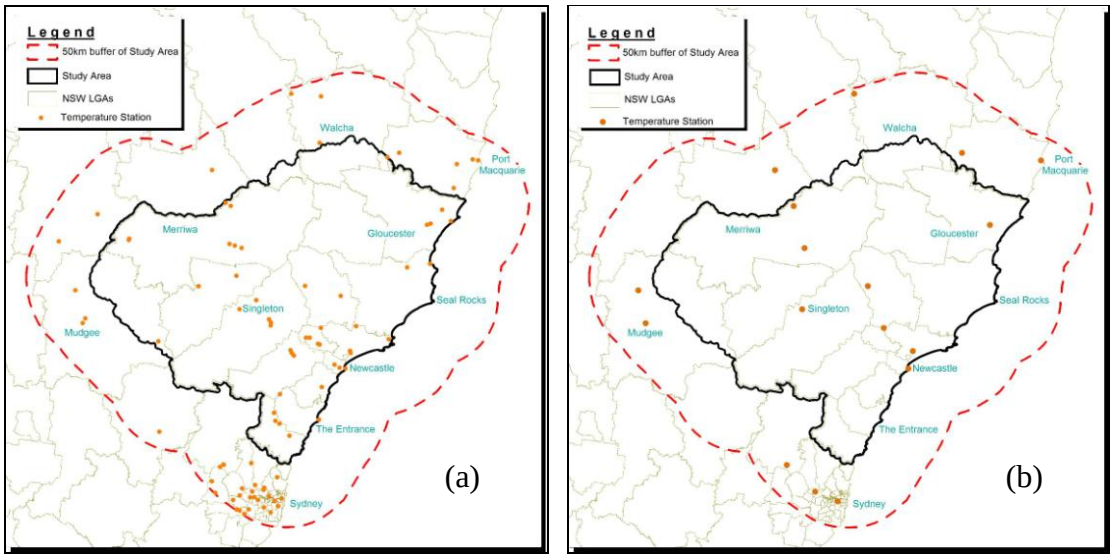

Figure 2.3. Potential (a) and final (b) daily maximum and minimum temperature stations

Each maximum and minimum temperature timeseries was checked for missing data between the years of interest (1970 and 2007) and this was converted to percentage completeness. It was determined that sufficient spatial coverage could still be maintained by restricting the final data set to include only those stations with daily maximum and minimum temperature data that is at least 90% complete. As for rainfall, a number of stations are clustered around the Sydney region. Two key Sydney stations were chosen for use in future analysis involving the interpolation of point source data to gridded data for the study region. A total of 17 stations satisfy the selection criteria. The locations of the temperature stations that that satisfied the criteria adopted for data selection are shown in Figure 2.3(b).

2.1.3 Australian 3 Hourly Temperature

Temperature data is available for 1730 sites across Australia at 3 hourly intervals which may be used to generate daily average temperatures (from the 9am and 3pm records). Of the 1730 sites, 91 are located within the study region and buffer zone, as shown in Figure 2.4(a). The record length and continuity of the data varies from station to station, with some of these stations recording temperature every three hours, while others have only recorded 9am and 3pm temperatures. Additionally, breaks in continuity of the timeseries are not handled with missing values, rather the dates for missing days/months/years are simply not present in the dataset. This poses problems for analysis; that is, determining the true

number of missing values is a complicated process.

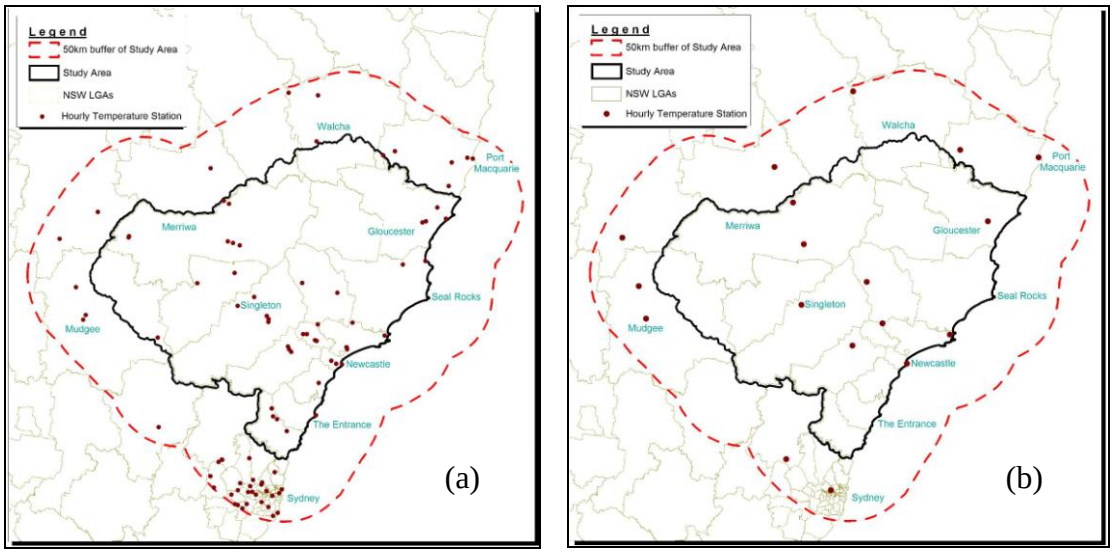

Figure 2.4. Potential (a) and final (b) 3 hourly temperature stations

Ignoring missing dates, station data were selected that span at least 1970 to 2007 (37 years) and are at least 90% complete (for 9am and 3pm temperature readings). Stations that have been discontinued and replaced by a secondary gauge at a nearby location were also considered for inclusion in the final data set using the quality assurance method outlined in Appendix A. A total of 18 stations were found to satisfy the selection criteria, as shown in Figure 2.4(b). Although an hourly temperature record is not available for each of the 14 LGAs, the available stations provide reasonable spatial coverage for a regional study. In particular, the data set provides information on both coastal regions and the Upper Hunter. However it is noted that further evaluation of the proportion of missing dates may result in fewer suitable stations.

2.1.4 Relative Humidity

Relative humidity data is available for 1730 number of sites across Australia, measured at 9am and 3pm (same stations as 3 hourly temperature). Of these, 91 are within the study region and buffer zone, as shown in Figure 2.5(a). As with the 3 hourly temperature data, omitted dates in the times series causes analysis issues.

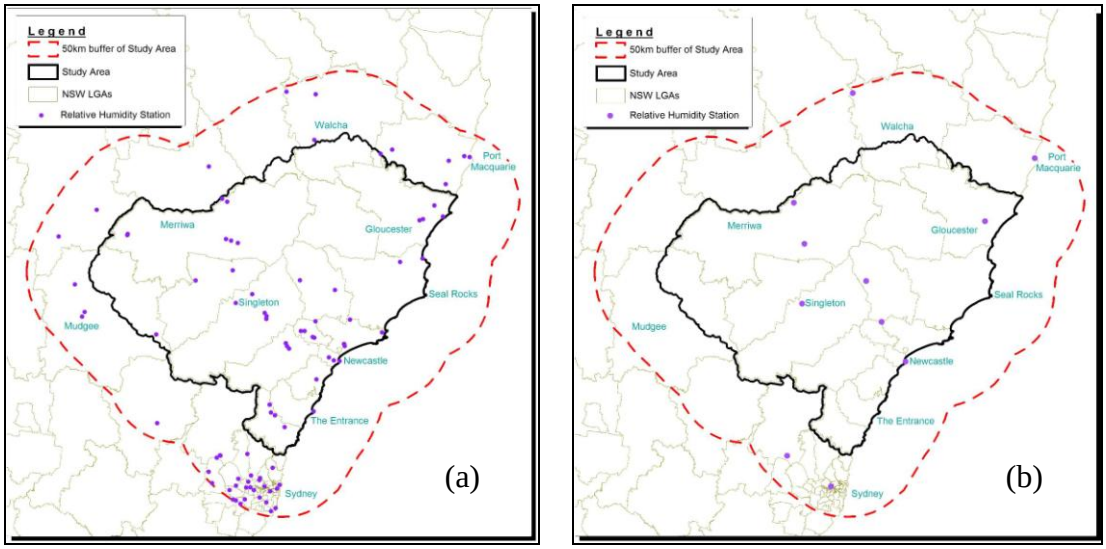

Figure 2.5. Potential (a) and final (b) 3 relative humidity stations

Ignoring omitted dates, data sets were chosen that span at least 1970 to 2007 (37 years) and are at least 90% complete. Stations that have been discontinued and replaced by a secondary gauge at a nearby location were also considered for inclusion in the final data set using the quality assurance method outlined in Appendix A. A total of 11 stations were found to satisfy the selection criteria as shown in Figure 2.5(b). Although the data set for relative humidity is smaller than for temperature and rainfall, it should still be possible to gain some insight into the spatial variability of relative humidity for the Hunter and Central Coast region.

2.1.5 Australian daily average wind speed

Daily windspeed data is available for 1823 number of sites across Australia. Of these, 96 are within the study region and buffer zone, as shown in Figure 2.6(a). As for all other climate records, the length and continuity of the data varies from station to station, with most records being less that 40 years.

Station data sets were chosen that span at least 1970 to 2007 (37 years) and are at least 90% complete. Stations that have been discontinued and replaced by a secondary gauge at a nearby location were also considered for inclusion in the final data set using the quality assurance method outlined in Appendix A. A total of 14 stations were found to satisfy the selection criteria as shown in Figure 2.6(b).

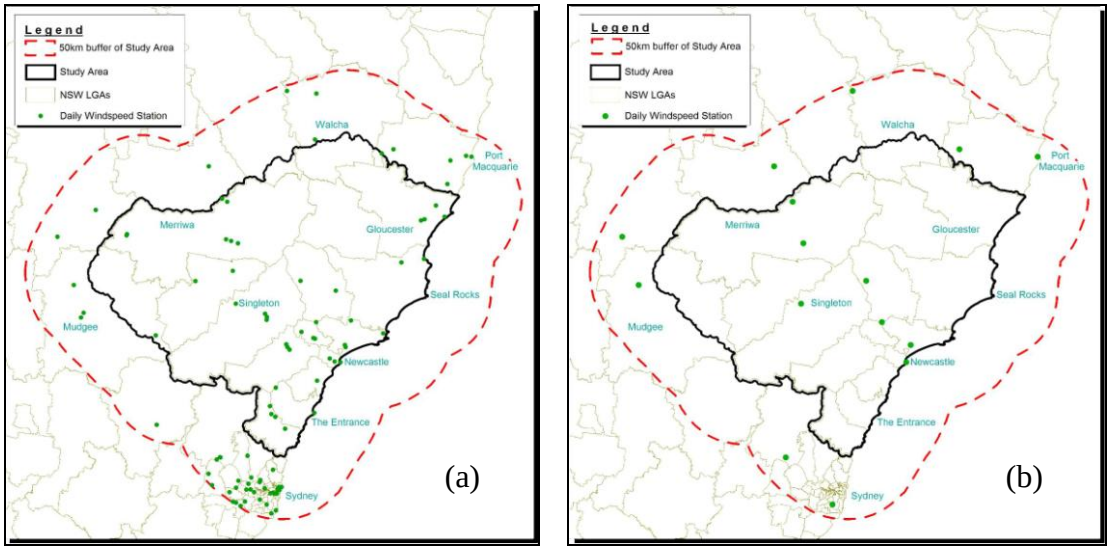

Figure 2.6. Potential (a) and final (b) daily average windspeed stations

Figure 2.6(b) shows that although the windspeed data set is smaller than for temperature and rainfall, the broad distribution of suitable station data within the study region and buffer zone may make it possible to gain some insight into the spatial variability of windspeed.

2.1.6 Maximum Wind Gust

Daily maximum wind gust data is available for 553 sites across Australia. Of these, only 26 are within the study region and buffer zone, as shown in Figure 2.7(a). As for all other climate records, the length and continuity of the data varies significantly from station to station. Data sets were chosen that span at least 1970 to 2007 (37 years) and are at least 90% complete. Maximum wind gust has not been monitored for a long period of time and the majority of stations do not have continuous data records for this variable. In fact, 14 of the 26 possible stations only began monitoring wind gust speed in 2003, while many other stations recorded this variable for a short period (less than 10 years). Only one station located within the study boundary (Williamtown) was found to satisfy the selection criteria (Figure 2.7(b)).

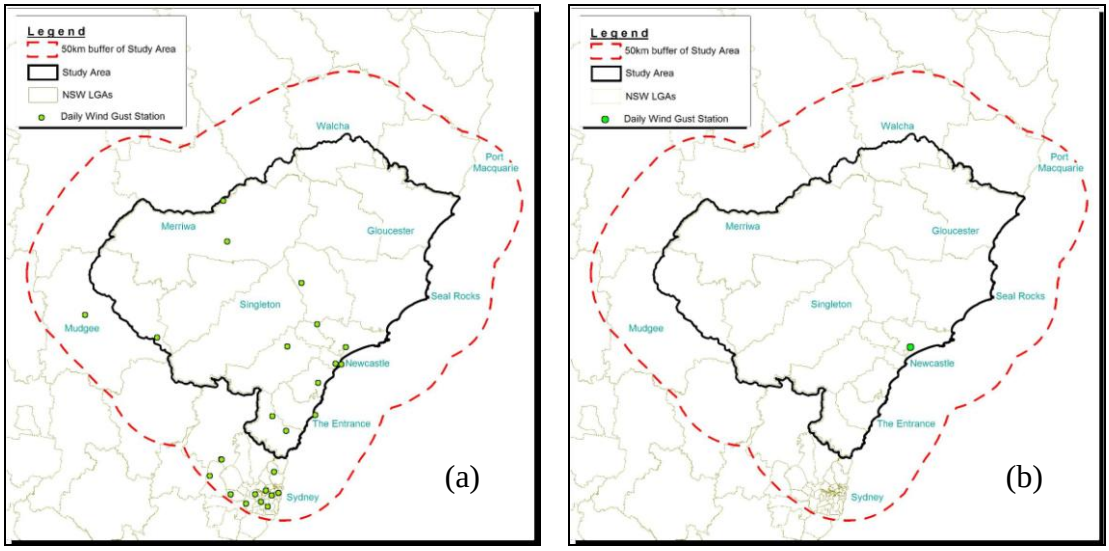

Figure 2.7. Potential (a) and final (b) daily maximum wind gust stations

Due to the limited data available for maximum wind gust, regional variability in climate variability/climate change impacts will not be able to be addressed. However, this data may be useful to study local impacts on extremes for Newcastle.

2.1.7 Daily Pan Evaporation

Daily pan evaporation data is available for 630 sites across Australia. Of these, 30 are located within the study region and buffer zone, as shown in Figure 2.8(a). Pan evaporation has only been measured for a relatively short period of time in Australia, with the majority of records being less than 35 years in length. Data sets were chosen that spanned at least 1974 to 2007 (33 years) and were at least 90% complete. A total of 7 stations were found to satisfy the selection criteria as shown in Figure 2.8(b).

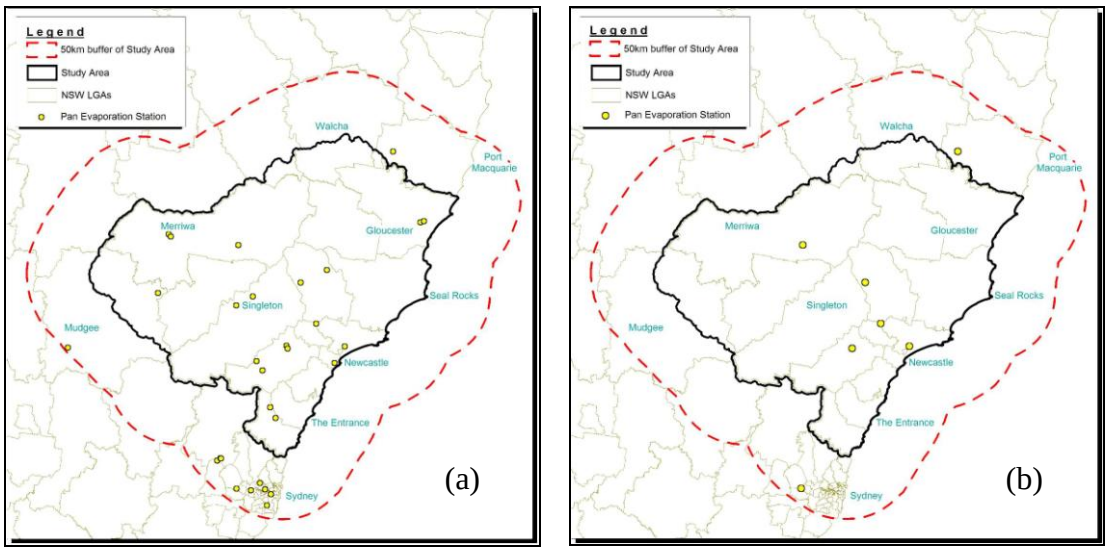

Figure 2.8. Potential (a) and final (b) daily pan evaporation stations

Due to the limited data available for pan evaporation, regional variability of pan evaporation may not be able to be addressed in great detail. However, it appears that sufficient data exits to study the broad scale variability of pan evaporation across a number of LGAs located both along the coast and inland.

2.2 Global reanalysis climate data

The US National Centers for Environmental Prediction (NCEP) and National Center for Atmospheric Research (NCAR) are cooperating in a project to produce a record of global analyses of atmospheric variables to support the needs of research and climate modeling communities. The record produced from this project is commonly known as the NCEP/NCAR reanalysis (NNR) data. The project uses a frozen state-of-the-art analysis/forecast system to perform data assimilation from past data (Kalnay, et al., 1996). The resultant assimilated data set is continually updated, and incorporates observations and global climate model output from 1 January 1948 to present.

Data is available at sub-daily, daily and monthly time scales on a global grid (2.5° x 2.5°) for 17 atmospheric pressure levels and 28 sigma levels. In all there are over 80 variables available, including air temperature, sea level pressure, geopotential height, maximum/minimum temperature, upper level winds to name a few. NCEP/NCAR reanalysis data for the January 1948 to December 2007 time period was obtained from the US National Oceanic & Atmospheric Administration (NOAA)[1]. Specifically, monthly mean sea level pressure and geopotential height (for all 17 levels) data was obtained.

In addition, the extended reconstructed sea surface temperature (ERSSTV3) data set was obtained. This data is constructed using the most recently available International Comprehensive Ocean-Atmosphere Data Set (ICOADS). The monthly data is available on a global grid (2.0° x 2.0°) beginning January 1854 to present. The entire data set was obtained for this research.

[1] *NCEP/NCAR Reanalysis data provided by the National Oceanic and Atmospheric Administration, Earth System Research Laboratory, Physical Sciences Division (NOAA/ESRL PSD), Boulder, Colorado, USA, from their Web site at http://www.cdc.noaa.gov/.*

3 Methodology

Three principal techniques are adopted in order to analyse sub-regional climate distributions and variability. These techniques involve the use of interpolation algorithms to create gridded surface data from point source data (BOM stations), statistical determination of regional climate zones and the use of self-organising maps (SOMS) to cluster global reanalysis data into key synoptic types or patterns. An overview of these techniques and parameters used in this research is provided in the following sections.

3.1 Interpolation of Point Source Data

Analysis of sub-regional climate distributions involves the consideration of spatial and temporal variability in key climate variables over the region. Data on key climate variables is provided by the BOM as point source data; that is, a timeseries of recorded values for particular climate variable at a particular point in space (i.e. precipitation in the preceding 24 hours recorded at each recording station). Analysis of the distribution of the values for these variables over the study region requires the interpolation of the point source data to a gridded surface for the study region. The ArcGIS 9.2 software program contains a number of suitable interpolation algorithms and is used for this research.

The gridded surfaces for key climate variables are obtained using the Kriging interpolation algorithm. The use of this algorithm follows recommendations from relevant literature (Childs, 2004; Earls & Dixon, 2007). Based on the most densely populated point layers (i.e. point locations of precipitation, minimum/maximum temperature stations), the resultant surfaces cover the geographic region from -33.87° to -30.96° latitude and 149.53° to 152.92° longitude. This extent is reduced for pan evaporation surfaces due to the limited station data available.

Annual average values are calculated for a calendar year from January to December inclusive. Seasonal averages are calculated for the months: December, January and February (Summer); March, April and May (Autumn); June, July and August (Winter); and, September, October and November (Spring). Thus some discrepancies arise between the annual and combined seasonal values due to the inclusion of previous year December values in Summer season calculations. Additionally, only data exceeding 90% complete is included in average calculations.

3.2 Climate Zonation

Climate zonation is a process for dividing a region into distinct sub-regions or zones where climatic similarity is maximised within zones and minimised between zones. The development of climate zones allows the analysis of sub-regional climate variability at a level above the individual BOM station data station. A number of techniques are available

for determining climate zones including defining regions based on plant hardiness, the presence of plant species, evapotranspiration and air mass origin. These techniques can combine both subjective and objective (statistical) approaches. In this research a purely statistical approach to determining climate zones was taken. The methodology adopted here is similar to that of Malmgren and Winter (1999) whereby principal components (PCs) analysis of key seasonal climate variables is conducted and these PCs are used as the basis for cluster analysis.

The key seasonal climate variables used for the zonation were summer, autumn, winter and spring precipitation, average minimum temperature and average maximum temperature. This resulted in a total of 12 climate parameters. As key climate variable data was not available for the same stations within the region (i.e. precipitation is recorded at 80 stations whereas temperature at only 17), spatial surfaces derived using the methodology described in section 3.1 were used. The regional 25m digital elevation model (DEM) was also used.

The ArcGIS 9.2 software program was used to perform the analysis. A principal components analysis (PCA) was conducted using the 12 seasonal surfaces and the DEM as raster input bands. The output of the ArcGIS PCA was evaluated to determine the appropriate number of principal components (i.e. those with eigenvalues above 1). In this case, the first 5 principal components were selected. These principal components were used as the input to the clustering process, which was performed using the ArcGIS Iso Cluster tool.

Iso Cluster performs clustering of the multivariate data combined in a list of input rasters. The tool uses an isodata clustering algorithm to determine the characteristics of the natural groupings of cells in multidimensional attribute space, producing a "signature file". The resulting signature file can be used as the input for the classification function; in this case Maximum Likelihood Classification (MLC) was used to produce an unsupervised classification raster. The resultant classification raster was then converted to a polygon feature layer to generate the climate zones. Different numbers of zones were produced (i.e. 2, 3, 4, 5 and 6) and evaluated by the project steering committee to determine the appropriate level of detail required for this project. A three zone classification was determined appropriate and is shown in Figure 3.1.

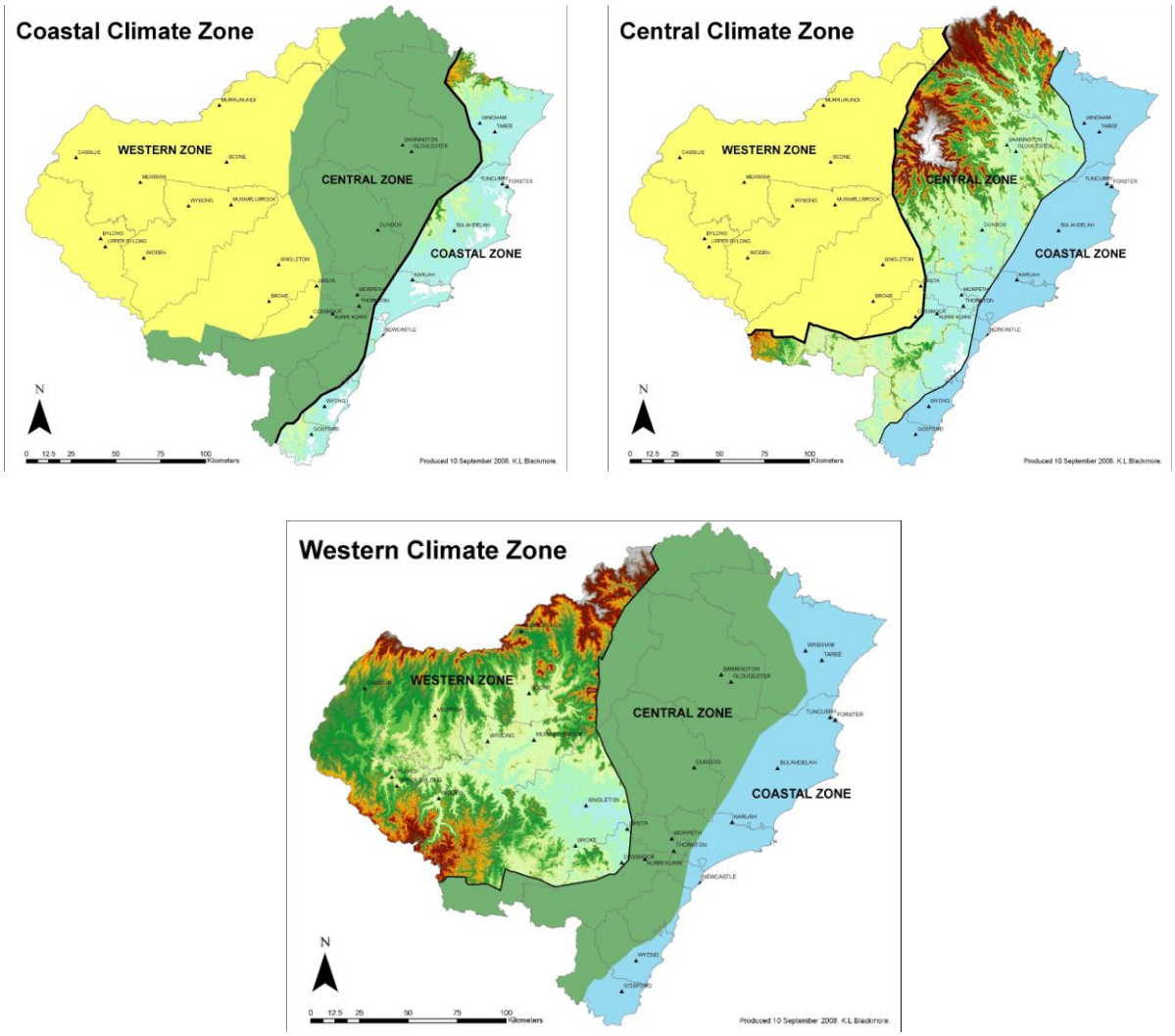

Figure 3.1. Coastal, central and western climate zones for the region.

3.3 Self Organising Map

The Self-Organising Map (SOM) algorithm is an iterative non-linear pattern recognition technique from the machine learning family of algorithms. The technique relies on a process known as vector quantitisation which essentially clusters like features together (Figure 3.2). Unlike other standard clustering techniques (i.e. K-means, nearest neighbour, etc), SOM produces a resultant "map" which arranges the clusters by similarity. That is, clusters with similar features will appear close together of the map.

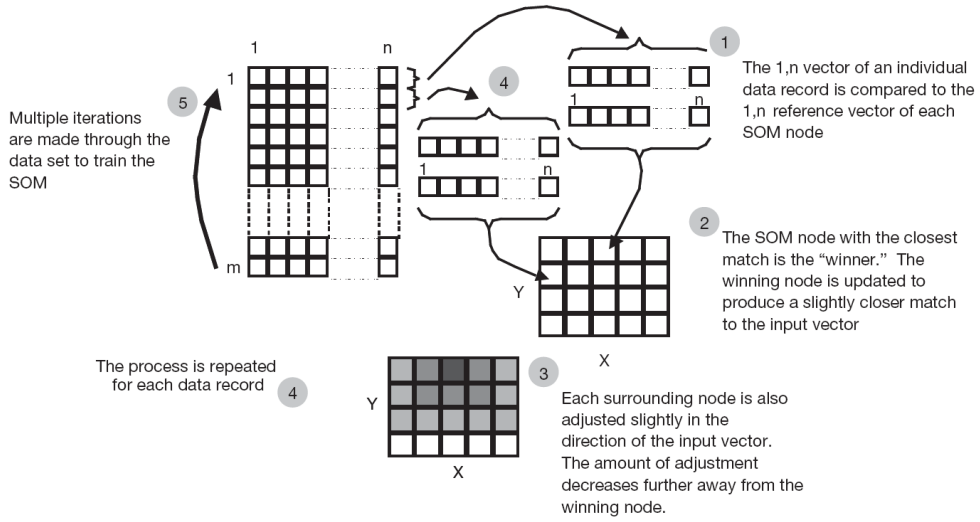

Figure 3.2. The iterative self-organising map (SOM) training procedure (reproduced from Crane & Hewitson 2003).

The output from the SOM process is a user specified number of prototype or representative vectors. These vectors represent each of the derived "clusters" in such a way that they span the entire input space. In this research, the resultant prototype vectors are used to generate interpolated surfaces using the ArcGIS software. The following sections provide information on the use of the SOM technique in this research.

A number of parameters are required to be set for the SOM training process. In this analysis, the batch training algorithm was selected, with an initial radius of 5 and a final radius of 1. Training was conducted for 50,000 iterations. These parameters follow those used by Hewitson and Crane (2003).

3.3.1 Clustering the Synoptic Types to Key Features

An important component of this study is to define the key synoptic patterns that drive the climate variability of the region. A review of literature revealed that synoptic patterns may be successfully identified from atmospheric pressure data using a SOM (Hewitson and Crane 2002; Hope, et al. 2006). The SOM methodology is particularly appropriate to synoptic climatology as there is no assumption of linearity (as with traditional Principle Component Analysis) (Kohonen 1997).

Synoptic climate typing has been performed on NCEP/NCAR reanalysis (see Section 2.2) monthly sea-level pressure (SLP) data for the region. This analysis is performed using available SOM software (Vesanto, et al., 1999). The analysis involves extracting the data from January 1948 to December 2007 for an appropriate geographic region from the global coverage. Data for the geographic region 112.5° to 177.5° longitude, -10° to -47.5° latitude

was selected for this research. This extent covers the land areas of Australia and New Zealand and allows the discernment of synoptic patterns that affect the Hunter, Lower North Coast and Central Coast region.

The SOM process requires the specification of the number of representative vectors *a priori*. Determination of the appropriate number of representative vectors is a function of the number of inherent clusters or groups in the input data and the required resolution of the output. In this research, various size SOMs were produced and evaluated to determine the required resolution. An initial SOM size of 5 x 7 (35 types) was adopted and evaluated. Although found to discriminate regional climate patterns, this size SOM produced some synoptic types that were too similar to allow analysis of synoptic differences. Evaluation of various alternative size SOMs (i.e. 4x5, 3x4, 2x3) resulted in the selection of a 3 x 4 (12 types) SOM as appropriate for this research.

The synoptic typing process has been conducted to produce twelve (12) types to allow the subtle discrimination of regional climate patterns on key climate parameters such as rainfall, evaporation and temperature. The 12 synoptic types (STs) generated are shown to capture a range of significant synoptic features that are known to influence the weather of the region, including the clear seasonal trend in the location and intensity of the subtropical anticyclone, the monsoonal trough the circumpolar trough, and the longwave features in the Pacific and Indian Ocean sectors. Each month from January 1948 through to December 2007 has been classified according to the 12 synoptic patterns, resulting in a monthly time series of synoptic types. Differentiation between Summer and Winter STs can be achieved, however differentiation between Spring and Autumn types is not possible. This is a limitation of the methodology, which is unable to discern the subtle shifts which characterise these seasons.

In addition to STs derived from SLP data, of key interest are the variations in SLP from the mean conditions that produce different climate conditions in the region. Thus the SOM process was also completed using SLP anomalies. These anomalies are created by subtracting the mean SLP value for the period from January 1968 to December 1996 (Kalnay, et al, 1996) for a given grid point from the actual value for the grid point. The anomaly data is then used as the input to the SOM process. The resulting anomaly types correspond to the SLP types, however they provide an improved visualisation. In this report, the SLP STs and corresponding anomaly STs are shown in Chapter 4 and a profile of each type is provided in Appendix C.

3.3.2 Clustering Thickness Types to Key Features

Following a similar process used to derive synoptic types from SLP data (Section 3.2.1), the SOM methodology is used to derive 12 thickness types. Again, the selection of a 12 type solution is somewhat arbitrary. NCEP/NCAR reanalysis (see Section 2.2) monthly geopotential height data for the region is used to derive thickness types. Geopotential

height is a measure (in meters) of the vertical distance above mean sea level of a given atmospheric pressure level. The thickness is obtained by subtracting the geopotential height at 1000mb from the geopotential height at 500mb.

The derived thickness measures provide the input or training data for the SOM algorithm. Clustering of thickness types to key features is conducted for the same geographic extent and time period as that used for SLP.

3.3.3 Clustering Sea Surface Temperature Anomaly Types to Key Features

The extended reconstructed sea surface temperature (ERSSTV3) data is available for monthly sea surface temperature (SST). Sea surface temperature anomalies are calculated as the difference between the recorded SST value from the ERSSTV3 data and the seasonal average (also calculated from the ERSSTV3 data). Unlike SLP and geopotential height data, SST data is provided on 2° x 2° global grid. Thus once SST anomalies were calculated, the data was resized (using Matlab) to match the NCEP/NCAR grid (i.e. resized to 2.5° grid). This resultant data set then provides the input for the SOM algorithm. Clustering of thickness types to key features is conducted for the same geographic extent and time period as that used for SLP.

4 Synoptic Climate Types and Climate Drivers

4.1 Overview of Southern Hemisphere Climate Modes

The large-scale atmospheric circulation patterns for the Southern Hemisphere are described by the time varying position of: (i) the longwave trough (LWT) and ridge (LWR) in the extratropics over the Southern Ocean and Southern Australia; (ii) the poleward-equatorward fluctuation in the position of the subtropical ridge (STR); and, (iii) the monsoonal trough (MT) over northern Australia. The spatial patterns of these climate features are time–varying on daily synoptic weather time scales, and seasonal to decadal climate time scales. The time-varying circulation is due to the interaction of the major climate modes of oscillating atmospheric pressure and sea-surface temperature in the Southern Hemisphere which are the El Nino-Southern Oscillation (ENSO) and the Southern Annular Mode (SAM). These are the dominant climate modes for the tropical and extratropical Southern Hemisphere, respectively. The spatial patterns of these modes in surface pressure are shown in Figure 4.1. These patterns control the growth and decay of synoptic weather systems over Australia.

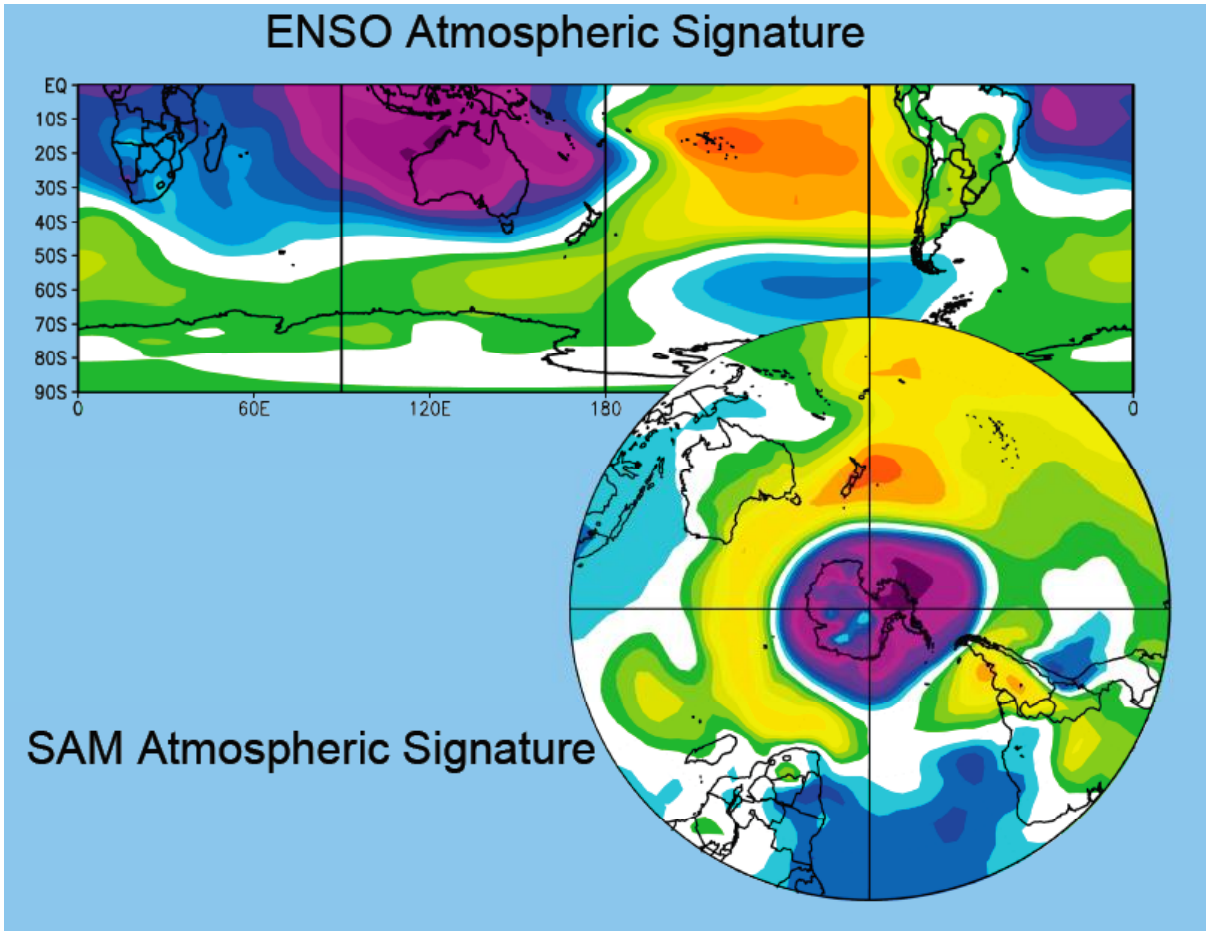

Figure 4.1. The sea level pressure (SLP) anomalies associated with the major tropical and extratropical climate modes, determined from the NNR reanalysis data set, with low SLP anomalies shown in purple and high anomalies shown in orange. The spatial pattern clearly identifies dipoles in east-west SLP in the tropics that describe the ENSO phenomenon, and

dipoles in north-south SLP in the extratropics that describe the SAM phenomenon. The most widely used statistic of the ENSO phenomenon is he Southern Oscillation Index (SOI) being the calculated difference in SLP between Tahiti and Darwin. The statistic used to describe the SAM is the SAM Index which is calculated from the difference in zonal SLP at 40° and 60° South.

In addition, the Southern Hemisphere extratropics, the secondary climate modes in the extratropics have been identified as propagating atmospheric wave trains across the Pacific sector, and are known as The Pacific-South American (PSA) teleconnection pattern (PSA1 is the ENSO mode, and PSA2 is the South Pacific Wave Train) (Ghil and Mo, 1991). The Pacific South American Mode 1 (ENSO Mode) originates from coupled atmospheric anomalies in the central to western tropical pacific region; and the Pacific South American Mode 2 (South Pacific Wave Train) originates from coupled atmospheric anomalies in the tropical north eastern Indian and northern Australian region. These patterns are shown in Figure 4.2.

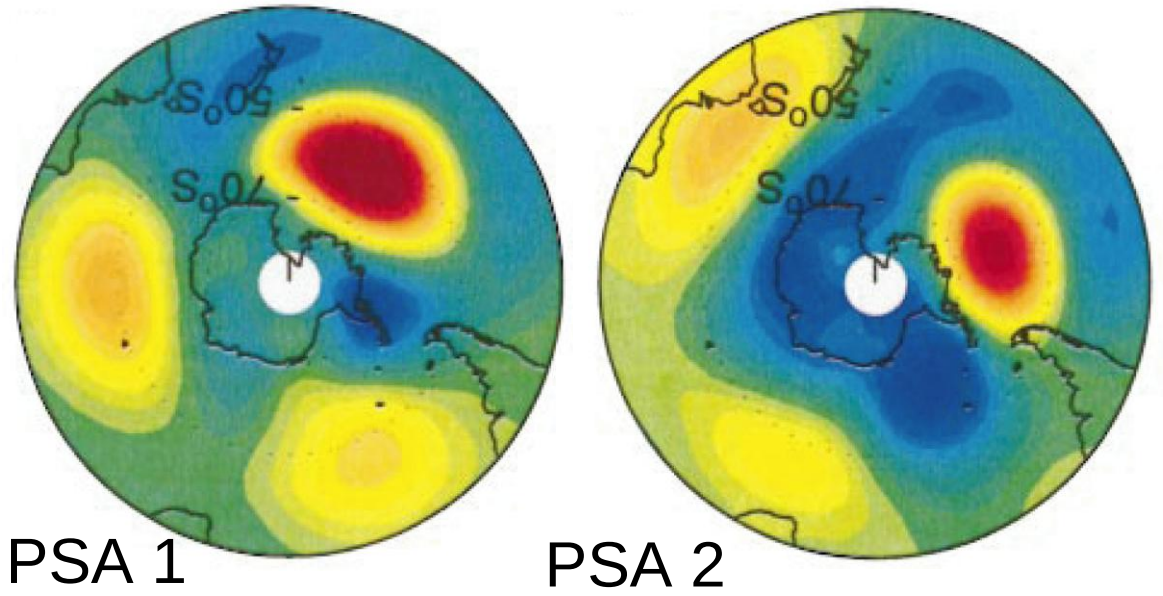

Figure 4.2. The spatial teleconnection patterns of the Pacific South American climate modes, showing regions of oscillating atmospheric pressure. PSA 1 or 2 are in there respective positive phases when SLP anomalies off Antarctica are positive (red).

4.2 Synoptic Types and Their Relationship to the Major Climate Modes

The synoptic typing process (see Section 3.2) has been arbitrarily conducted to produce 12 types to allow the subtle discrimination of regional climate patterns on key climate parameters such as rainfall, evaporation, air and sea-surface temperature. The 12 synoptic types are generated using both monthly sea-level pressure (SLP) data, and monthly sea-level pressure anomaly (SLPA) data. The SLPA data were calculated from the 1960-1990 mean climatology. The SLPA capture a range of significant large-scale synoptic features that are

known to influence the weather of the region, including the clear seasonal trend in the location and intensity of the subtropical anticyclone, the monsoonal trough, the circumpolar trough, and the longwave trough and ridge features in the Pacific and Indian Ocean sectors. These monthly ST represent an average of the synoptic weather system occurrence at the daily time scale, including: cold frontal systems, including: simple and complex cold fronts, frontal waves, Southern Tasman Lows and cold-cored cut-off lows from the westerly airstream; the northern Australian monsoonal trough; warm-cored cyclones such as East Coast Lows and Easterly Dips; and, anticyclonic intensification over south-east Australia and blocking anticyclones over the Tasman Sea and New Zealand region (Sturman and Tapper, 2006).

The 12 synoptic patterns that have been generated using the SOM methodology and monthly NNR SLP and SLPA data are shown in Figure 4.3 a and b, respectively, according to a 3 x 4 matrix. The ST's are most similar to the adjacent types and most dissimilar to the most diagonally opposite. A monthly time series of ST's was generated from January 1948 to March 2007.

A.

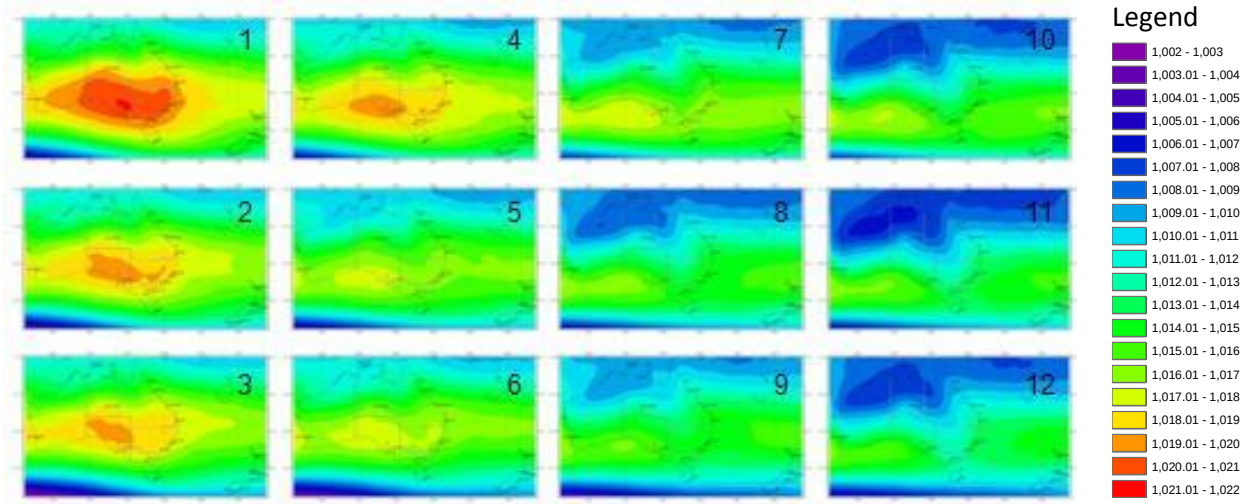

B.

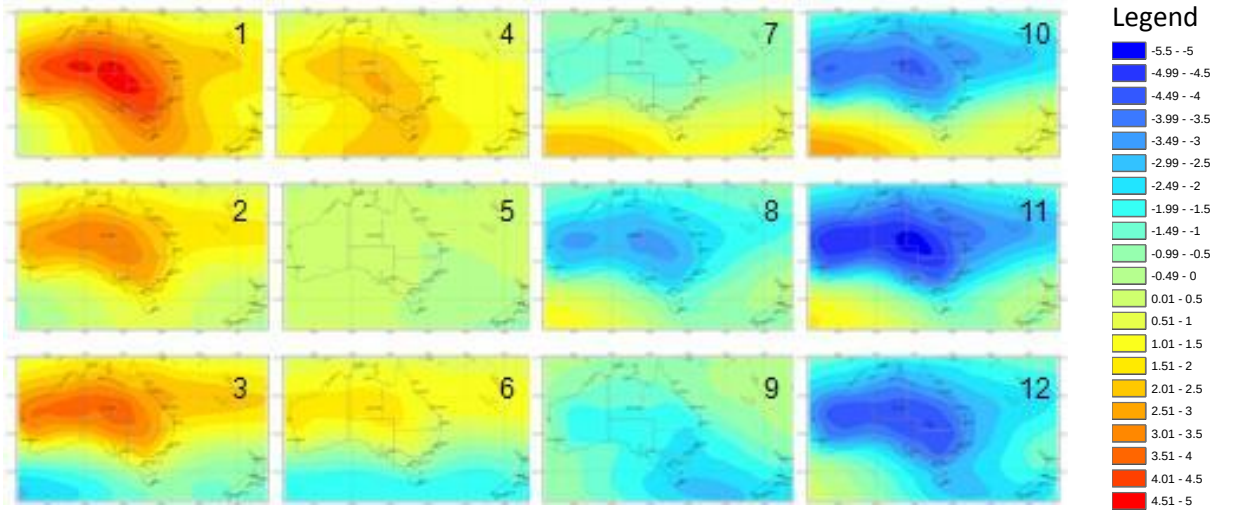

Figure 4.3. 12 key synoptic types (A) and corresponding anomaly types (B) derived using the SOM methodology

The NCEP-NCAR (NNR) monthly time series was analysed to characterise each of the ST's into the associated major large-scale climate mode, using the SOI Index (BOM, Troup SOI Index) and the SAM and PSA1 and 2 indices from Visbeck and Hall (2004). The results are shown in Figure 4.4 below. The ST's most reliably explain the variance in the SAM and the PSA2 modes, and have a variable correlation with the ENSO and related PSA1 modes, due to the time-varying interaction of the tropical and extratropical circulations. A vertical transition (columns) between ST's describes the climate pattern shift from the +ve SAM (zonal and more poleward westerly circulation) such as ST 1, 4, 7 and 10 to -ve SAM (meridional and more equatorward westerly circulation) such as ST 3, 6, 9 and 12. A vertical shift from PSA2+ve (South Pacific Wave) circulation (ST's 1, 4, 7 and 10) is evident down the matrix, to a dominance of PSA2-ve on the bottom row (ST's 3, 6, 9 and 12).

The statistical relationship between the ST's and the SOI Index is weak and not significant, and is revealed by a shift in the dominance of PSA1 (ENSO) mode from El Nino-like (+ve

phase) climate to La Nina-like (-ve phase) climate patterns, moving horizontally (rows) across the matrix. The lack of correlation significance between the ST's and ENSO indicates that the synoptic typing is biased towards the representation of mid-latitude climate variability, that is most applicable to investigating climate variability and change in South-east Australia.

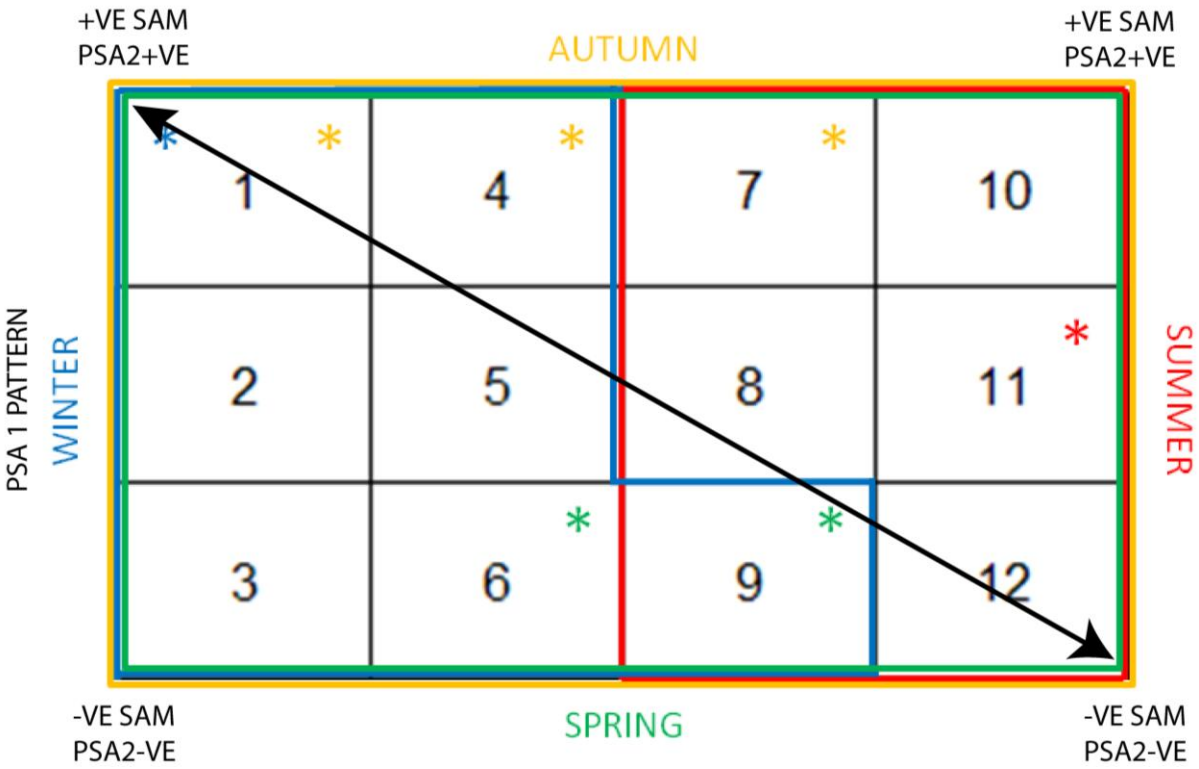

Figure 4.4 showing the dominant ST's by season: red occurring in summer (DJF); yellow occurring in autumn (MAM); blue occurring in winter (JJA); and, green occurring in spring (SON). The most dominant types in the respective seasons are shown by asterisks.

The most frequent seasonal ST's that account for ~20 % of frequency are: ST 10, 11 and 12 in summer; ST 1, 4 and ST 6 in autumn; ST 1 and 3 in winter; and ST 6 and ST 9 in spring. The individual ST's represent the dominant large scale circulation for each month in the record, and many of the ST's can be associated with frequent occurrence or persistence of synoptic weather conditions. Synoptic weather systems and their associated ST's are listed in Table 4.1 below.

SYNOPTIC WEATHER SYSTEM	SYNOPTIC CLIMATE TYPE
Southern Tasman Sea Lows	ST's 2 (eastern Tasman Sea), 3, 5, 6, 9
Frontal waves in the Southern Tasman Sea	ST's 3, 6, 12
Cut-off or Southern Secondary Low (central to southern Tasman Sea)	ST's 1, 2
Blocking Highs over Tasman and New Zealand	ST's 7, 8, 10, 11
Northern Australia or Monsoon Trough	ST's 7, 8, 10, 11, 12
SE Australia Longwave Ridge	ST 1, 2, 4, 7
SE Australia Longwave Trough	ST 8, 9, 11, 12
Easterly Dips	ST's 7, 8, 10, 11
East Coast Lows	ST 1
Anticyclone intensification	ST's 1, 2, 3,

Table 4.1. Synoptic weather systems and their associated synoptic types

4.3 Synoptic Types and Interdecadal Variability

Interdecadal variability within the Australasian and South West Pacific regions is associated with the Interdecadal Pacific Oscillation (IPO). During the time period from 1948 to 2007 there have been two phases of this oscillation: IPO –ve phase (La Nina-like) from 1948 to 1976; and, IPO +ve phase (El Nino-like) from 1977 to 2007. To investigate the climate variability of the region, the ST time series was stratified according to these two time periods. For purposes of comparison, the frequency of ST's for: (i) all years , 1948 to 2007; (ii) 1948 to 1976; and, (iii) 1977 to 2007, are shown below in Figures 4.5, 4.6 and 4.7 respectively.

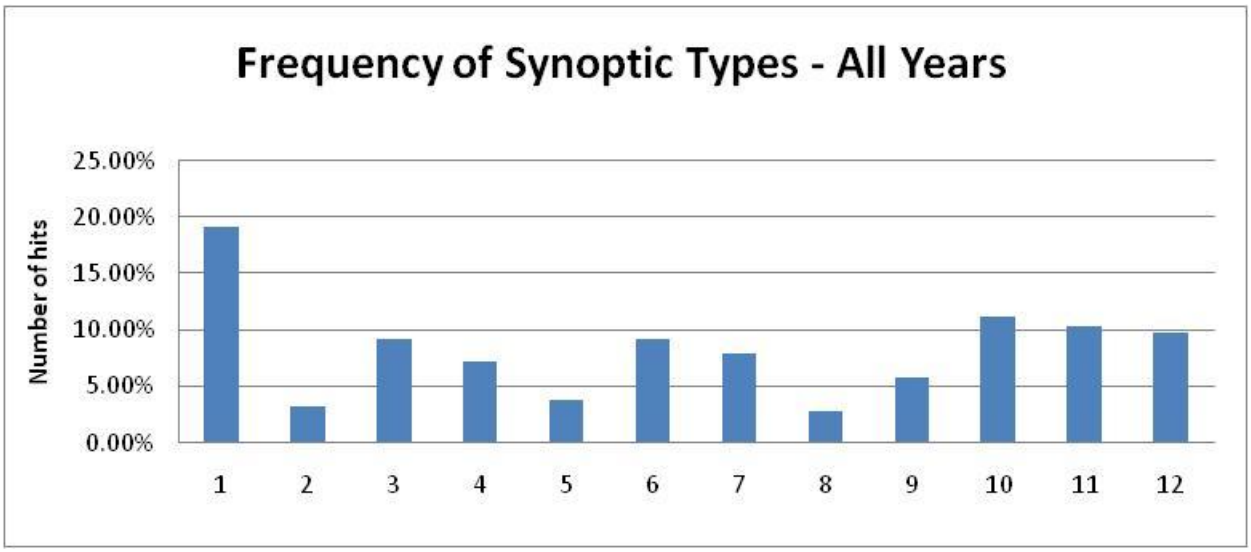

Figure 4.5. Frequency of occurrence of synoptic types from Jan 1948 to Dec 2007.

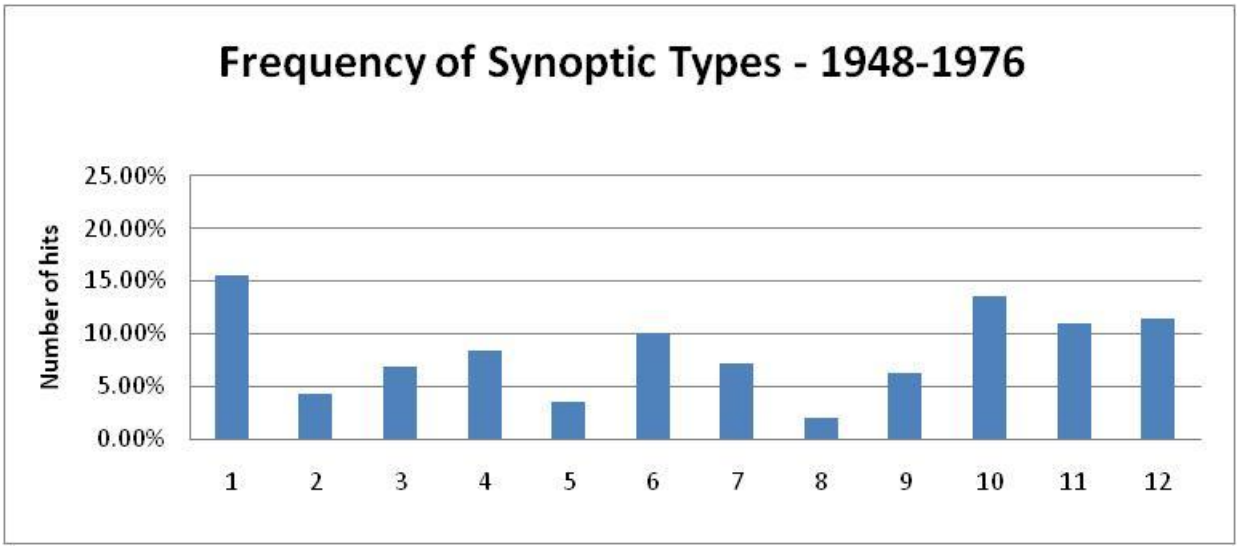

Figure 4.6. Frequency of occurrence of synoptic types from Jan 1948 to Dec 1976.

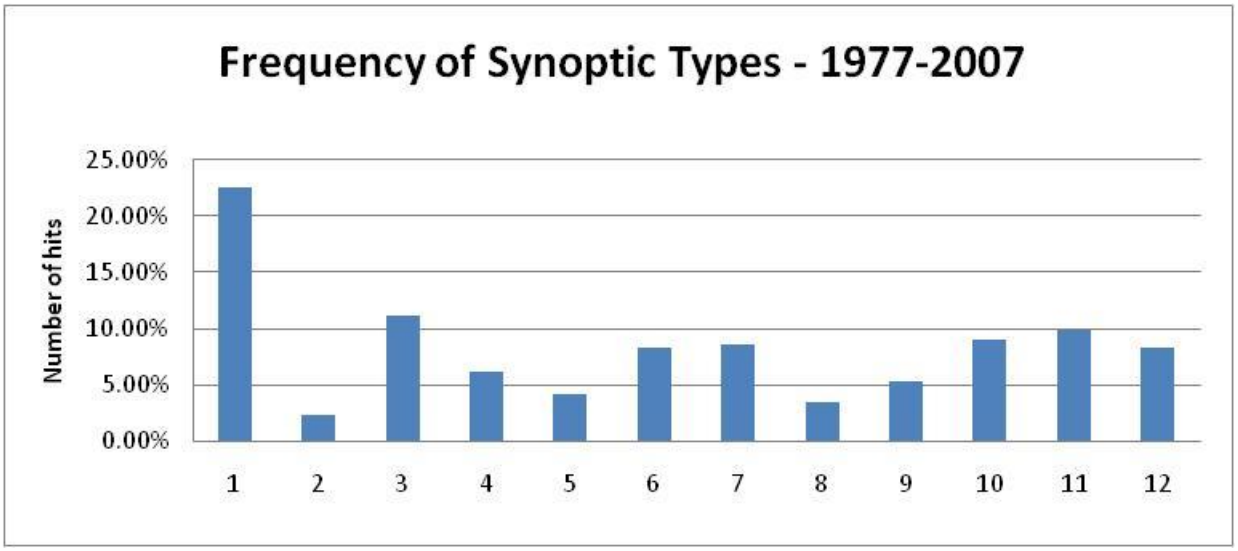

Figure 4.7. Frequency of occurrence of synoptic types from Jan 1977 to Dec 2007.

A plot showing the difference in frequency of the ST's between IPO periods is shown below in Figure y. The most variable ST's that are statistically significant between the two IPO periods are: ST 1, 3, 10 and 12. During the IPO +ve phase (1977 to 2007) the dominant ST's change to the following:

(i) Summer: ST 10 decrease in frequency, and ST 7, 8 and 12 have a small increase;
(ii) Autumn: ST 6, 9 and 10 decreases in frequency whilst, ST 1 and 4 increase;
(iii) Winter: ST 2 and 6 decrease in frequency whilst, ST 1 and 3 increase;
(iv) Spring: ST 4 and 12 decrease in frequency whilst, ST 1 and 6 increase.

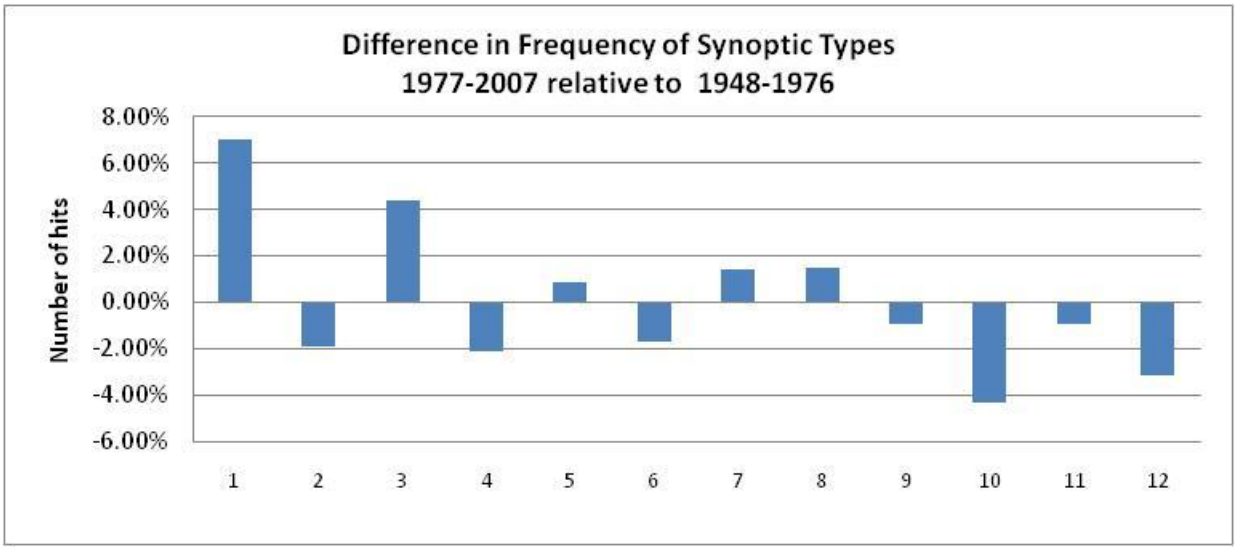

Figure 4.8. Difference in the frequency of occurrence of synoptic types between 1948-1976 and 1977-2007.

These results demonstrate a weakening of the atmospheric circulation during the DJF seasons together with an eastward shift in the longwave trough south-east of Australia. During winter the Australian anticyclone (high pressure (STR) over southern Australia) has strengthened as demonstrated by the shift in ST from 2 to 1 and ST 6 to 3. The longwave ridge is quasi permanent over south-east Australia and an associated eastwards displacement of the frontal wave towards New Zealand has also occurred. During autumn ST 10 has been replaced by ST's 1 and 4, showing that the monsoonal trough extension into southern Australia has been replaced by the strengthened STR, which is the driver of the higher frequency of drought conditions for southern Australia. During spring ST 4 and 12 have been replaced by ST 1 and 6 which is indicative of a strengthened STR across central and eastern Ausralia and the South-West Pacific. In a broader context the sum of these changes in ST can be seen in Figure 4.9 where the seasonal SLP anomalies in hPa for the difference between IPO phase circulations (1977 to 2007 minus 1949 to 1976) is shown. An increase in the latitudinal SLP gradient from the Coral Sea to southern Tasman Sea and an increase in SLP in the western Coral and Tasman Seas and over northeastern NSW and southeastern Queensland.

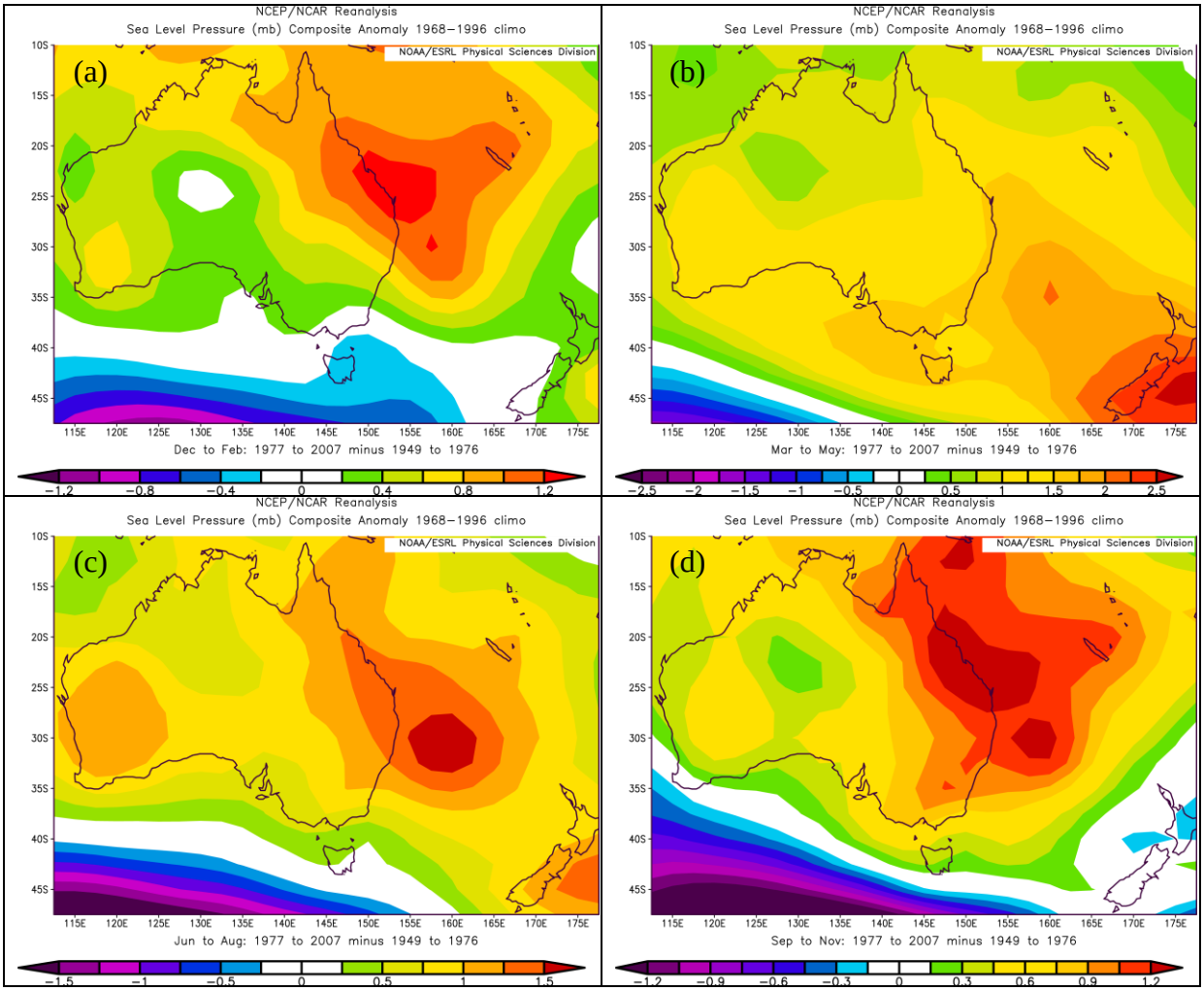

Figure 4.9 shows the seasonal SLP anomalies in hPa for the difference between IPO phase circulations (1977 to 2007 minus 1949 to 1976), (a) summer, (b) autumn, (c) winter, and (d) spring.

5 Sub-regional Climate Distributions

Sub-regional climate distributions for the region are discussed in terms of annual and seasonal variability (Section 5.1), inter-annual and inter-decadal variability (Section 5.2) and extreme events (Section 5.3).

Results are presented in this section for the coastal, central and western climate zones. The methodology used to derive these zones or sub-regions is discussed in Section 3.2 (page 13) of this report. A diagram (Figure 3.1) showing the boundaries of these climate zones within the study region is also provided (page 15).

5.1 Annual and Seasonal Variability

5.1.1 Precipitation

The spatial distribution of precipitation varies within the region and is influenced by terrain and the ocean. A regular decrease in precipitation is evident from along the coast in the east, to west (Figure 5.1). The highest annual rainfall is recorded in the Bulga and Comboyne Plateau area in the north east of the region, averaging over 1900mm per annum. In contrast, the western most area of the region, south west of Muswellbrook, receives an average of 630mm per annum, approximately one third of that received in the north east of the region.

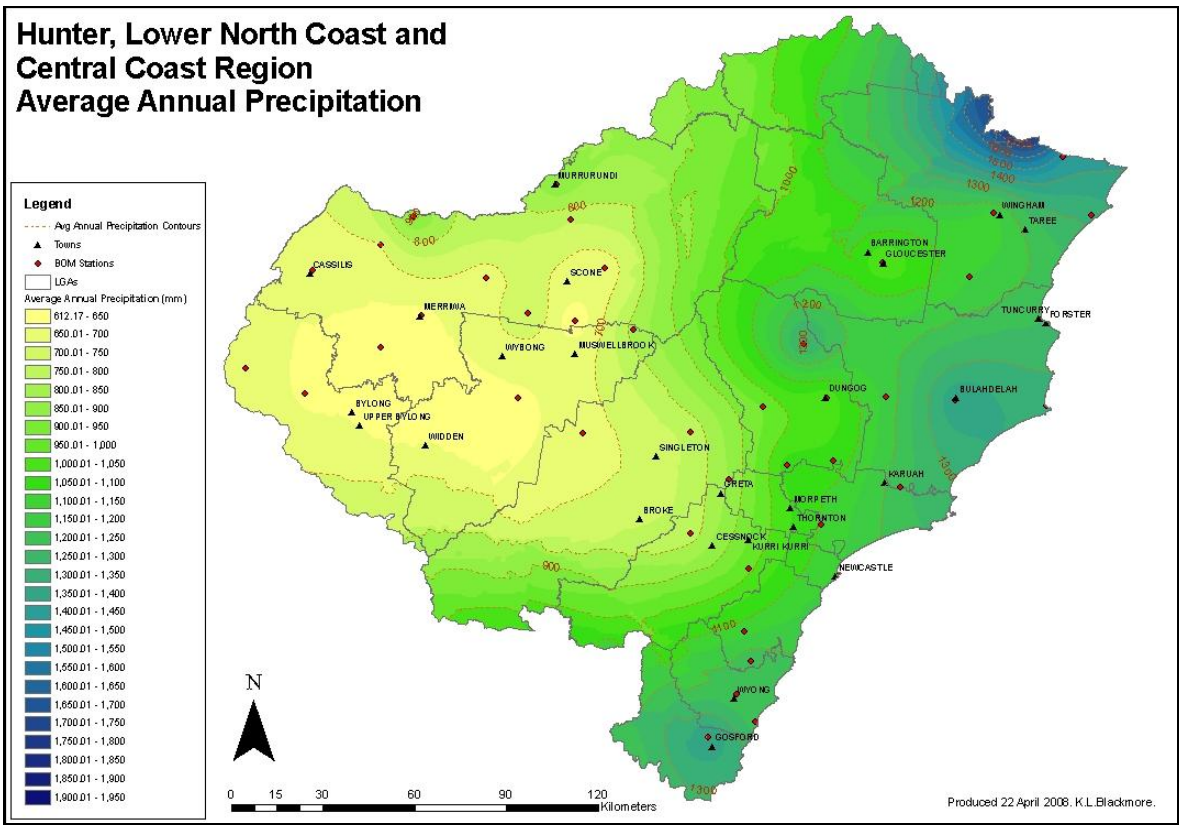

Figure 5.1. Average Annual Precipitation (mm) in the Hunter, Lower North Coast and Central Coast Region

The majority of the regions rainfall occurs in the summer and autumn seasons. Variation in the seasonal spatial distribution of precipitation is evident, with two distinct seasonal trends (Figure 5.2). The spatial pattern of precipitation in the summer and autumn seasons dominates the annual pattern. The highest rainfall occurs in summer in the Barrington Tops, however all areas generally receive more than 70mm per month of summer rain. Summer monthly rainfall in the central and coastal areas averages over 120mm per month, whereas the west of the region averages around 80mm. The coastal effect is clearly evident in the autumn months, with the coastal region receiving average autumn monthly rainfall of over 125mm, compared to just over 50mm in the western parts of the region.

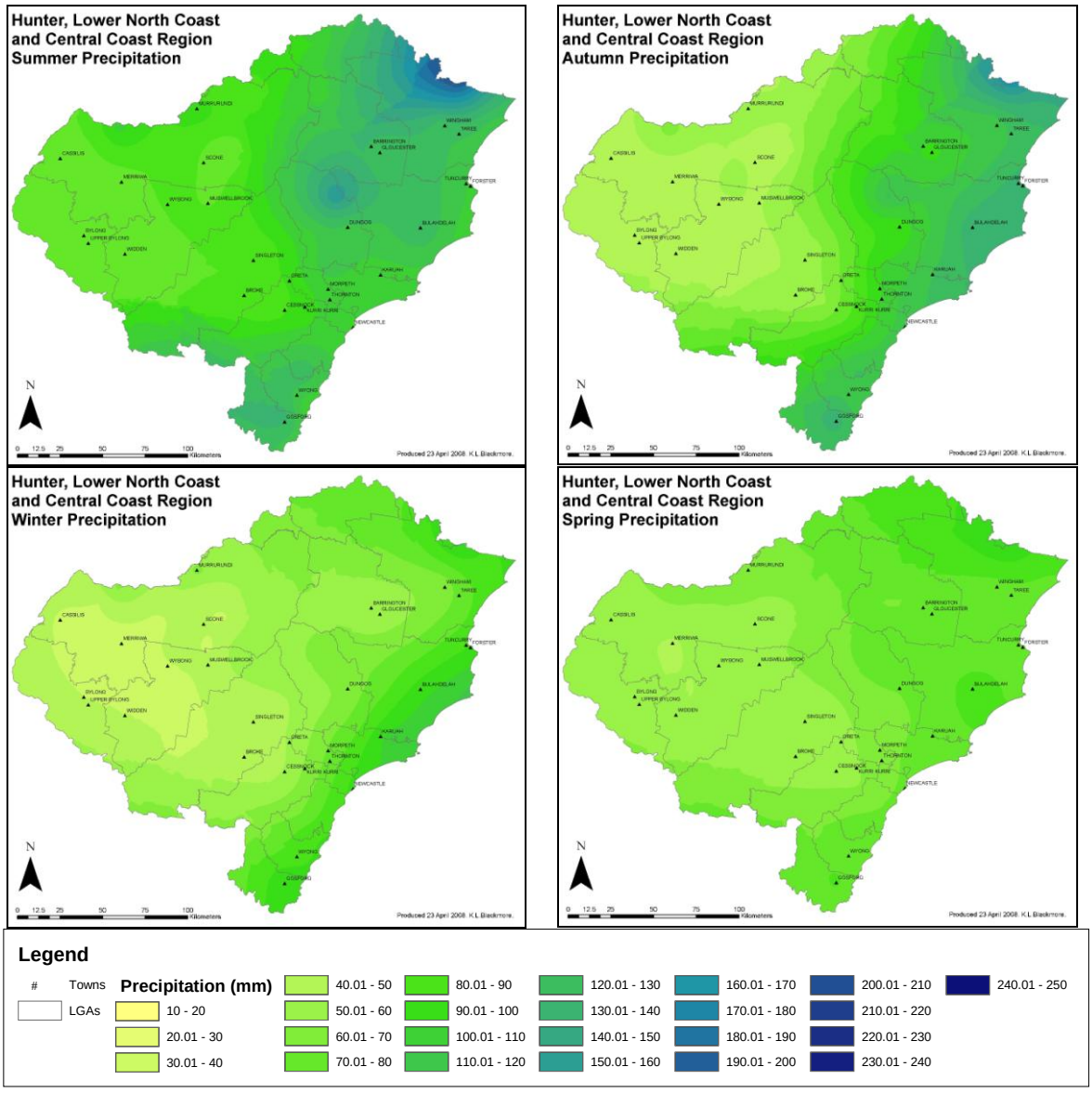

Figure 5.2. Average Seasonal (summer, autumn, winter, spring) Precipitation (mm) in the Hunter, Lower North Coast and Central Coast Region

By July, precipitation further retracts to the coastal areas with an average of 90mm per month of winter rainfall; the western areas receive approximately 45mm. By spring the most even distribution of rainfall across the region occurs, with just over 20mm variation in averages across the region. Western areas receive ~ 55mm of winter rainfall compared to ~ 75mm on the coast. Thus the winter and spring seasons combine to define the region's dry season.

The average monthly precipitation is plotted against ST for the 3 sub-regions (Figure 5.3). The highest monthly precipitation in the coastal and central zones occurs during ST's 7, 10 and 11 when the Subtropical Anticyclone is most polewards. Precipitation in the western zone is also highest during ST's 7, 10 and 11. Lowest monthly precipitation in the coastal and central zones occurs during ST's 3, 6 and 9. Lowest monthly precipitation in the western zone occurs during ST's 1, 3 and 6.

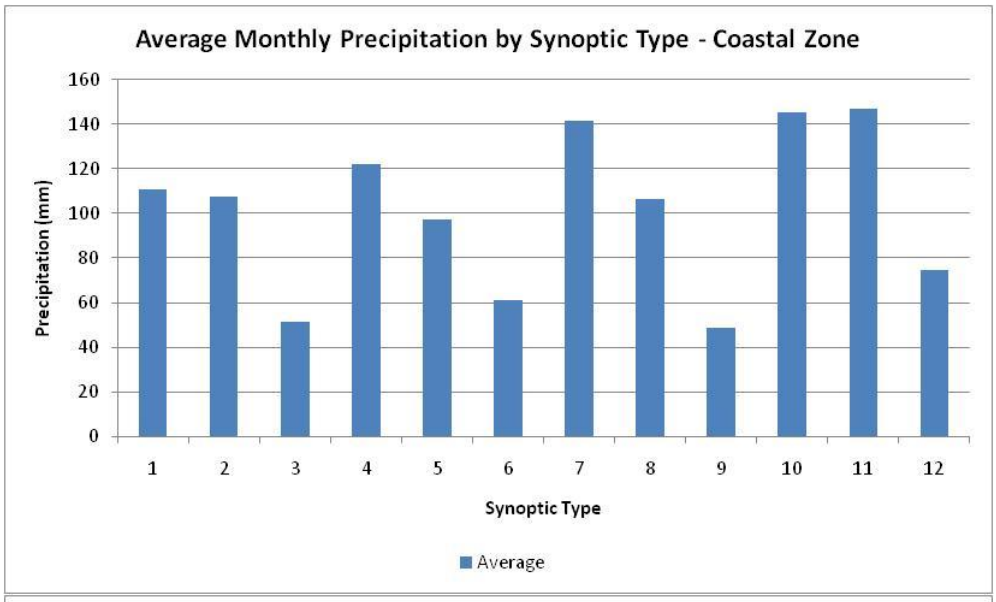

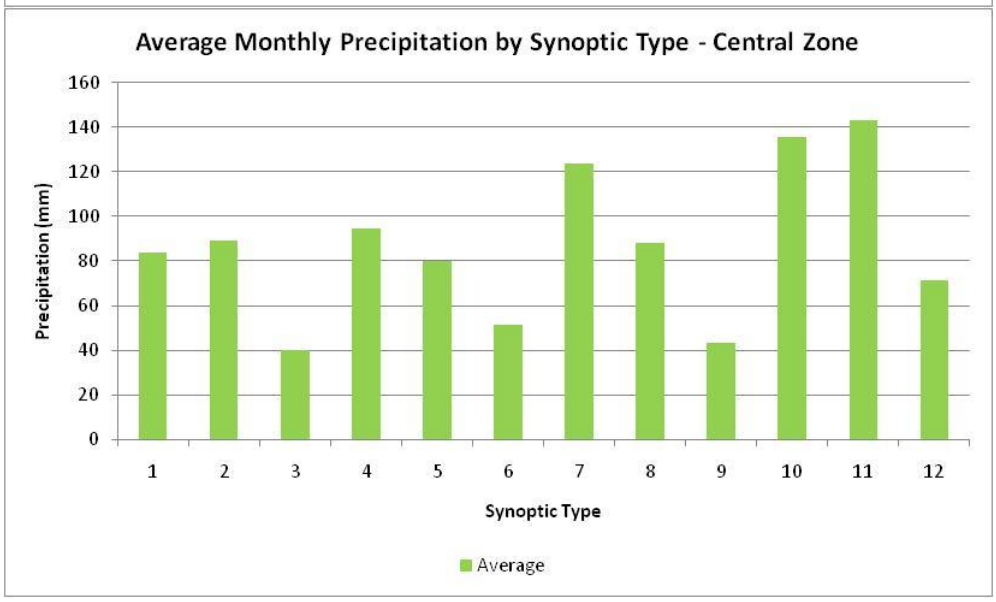

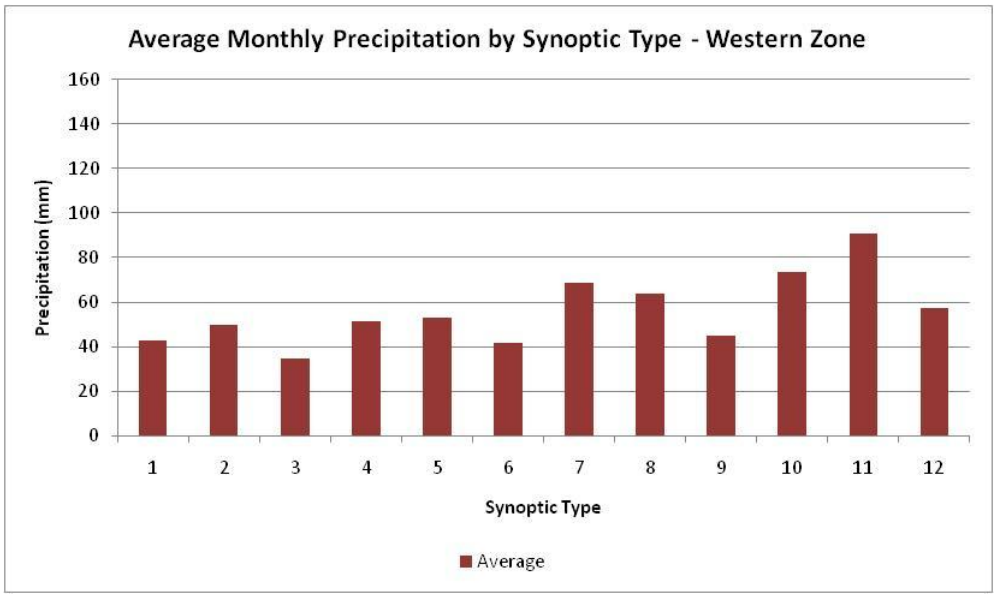

Figure 5.3. Average Monthly Precipitation (mm) by Synoptic Type

5.1.2 Maximum and Minimum Temperature

The mean annual maximum temperature for the region is 23.2°C and shows relatively little variation across the region (Figure 5.4). Mean annual maximum temperatures range from 23.5°C in the north, to 17.5°C at the most southerly extent. Average annual maximum temperatures above 24.5°C are recorded in the north (Taree) and central (Singleton) parts of the region. As would be expected, the generated annual maximum temperature spatial surface shows a general latitudinal decrease in temperatures from North to South.

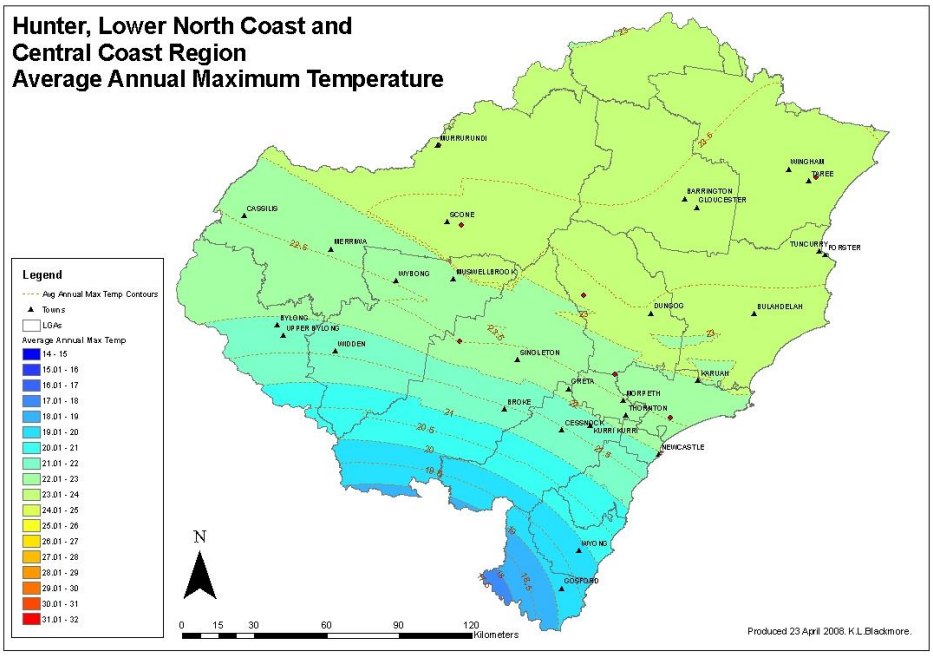

Figure 5.4. Average Annual Maximum Temperature (°C) in the Hunter, Lower North Coast and Central Coast Region

Seasonal sub-regional maximum temperature distributions again show minimal variation within season, however strong inter seasonal variations are evident (Figure 5.5). Coastal influences impact on summer maximum temperatures, with temperatures ranging between 25°C on the coast (Nobby's Head at Newcastle) and 30.2°C in the west (Scone). On average, the maximum summer temperature for the region is around 28.5°C. By autumn, the average maximum temperature for the region drops 5°C and coastal influences become less apparent. Cool westerly winds negate any coastal influences in winter, with average maximum temperatures between 16-19°C and a regional average of 17.4°C. spring sees a return to cooler coastal temperatures, with the coastal areas approximately 1°C lower than inland areas. The regional average maximum temperature is 23.5°C, with a range of maximum temperatures between 21.5°C (Nobby's Head at Newcastle) and 25.5°C (Jerrys Plains).

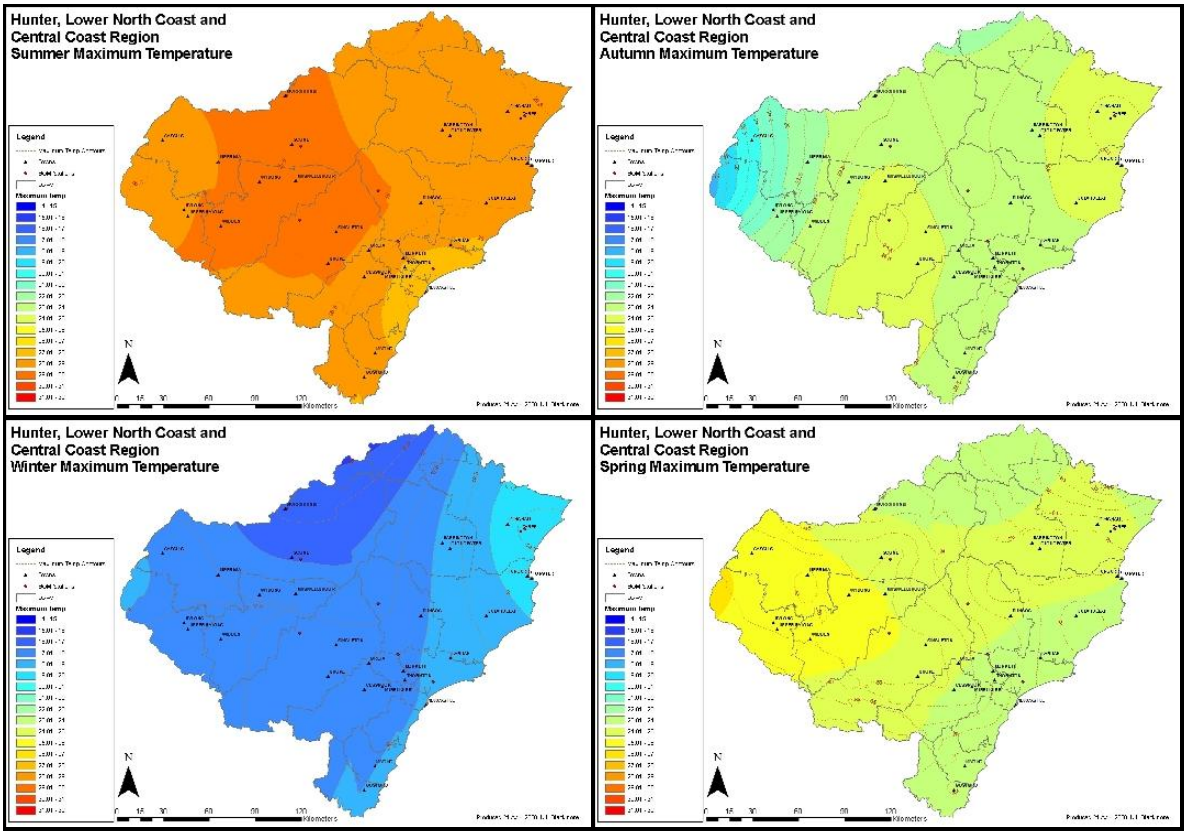

Figure 5.5. Average Seasonal (summer, autumn, winter, spring) Maximum Temperature (°C) in the Hunter, Lower North Coast and Central Coast Region

The average monthly maximum temperature is plotted against ST for the 3 sub-regions in Figure 5.6. The highest monthly maximum temperature in the coastal and central zones occurs during ST's 7 to 12. Maximum temperature in the western zone is also highest during ST's 7 to 12.

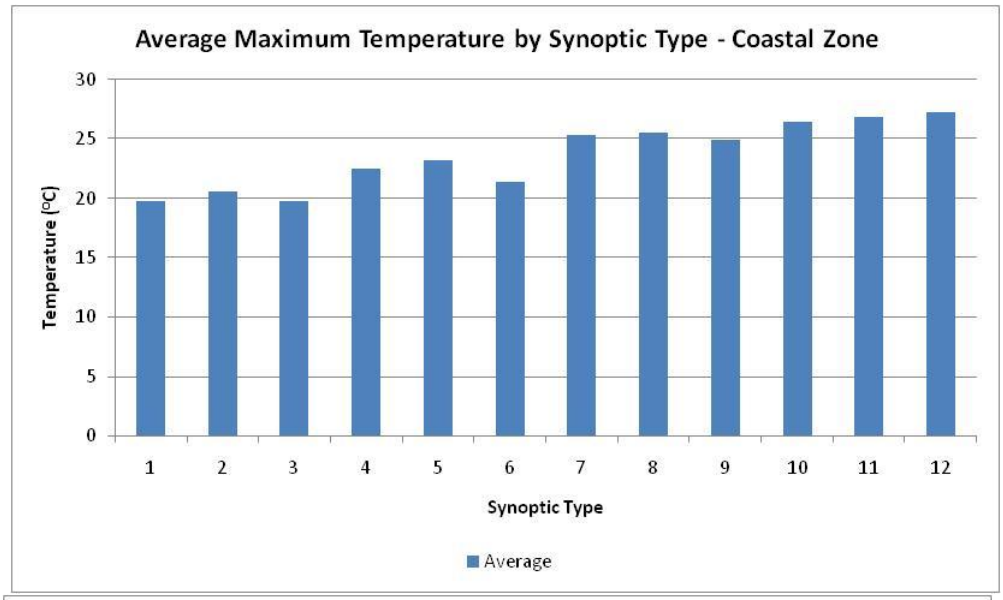

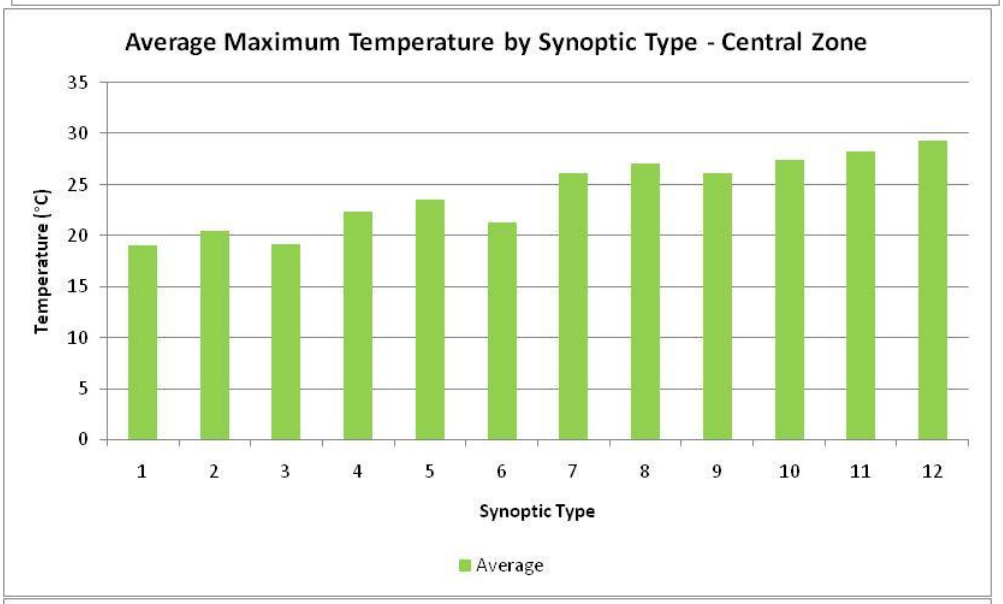

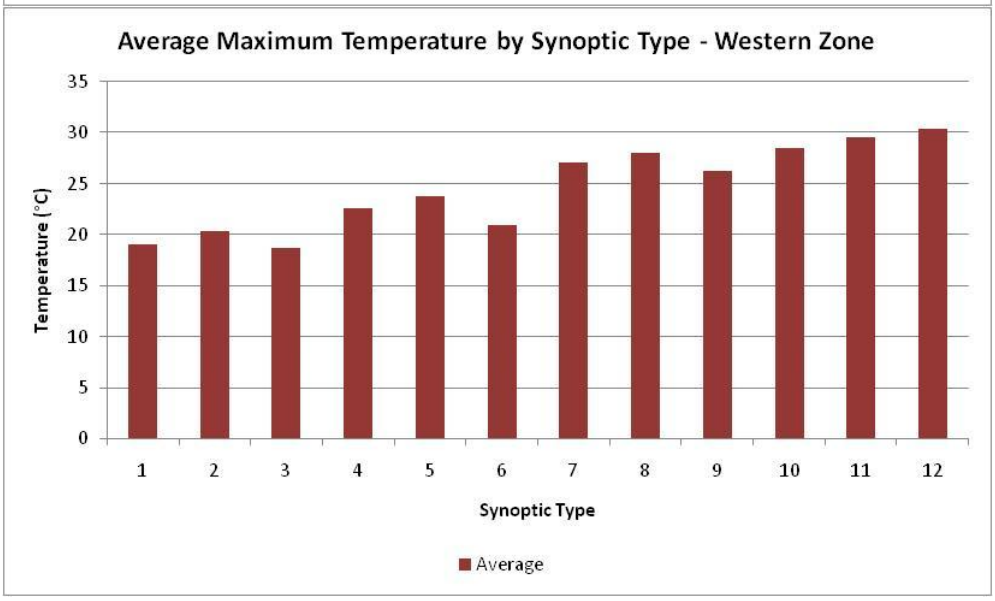

Figure 5.6. Average Maximum Temperature (°C) by Synoptic Type

The spatial distribution of annual mean minimum temperatures is significantly different to that of maximum temperatures. Annual mean minimum temperatures are highest along the coast, showing a gradual decrease to the west of the region. The region as a whole has an average annual minimum temperature of 11°C. The coastal area of the region averages 12.5°C, decreasing to 10.5°C through the central areas to lows of below 9°C in the far west. The coastal and terrain influences dominate; the latitudinal influence evident in the average annual maximum temperature spatial distribution does not impact. A clear longitudinal effect is evident (Figure 5.7).

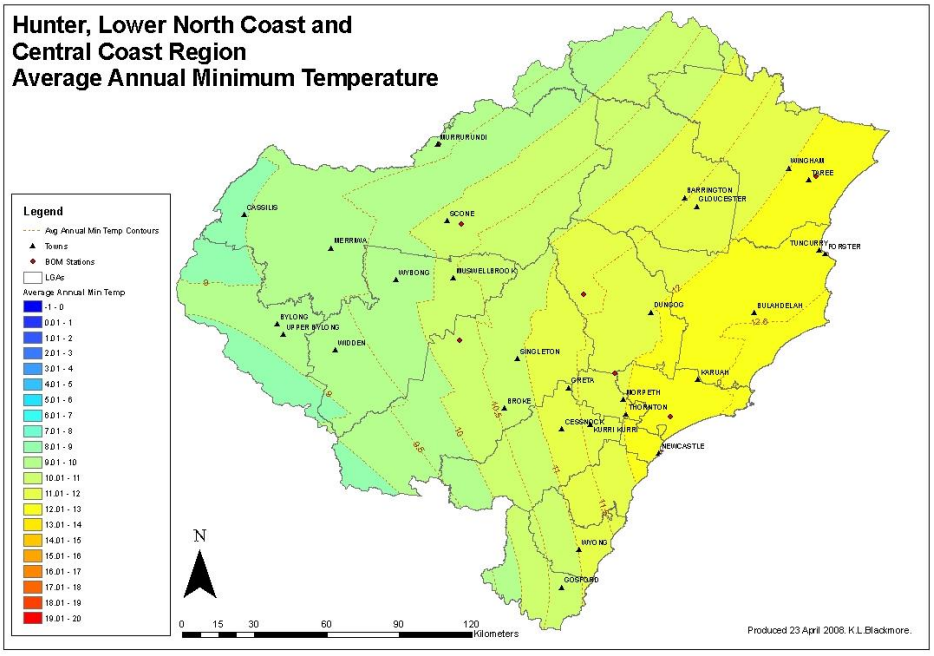

Figure 5.7. Average Annual Minimum Temperature (°C) in the Hunter, Lower North Coast and Central Coast Region

Seasonal average minimum temperatures show a clear coastal influence throughout the year (Figure 5.8). Whereas prevailing sea breezes aid in keeping maximum temperatures down during the summer months, the lower elevations along the coast impact on average minimum temperatures. This results in warmer coastal temperatures throughout all seasons. Summer minimum temperatures average 16.7°C, however this varies from 14°C in the west of the region (Murrurundi) to just over 19°C on the coast (Nobby's Head at Newcastle). Autumn sees average minimum temperatures reduced to 11.8°C, with winter average minimum temperatures for the region down to 5.4°C. Individual daily minima below 0°C are common in the west of the region during winter.

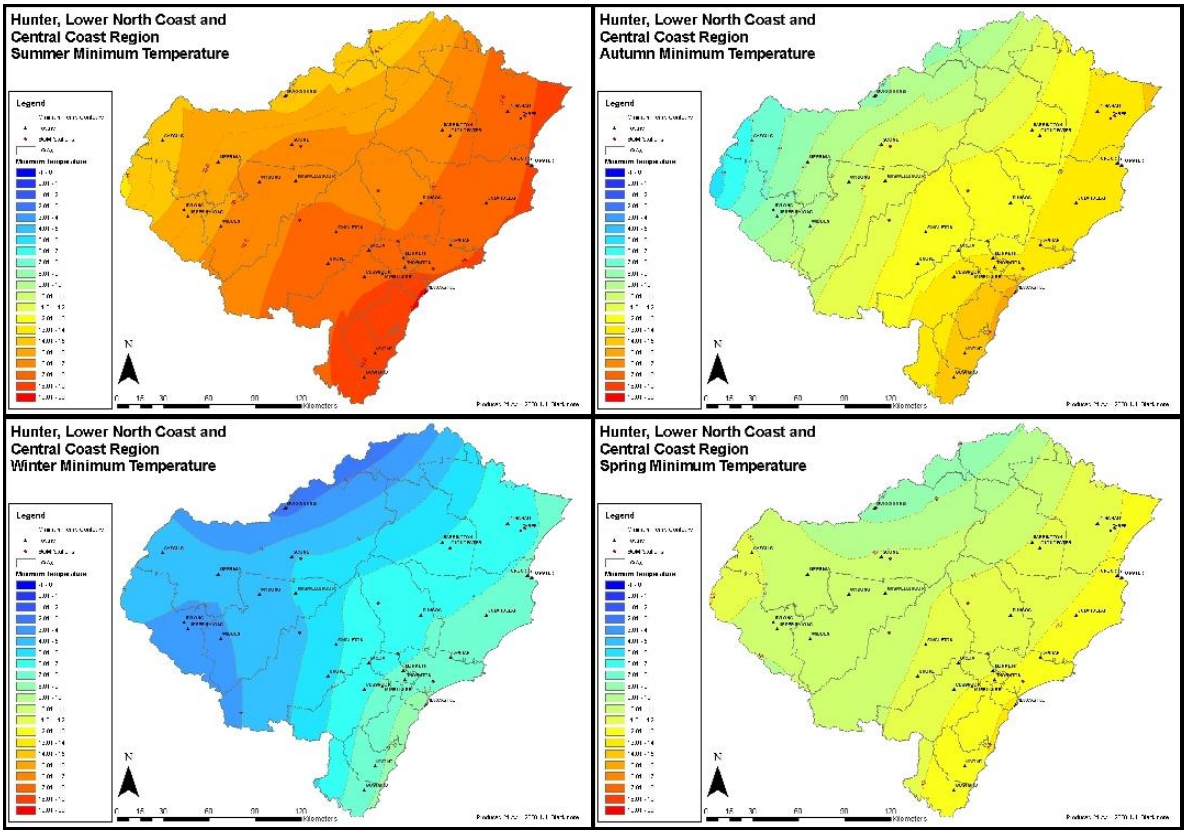

Figure 5.8. Average Seasonal (summer, autumn, winter, spring) Minimum Temperature (°C) in the Hunter, Lower North Coast and Central Coast Region

The average monthly minimum temperature is plotted against ST for the 3 sub-regions in Figure 5.9. The highest monthly minimum temperature in the coastal, central and western zones occurs during ST's 10 to 12. The lowest minimum temperatures occur during ST's 1 to 3 and 6.

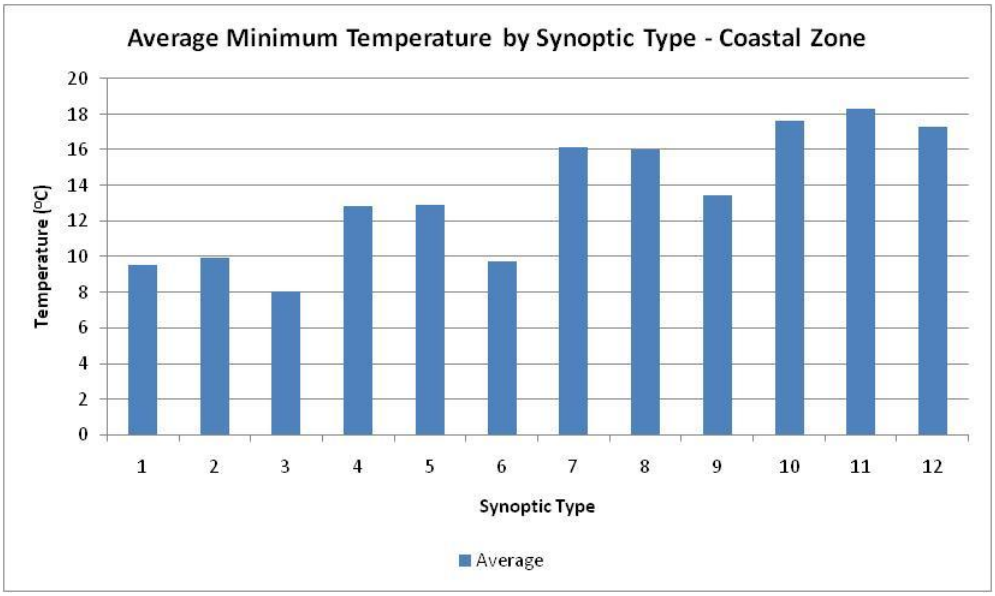

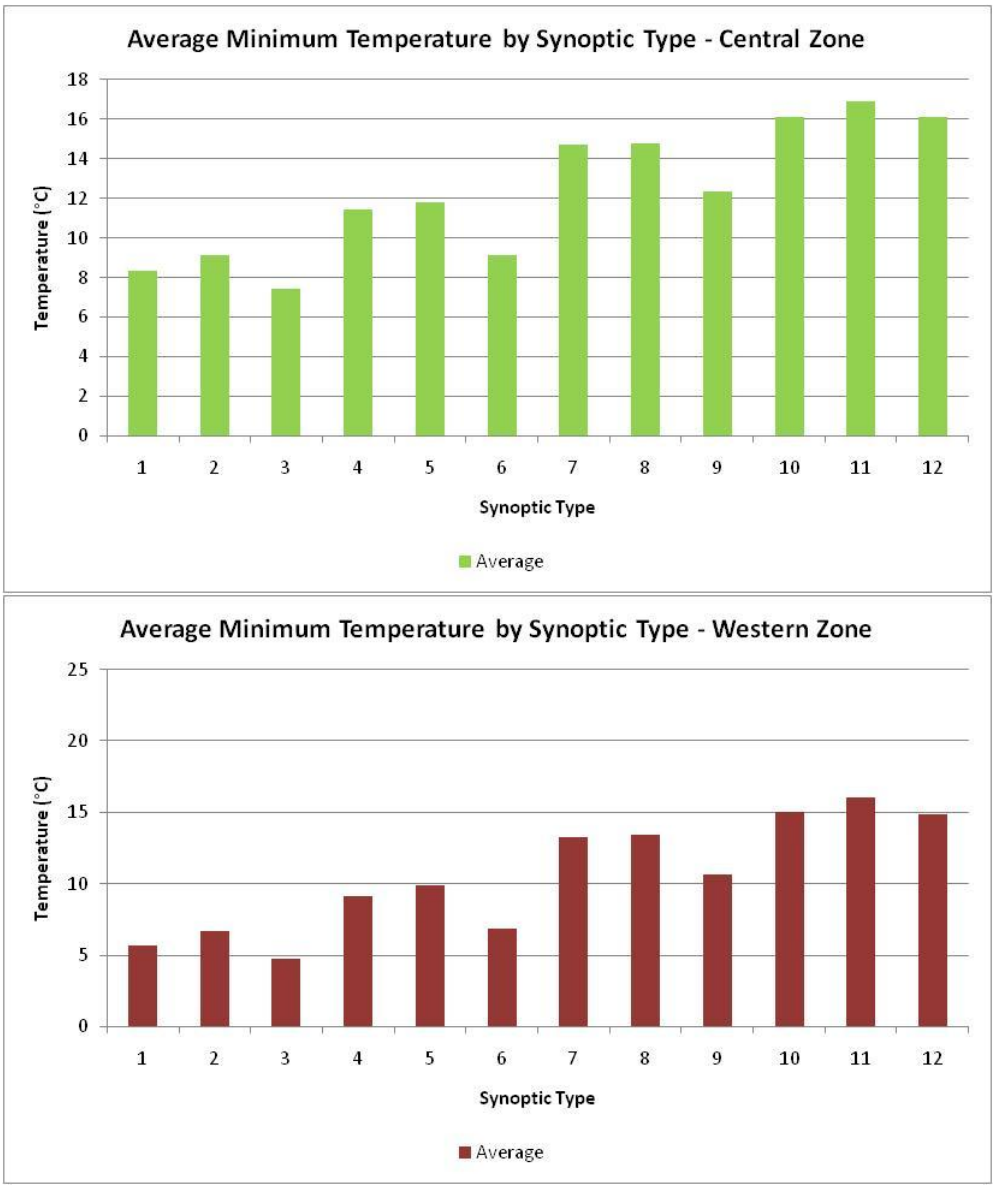

Figure 5.9. Average Minimum Temperature (°C) by Synoptic Type

5.1.3 Average Wind Speed and Maximum Wind Gust

Directional information for average daily wind speed records are not available, limiting the ability to visualise the data over the region in map form. Seasonal and annual averages for stations in the study region and buffer zone are calculated and presented in Table 5.1 (refer to Figure 2.6 for a map showing the location of the recording stations). Annual average wind speeds show a distinct coastal influence, which decreases inland. In winter, winds along the coast and in the central areas of the region increase, presumably under dominant westerly trends. This trend continues through to the end of spring.

		AVERAGE DAILY WIND SPEED (KM/H)				
STATION NO.	STATION NAME	SUMMER	AUTUMN	WINTER	SPRING	ANNUAL
55049	QUIRINDI	4.45	3.02	2.61	4.08	3.54
55136	WOOLBROOK	8.85	8.03	7.95	10.01	8.71
60026	PORT MACQUARIE	13.88	12.40	12.33	15.03	13.41
60085	YARRAS	7.53	5.76	6.64	9.03	7.24
61051	MURRURUNDI	7.71	6.32	7.06	8.77	7.47
61055	NEWCASTLE	27.09	24.64	26.42	28.13	26.57
61078	WILLIAMTOWN	14.17	11.10	14.09	14.59	13.49
61086	JERRY'S PLAINS	10.92	9.55	10.96	12.01	10.86
61089	SCONE	10.28	8.44	9.34	11.32	9.85
61250	PATERSON	9.94	8.46	12.93	13.10	11.11
61288	LOSTOCK DAM	5.94	6.55	10.55	8.87	7.98
62013	GULGONG	8.73	6.64	7.56	9.80	8.18
64009	DUNEDOO	17.50	14.55	12.83	16.48	15.34
66037	SYDNEY AIRPORT	16.23	12.48	12.68	15.77	14.29
67033	RICHMOND	9.38	6.33	7.14	9.95	8.20
	AVERAGE:	11.51	9.62	10.74	12.46	11.08

Table 5.1. Seasonal and annual average daily wind speed.

The average wind speed is plotted against ST for the 3 sub-regions in Figure 5.10. In the coastal zone, little variation in average wind speed occurring under each of the synoptic types is evident. The central and western parts of the region exhibit similar average wind speeds, with ST's 6 and 9 highest.

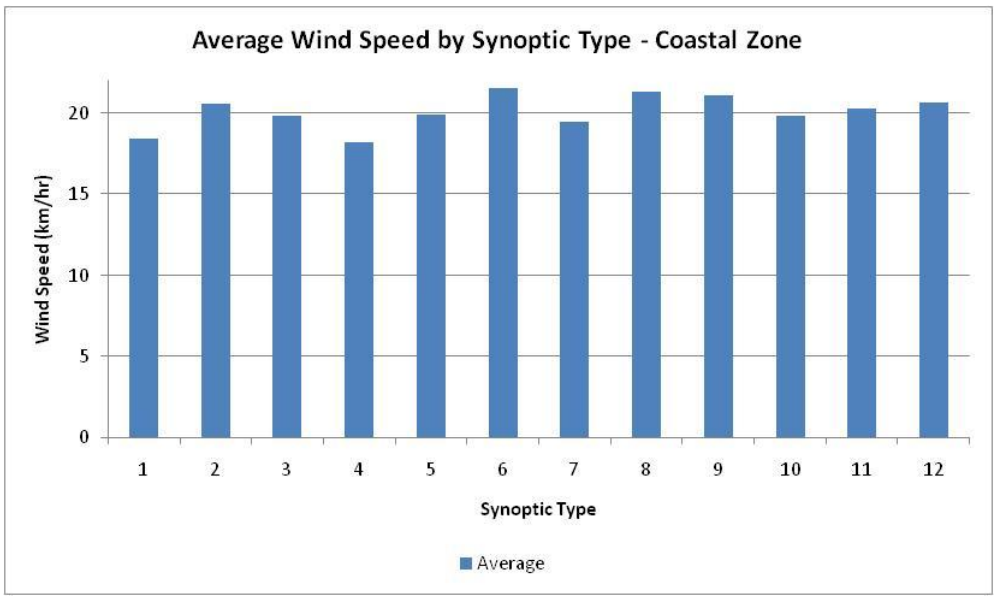

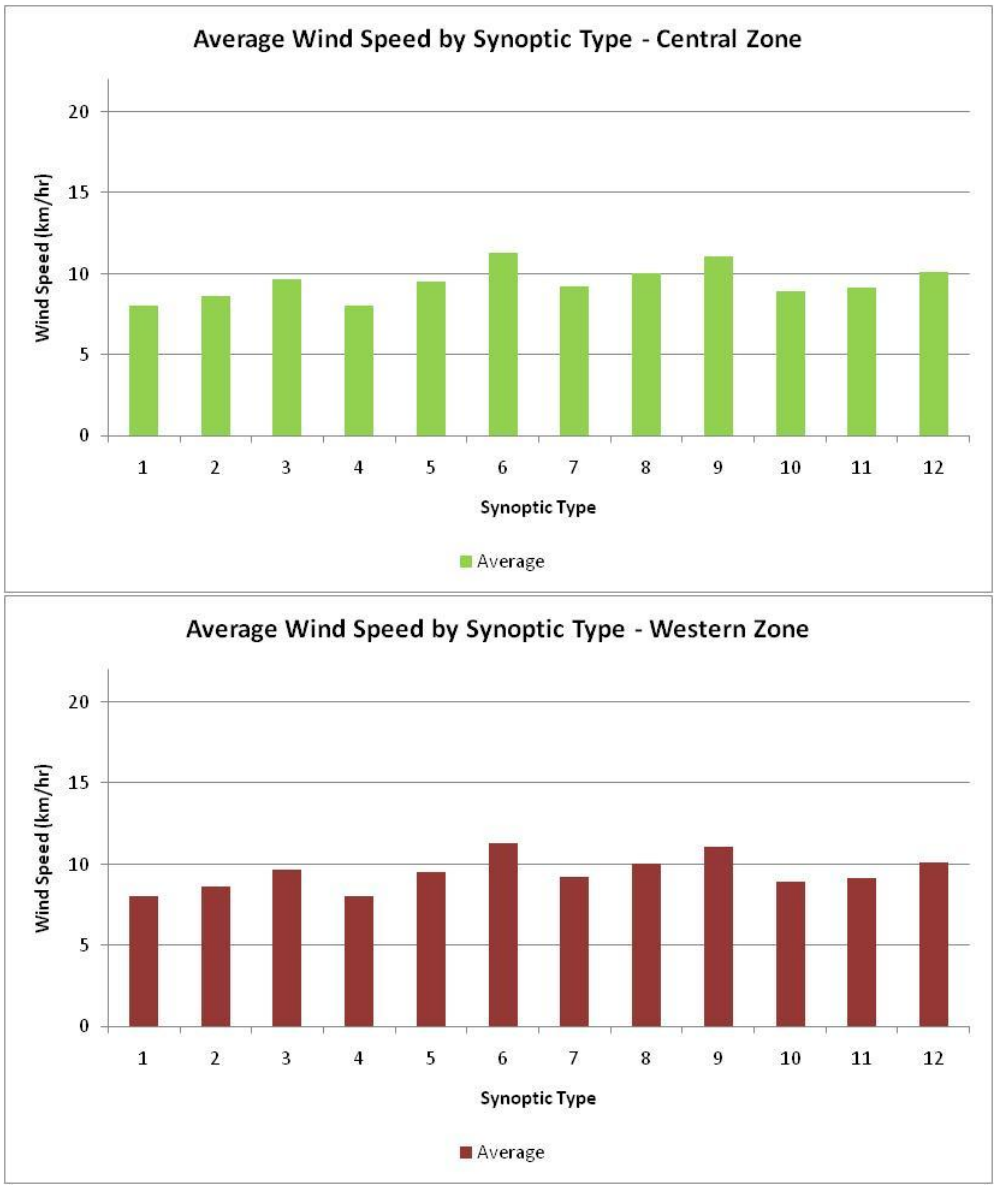

Figure 5.10. Average Wind Speed (km/hr) by Synoptic Type

Suitable (i.e. of a sufficient duration) maximum wind gust data is available from only one station in the study region. As such, spatial interpolation from point source data is not possible. Although wind gust station data records from Williamtown RAAF begin 1/10/1942, consistent recording of data does not commence until 1/10/1956. Maximum wind gusts average 44km/hr during summer from a south easterly direction. Autumn and spring wind gusts tend southerly (37.5km/hr and 45.7km/hr respectively). Winter winds tend south westerly with average gusts at 42km/hr. The wind rose diagram in Figure 5.11 clearly shows the dominance of the westerly wind gusts in the region.

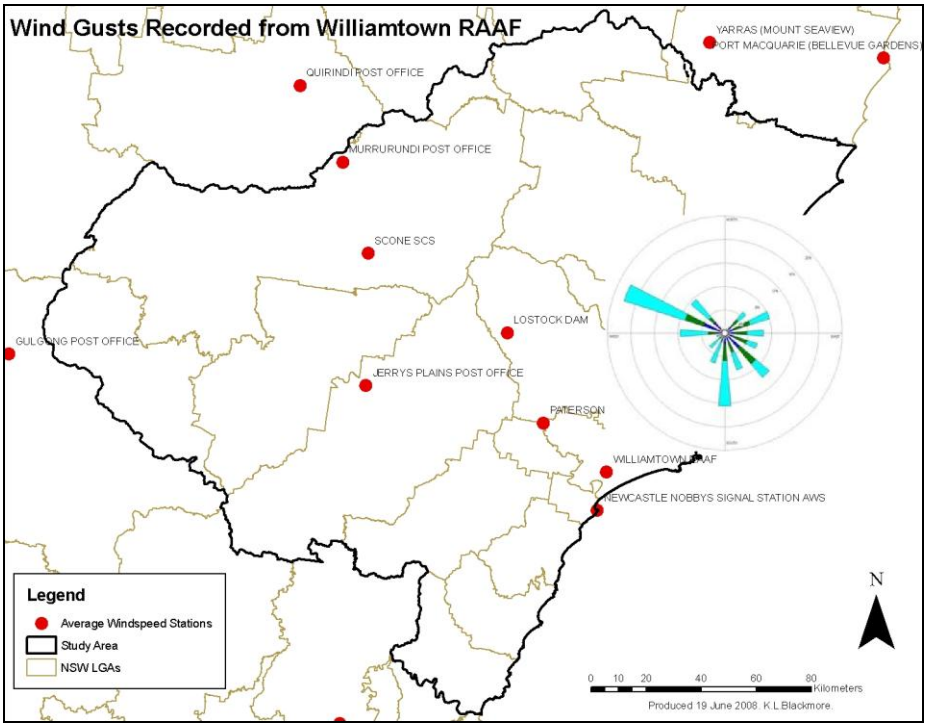

Figure 5.11. Wind rose diagram of wind gusts recorded from Williamtown RAAF.

The maximum monthly wind gust is plotted against ST Figure 5.12. The highest average monthly wind gusts occur during ST's 7, 9 and 12. Note though that variability in maximum wind gusts is high. The highest maximum wind gusts are recorded under ST's 3 and 6.

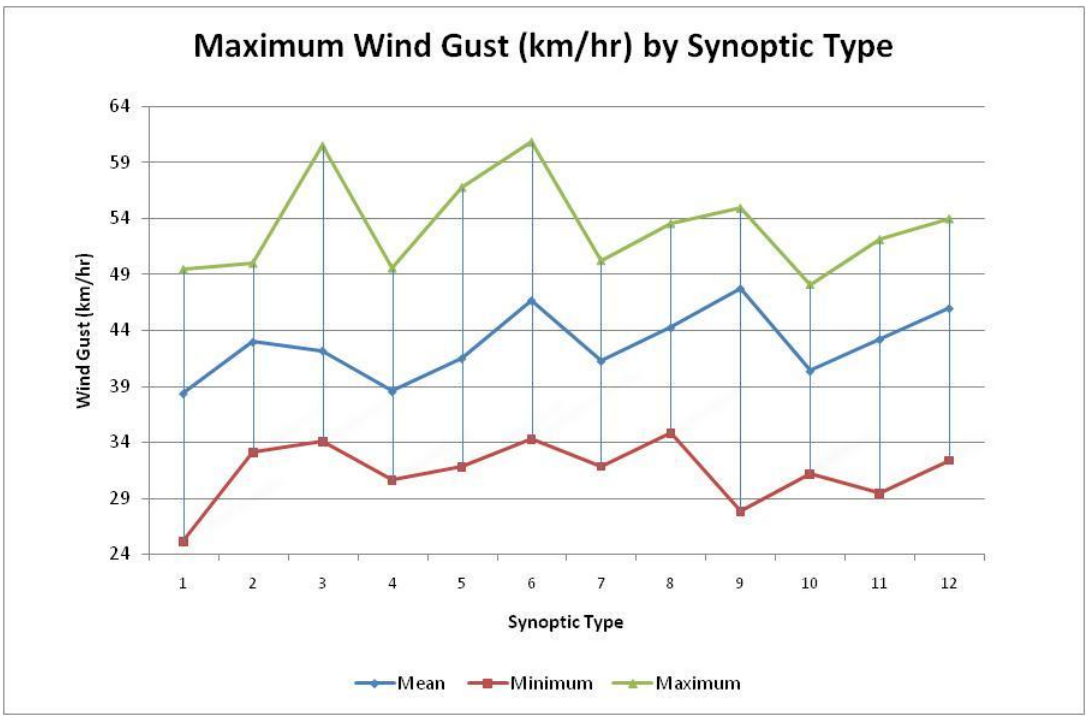

Figure 5.12. Maximum Wind Gust (km/hr) by Synoptic Type (recorded at Williamtown).

5.1.4 Pan Evaporation

Limited station data for the region results in incomplete spatial coverage for the interpolated pan evaporation surfaces. The generated surfaces do provide some insight into the sub-regional distribution and season variability of pan evaporation for the region however. Pan evaporation is measured in millimetres per 24 hours and combines the effects of a number of climate variables (i.e. temperature, humidity, solar radiation and wind). From the available data, on average annual pan evaporation is highest along the coast (Williamtown) at 4.7mm/24hr and in the west of the region (Scone) at 4.5mm/24hr (Figure 5.13). The central areas record the lowest average annual pan evaporation at 3.7mm/24hr (Cessnock).

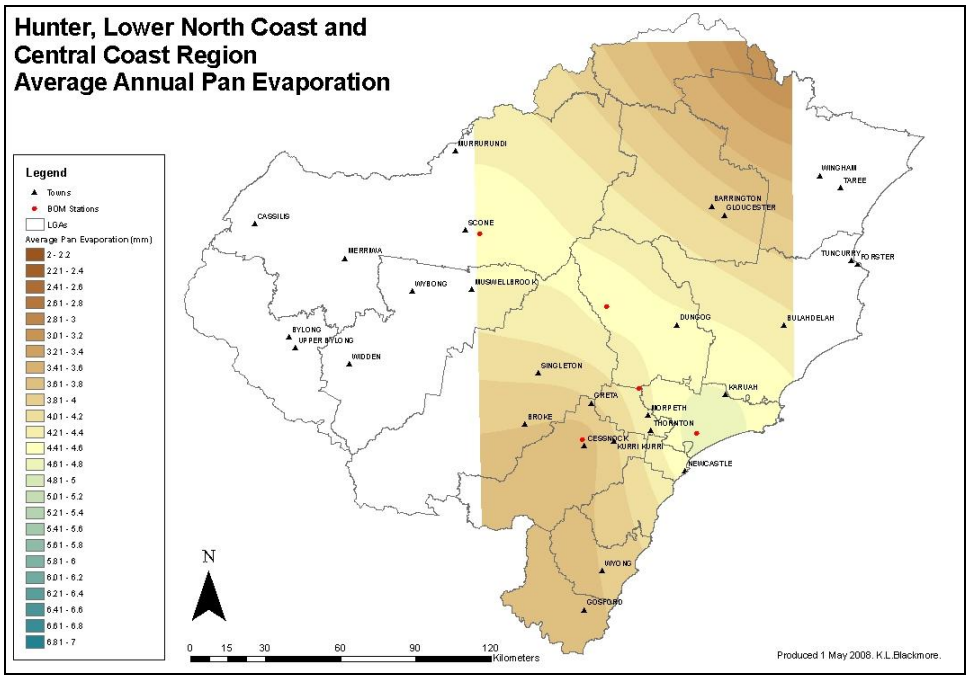

Figure 5.13. Average Annual Pan Evaporation (mm/24hr) in the Hunter, Lower North Coast and Central Coast Region

Strong seasonal variations in pan evaporation are evident (Figure 5.14), with spring and summer seasons recording higher average evaporation than the autumn and winter seasons. Very little variability occurs during winter, with average pan evaporation of 2.3mm/24hr. In contrast, summer averages 6mm/24hr across the region, ranging from a maximum of 6.9mm/24hr in the west (Scone) to 5.5mm/24hr in the Cessnock area.

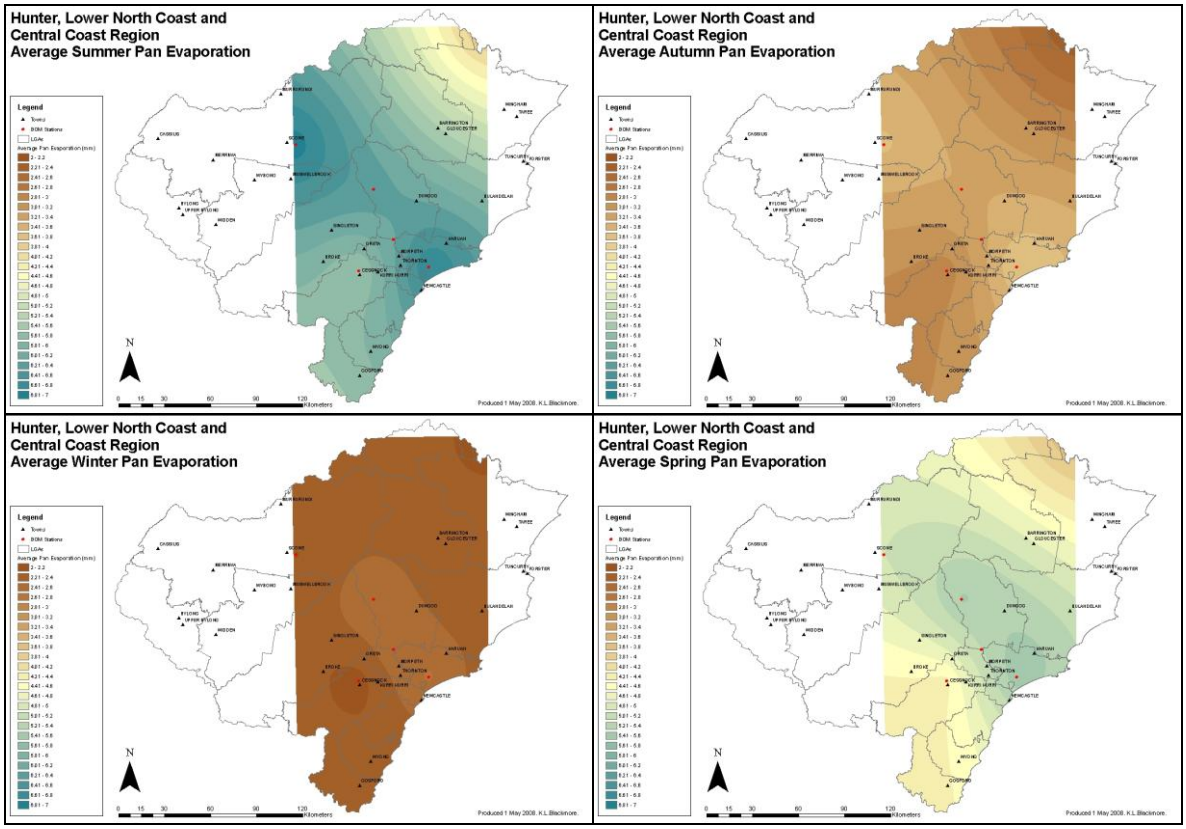

Figure 5.14. Average Seasonal (summer, autumn, winter, spring) Pan Evaporation (mm/24hr) in the Hunter, Lower North Coast and Central Coast Region

The average monthly evaporation is plotted against ST for the 3 sub-regions in Figure 5.15. The highest average monthly evaporation in all zones occurs during ST's 8, 9 and 12. Average monthly evaporation is lowest during ST's 1 and 3.

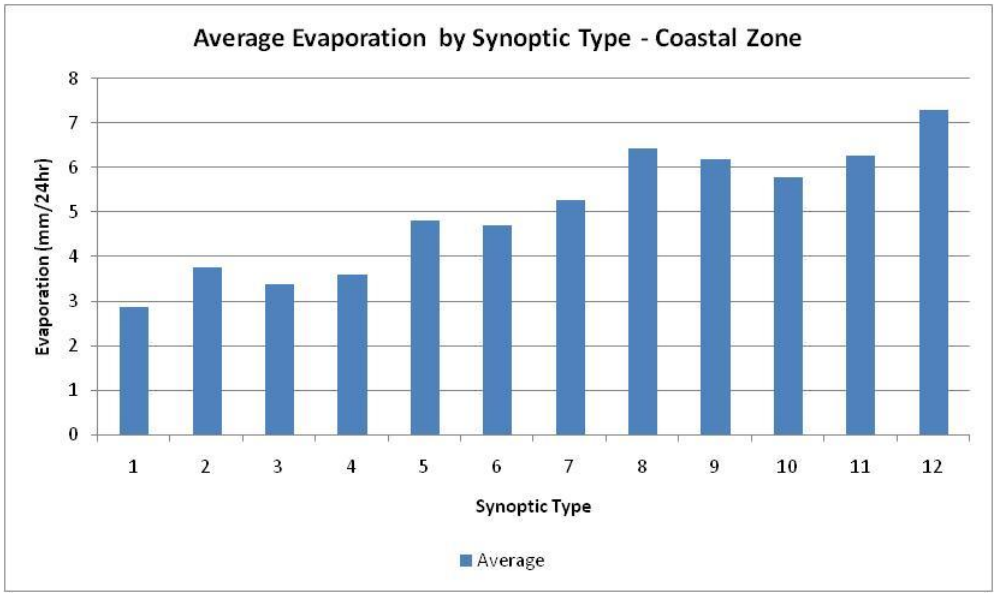

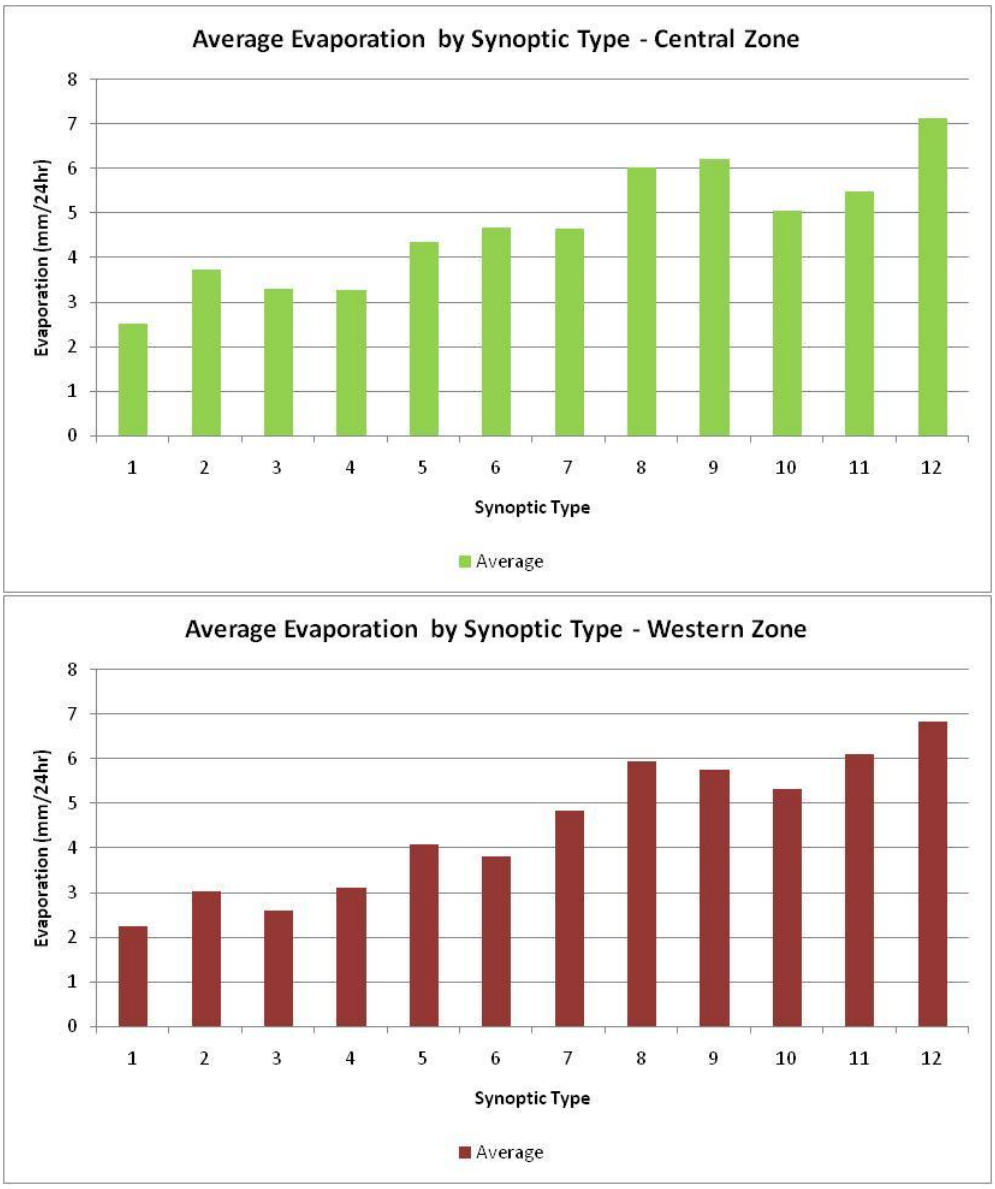

Figure 5.15. Average Pan Evaporation (mm/24hr) by Synoptic Type

5.1.5 3 Hourly Temperature and Humidity

A number of issues exist with this data set that limits the ability to provide a full analysis of spatial variability. The regularity that three (3) hourly temperature and humidity data is recorded varies widely within and across stations. For example, not all stations record data at the same 3 hourly intervals and data not available for a given day/time is completely omitted from the data set. Thus, two time intervals (9am and 3pm) were selected for the analysis, and all available station data for these times was included from January 1970 to April 2007.

	Average 9am Temperature (°C)							
	Port Macquarie	Taree	Yarras	Newcastle	Jerrys Plains	Scone	Paterson	Lostock Dam
Annual	18.24	17.76	16.68	17.19	17.25	16.77	17.55	15.78
Summer	22.52	22.44	21.15	21.42	22.80	22.17	22.29	20.49
Autumn	18.90	18.27	17.19	18.07	17.65	16.99	17.86	15.88
Winter	12.90	12.10	11.01	11.85	10.45	10.38	11.85	10.26
Spring	18.82	18.70	17.51	17.35	18.32	17.83	18.44	16.65

Table 5.2. Average annual and seasonal temperatures recorded at 9am

	Average 3pm Temperature (°C)					
	Port Macquarie	Taree	Yarras	Newcastle	Jerrys Plains	Paterson
Annual	21.44	22.89	22.85	20.14	23.68	22.61
Summer	24.86	27.36	27.21	23.11	29.51	27.76
Autumn	22.30	23.30	22.75	21.10	23.92	22.80
Winter	17.87	18.42	17.98	16.69	17.43	14.35
Spring	20.85	22.93	23.59	19.63	22.98	22.98

Table 5.3. Average annual and seasonal temperatures recorded at 3pm

Average annual temperatures recorded at 9am range from 15.8°C to 18.2°C, with coastal areas expectedly tending warmer than inland parts of the region (Table 5.2). These variations are due to coastal influences and terrain elevation. This trend is more significant during autumn and winter. Average annual temperature recorded at 3pm shows a reverse trend, with inland areas recording slightly higher temperatures (Table 5.3).

Season variations in 9am and 3pm temperatures are evident across the region (Tables 5.3 and 5.4). Average seasonal temperatures at 9am vary significantly across seasons, however very little spatial variation across the region is evident within seasons. Average summer temperatures at 3pm range from 23.1°C at Newcastle to 29.5°C at Jerrys Plains. Variations in 3pm temperatures across the region are reduced during autumn and spring, with some spatial variation evident through winter. These seasonal variations are consistent for temperature recorded at 9am and 3pm (Figure 5.16).

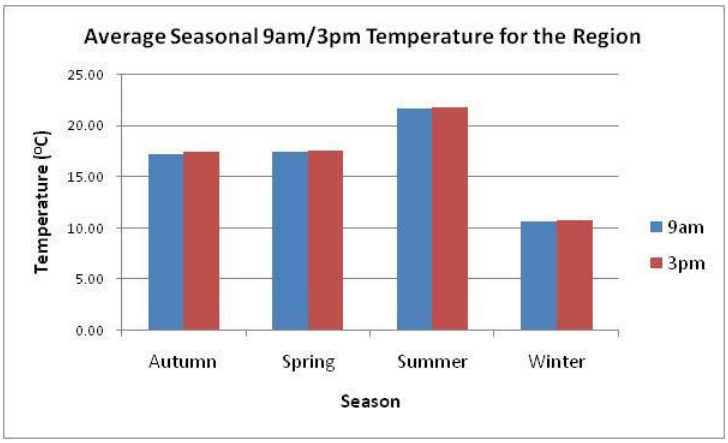

Figure 5.16. Average seasonal 9am/3pm regional temperature

Annual average relative humidity at 9am ranges from 69% at Scone through to 77% at Newcastle and Lostock Dam (Table 5.4). Generally, relative humidity in the region is highest along the coast, with the west of the region showing no spatial variation (Bridgman, 1984). Seasonal variations in humidity at 9am are lowest along the coast. Regional 9am humidity is highest during autumn (average of 78%), decreasing by 2.5% during winter and again during summer, to lowest levels during spring (average of 66%).

	Average 9am Humidity (%)					
	Port Macquarie	Newcastle	Jerrys Plains	Scone	Paterson	Lostock Dam
Annual	74.25	76.77	71.20	69.05	72.92	77.06
Summer	77.57	79.85	69.20	67.95	73.68	78.29
Autumn	78.09	79.60	75.15	73.20	78.72	82.29
Winter	72.86	76.12	77.29	73.65	74.38	77.86
Spring	68.53	71.32	62.87	61.03	64.74	69.71

Table 5.4. Average annual and seasonal relative humidity recorded at 9am

	Average 3pm Humidity (%)			
	Port Macquarie	Newcastle	Jerrys Plains	Paterson
Annual	65.02	67.10	47.03	52.94
Summer	70.31	74.18	45.64	52.13
Autumn	66.65	69.17	50.13	57.89
Winter	58.02	59.60	49.89	53.62
Spring	65.29	65.35	42.30	47.93

Table 5.5. Average annual and seasonal relative humidity recorded at 3pm

Both within and across season variations occur in relative humidity in the region. (Figure 5.17). While spring is associated with the lowest levels of relative humidity in the region (65.8% at 9am and 52.9% at 3pm), the greatest differential between 9am and 3pm recordings occurs during winter. Relative humidity reduces by 21.5% between 9am and 3pm during winter, compared to 15.5%, 18.0% and 12.9% for summer, autumn and spring respectively.

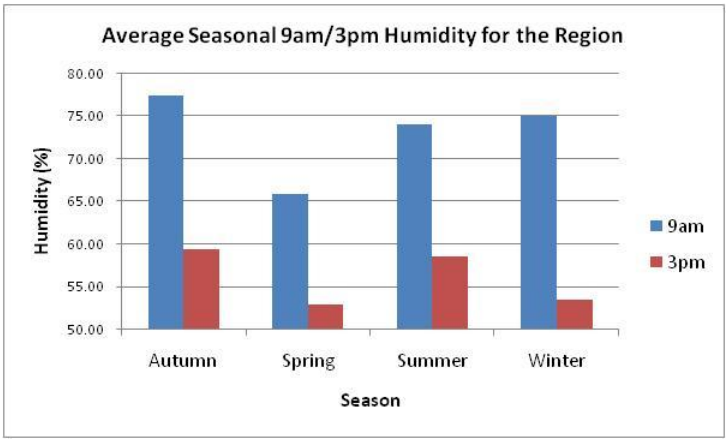

Figure 5.17. Average seasonal 9am/3pm regional relative humidity

The average relative humidity is plotted against ST for the region in Figure 5.18. Sub-regional analysis is not possible due to the limited number of recording stations available. The highest monthly 9am humidity occurs during ST's 1, 10 and 11. 3pm humidity for the region is highest during ST's 4, 7, 10 and 11.

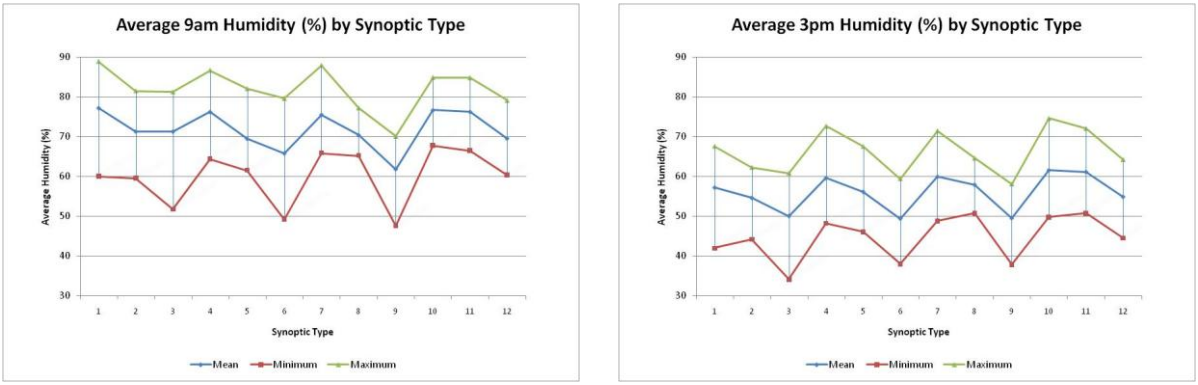

Figure 5.18. Average Relative Humidity Recorded at 9am and 3pm by Synoptic Type

5.1.6 Sea Surface Temperature

The SOMS methodology was also conducted on the NOAA extended monthly Sea Surface Temperature (SST) data, to produce a monthly time series of 12 SST anomaly types. Figure 5.19 shows the spatial patterns for each type. These types will be used in Stage 3 of the project to assess the future projections for climate change. However, an analysis of the interdecadal variability between the two IPO phases was undertaken. The seasonal SST anomalies for summer and winter in °C for the difference between IPO phase circulations (1977 to 2007 minus 1949 to 1976) are shown in Figure 5.20. The seasonal SST's off the NSW central and south coasts were up to 0.5°C warmer during the 1977 to 2007 period, which has been related to the shift in El Nino-like climate and to the observed changes in the ocean dynamics associated with the increase in the East Australian Current flow (Ridgway, 2007; Cai, et al. 2005).

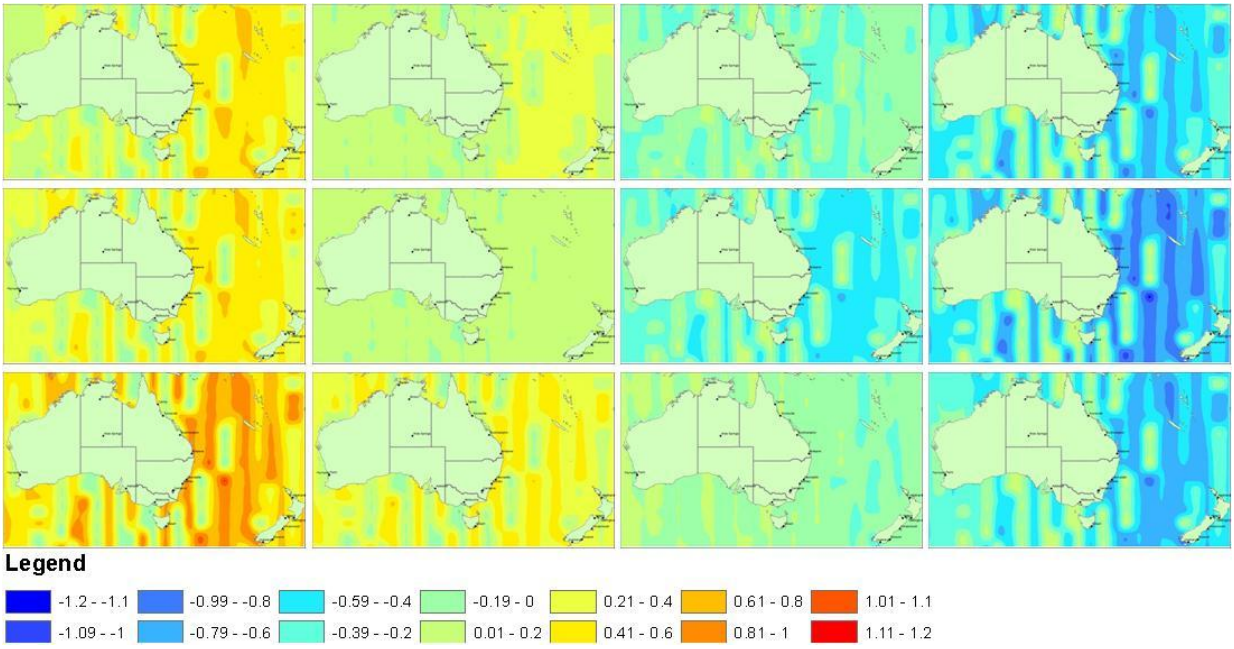

Figure 5.19. Key synoptic sea surface temperature anomaly types derived using the SOM methodology. Anomalies are shown as a + or – deviation from the seasonal mean in °C.

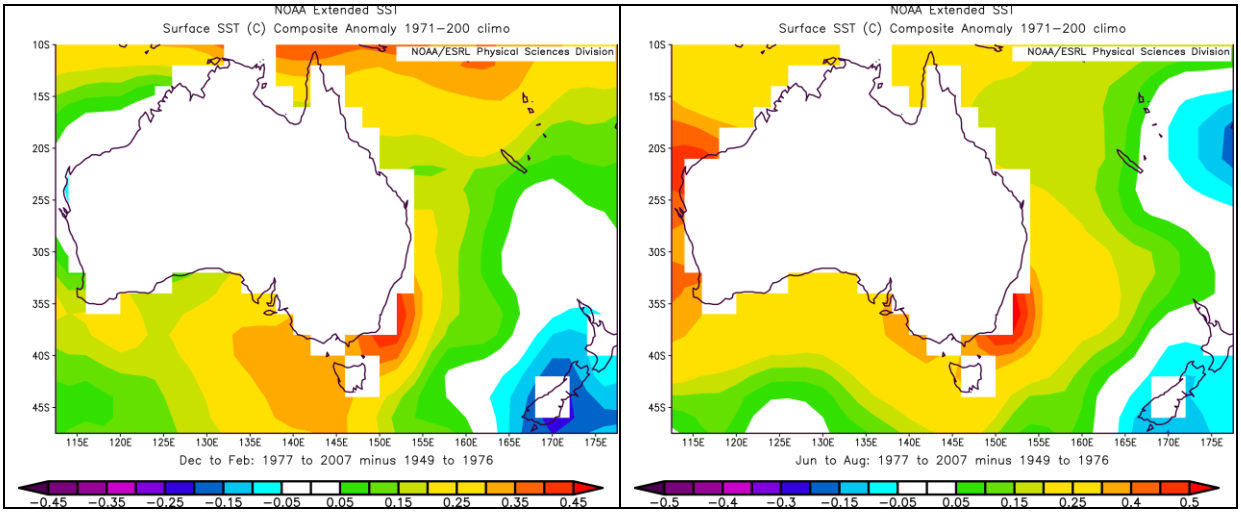

Figure 5.20. shows the seasonal SST anomalies in °C for the difference between IPO phase circulations (1977 to 2007 minus 1949 to 1976), (a) summer, and (b) winter.

5.1.7 Sea-Level Rise and Extreme Sea Levels

Relative sea level has risen by 0.1 to 0.15 m along the east coast of Australia over the past 150 years (Church et al., 2004). The annual mean monthly relative sea-level time series from Fort Denison, Sydney Harbour is shown in Figure 5.21. Superimposed on the trend in sea-level rise are the observed interannual fluctuations of between ± 0.05 to ±0.075 m due to both the El Nino-Southern Oscillation (ENSO) and the Interdecadal Pacific Oscillation (IPO) phenomena (Goodwin, in prep). The high (and low) sea-level anomalies occur during La Niña (El Niño) climate phases. Hence, mean annual sea level along the Central, Hunter and Lower North Coast NSW can vary by as much as 0.150 m between years, without any long-term trend in sea level (Figure 5.22). The annual mean sea-level time series from Newcastle Harbour is shown in Figure 5.23 for the shorter time period from 1966 to 2006, and shows a sea-level rise of 1.15 mm/year.

The return period of extreme sea levels due to storm surges and high waves during storm events is an important consideration for coastal management. The storm systems that produce these elevated sea levels are East Coast lows, Southern Secondary Lows or cut-off lows and southward moving tropical cyclones. Church et al. (2004) found that extreme sea levels were 2-3 times more frequent in the period since 1950 when compared to the pre 1950 period, and that enhanced interannnual variability due to ENSO and the IPO was contributing to this. Lord and Kulmar (2000) calculated that the return period for severe storms such as those in 1974 was 1 in 70 years for peak wave height and 1 in 200 for extreme water level. The probability of such an event impacting t he central and mid-north coast NSW is higher during La Niña years in the ENSO cycle (You and Lord, 2007), and further increased during the La Nina-like phase of the IPO.

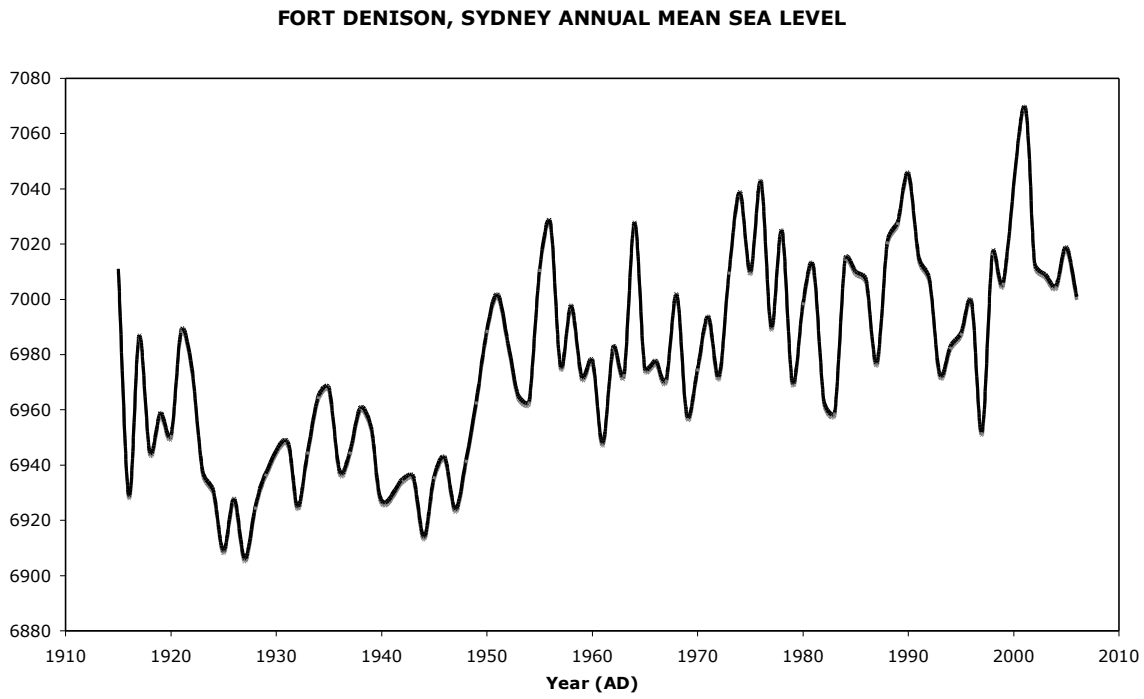

Figure 5.21. Annual Mean Sea Level Recorded at Fort Denison, Sydney

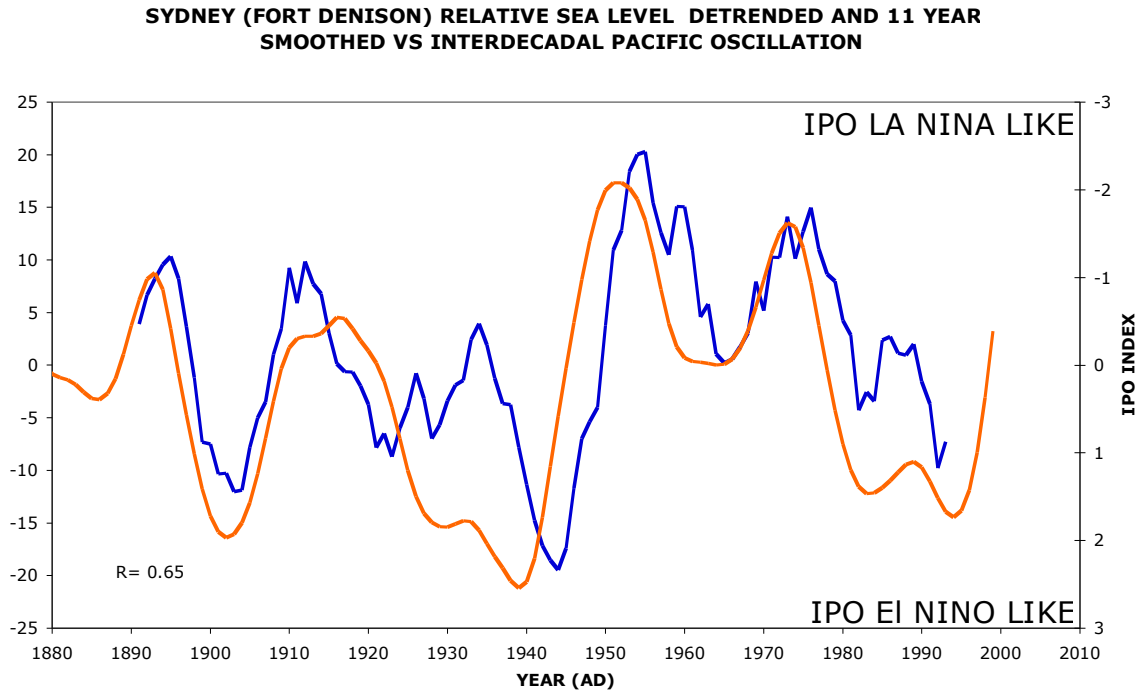

Figure 5.22. Relative Sea Level Detrended and 11 Year Smoothed Versus Interdecadal Pacific Oscillation Recorded at Fort Denison, Sydney

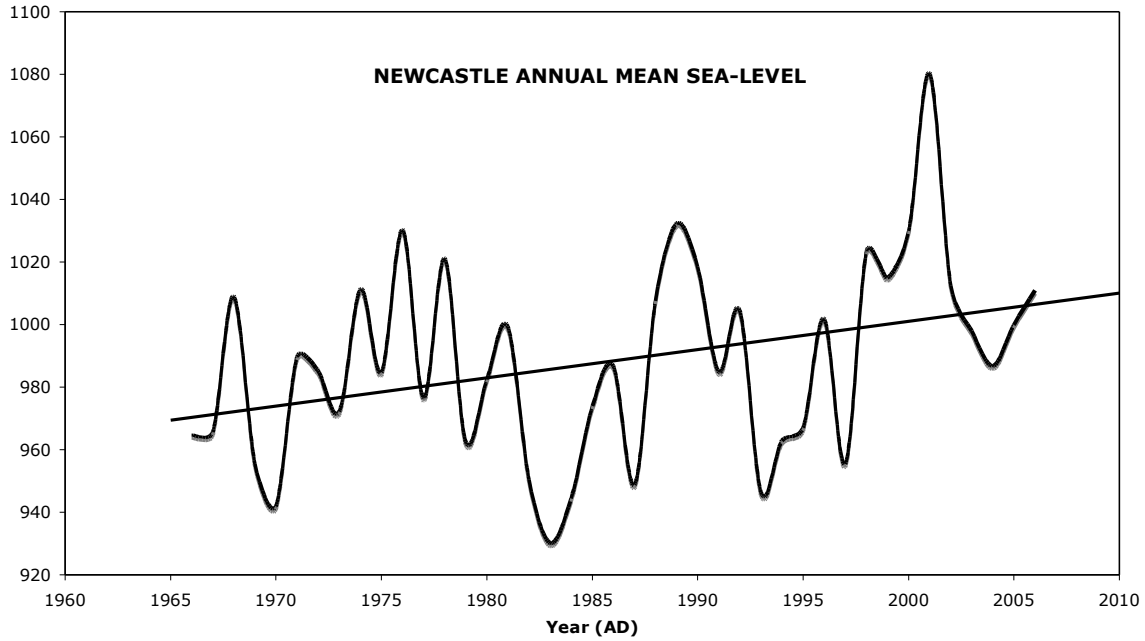

Figure 5.23. Annual Mean Sea Level Recorded at Newcastle.

5.1.8 Wave Climate

Comparison of wave direction records measured by waverider buoys at Sydney and Crowdy Head show that the annual mean wave direction along the NSW coast is equivalent, with Sydney and Crowdy Head receiving waves from the SE to S direction 65.7% of the time respectively, and from the NNE to ESE, 33.3% of the time respectively (M. Kulmar, Pers. Comm., 2005, Manly Hydraulics Laboratory, NSW Department of Commerce).

Goodwin (2005) reported a hindcast mean wave direction time series for Sydney and the NSW coast, from 1878 to 2002. The monthly mid-shelf mean wave direction (MWD) time series for south-eastern Australia, is based on the monthly, Trans-Tasman mean sea-level pressure (MSLP) difference between northern NSW (Yamba) and the north island of New Zealand (Auckland). The MSLP index is calibrated to instrumental (Waverider buoy) MWD data for the Sydney shelf and coast. Positive/negative Trans-Tasman MSLP difference is significantly correlated to southerly/easterly NSW mean wave direction (MWD), and to long/short mean wave periods. The 124 year, NSW annual (MWD) time series, shown in Figure 5.24, displays multidecadal variability, and identifies a significant period of more southerly annual MWD during 1884 to 1914, than in the period since 1915. The NSW MWD is significantly correlated to the Southern Oscillation Index (SOI). The correlation with the SOI is enhanced during periods when the IPO is in its negative (La Nina-like) state and warm SST anomalies occur in the south-west Pacific region. The NSW MWD was found to be associated with Pacific basin-wide climate fluctuations associated with the El Niño-Southern Oscillation (ENSO). Southerly/easterly NSW MWD is correlated with low/high MSLP anomalies over New Zealand and the central Pacific Ocean. Southerly/easterly NSW MWD is also correlated with cool/warm SST anomalies in the south-west Pacific, particularly in the

eastern Coral Sea and Tasman Sea. Further work has shown that the variability of MWD on the Central, Hunter and Lower North Coasts is also significantly driven by fluctuations in the Southern Annular Mode (SAM) and its influences on the generation of northward propagating wave energy from the Southern Tasman Sea.

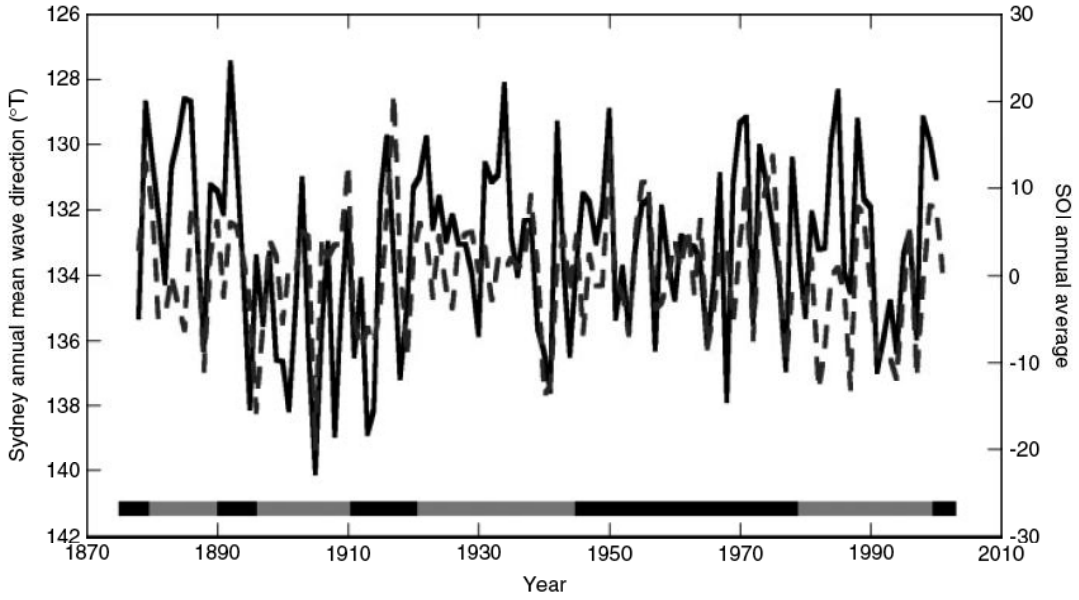

Figure 5.24. The hindcast annual MWD (solid line) plotted against the annual mean SOI (dashed line) for 1878 to 2001 (from Goodwin, 2005). Also shown in the bar at the bottom of the plot are the positive (grey) and negative (black) phases of the Interdecadal Pacific Oscillation (IPO).

Storm Frequency and Wave Climate

The Central, Hunter and Lower North Coasts of NSW receive storm wave energy from both tropical cyclones and from intense low pressure systems (known as East Coast Lows) over the southern Coral Sea and northern Tasman Sea. Significant wave heights at Sydney that are associated with East Coast Lows or Southern Secondary Lows can be in excess of 7 m. These high significant wave heights and the ensuing storm wave erosion are more frequent during the La Niña phases of the ENSO and IPO. The greatest number of significant storm events over the past century occurred during the IPO La Niña-like phase between 1950 and 1976. East Coast Lows and Southern Secondary Lows occur during the respective Synoptic Types1, 2 and 3.

Monthly Wave Climate and Synoptic Type

The monthly mean wave statistics (Significant Wave Height (Hsig), Maximum Wave Height (HMax), Peak Period (TP1), and Wave Direction (WD) (Sydney only) measured by waverider buoys off Sydney (July, 1987 to June, 2007) and Crowdy Head (1985-2007) were analysed to the corresponding monthly time series of Synoptic Types (ST). Mean wave statistics were then calculated for each monthly ST. Figure 5.25 shows the rose diagrams for significant

wave height and mean wave direction at Sydney for the 4 dominant seasonal ST 1, 7, 9 and 11. The wave statistics for the 12 ST's will be used in Stage 3 to assess the future projected changes in wave climate.

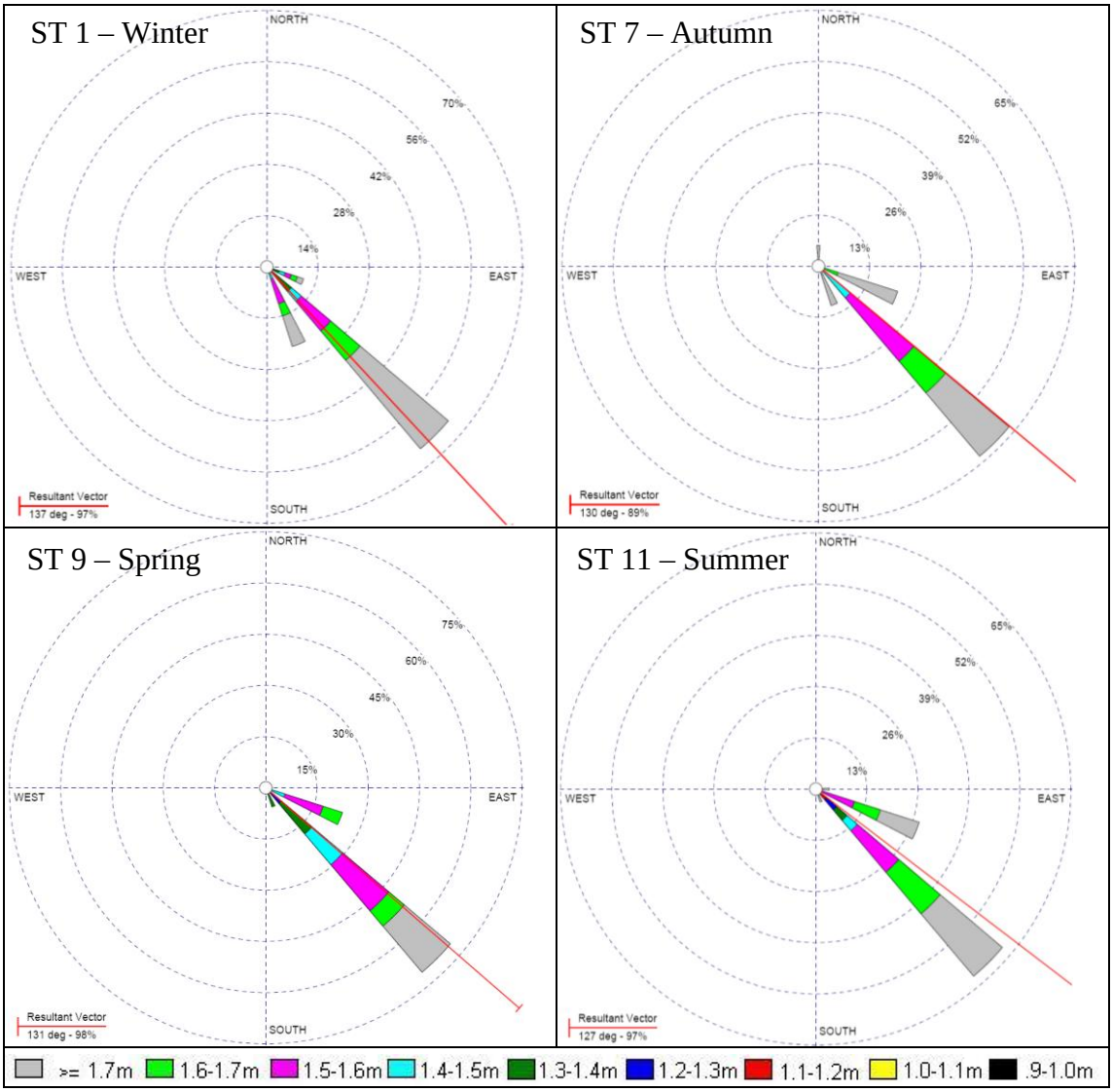

Figure 5.25. Rose diagrams for significant wave height and mean wave direction at Sydney for the 4 dominant seasonal ST.

5.2 Interannual and Interdecadal Variability

This section considers interannual and interdecadal[2] variability of key climate variables. Linear trend lines are shown on all graphs in this section; interdecadal variability graphs also include a ten year moving average (10 year MA). A 10 year MA is used to smooth out short-term fluctuations, thus highlighting longer-term trends or cycles.

[2] The time periods from 1948 to 1976 (29 years) and 1977 to 2007 (30 years) are contrasted where possible. The selection of these time periods is based on the IPO periods (see Section 4.3).

Linear trend lines are shown on all graphs in this section. The change occurring per annum (Change PA), the change occurring over the entire available time period (Total Change), the statistical significance of the linear trend as indicated by the r squared value (R^2) and the overall percentage change (%) for all variables are shown in Table 5.6. The r squared value is a statistical measure of fit of the linear trend line to the data points. An r squared value of 1.0 indicates a perfect fit; thus the closer to 0 the r squared value is, the less reliance can be placed on the statistical significance of the linear trend. Using the commonly accepted threshold of 0.7 to determine the "fit" of the trend to the linear trend line, no trends identified for the key climate variables are considered to be significant. A possible explanation for the lack of significance associated with the apparent linear trends in the key climate variables lies in inherent or natural variability.

	ALL YEARS					
Variable	Start	End	Change PA	Total Change	R^2	%
Precipitation	1948	2007	-3.33mm	-196.23mm	0.07	-19%
Max Temp	1970	2007	0.03°C	0.96°C	0.24	4%
Min Temp	1970	2007	0.01°C	0.22°C	0.02	2%
Pan Evap	1969	2007	-0.01mm/24hr	-0.27mm/24hr	0.06	-6%
Humidity (9am)	1970	2006	0.01%	0.36%	0.00	0%
Humidity (3pm)	1970	2006	-0.07%	-2.38%	0.10	-4%
	BEGINNING-1976					
Variable	Start	End	Change PA	Total Change	R^2	%
Precipitation	1948	1976	-5.38mm	-150.752mm	0.04	-14%
Max Temp	1970	1976	0.00°C	0.01°C	0.00	0%
Min Temp	1970	1976	0.11°C	0.65°C	0.16	6%
Pan Evap	1969	1976	-0.01mm/24hr	-0.08mm/24hr	0.01	-2%
Humidity (9am)	1970	1976	0.71%	4.24%	0.64	6%
Humidity (3pm)	1970	1976	0.17%	1.02%	0.08	2%
	1977-2007					
Variable	Start	End	Change PA	Total Change	R^2	%
Precipitation	1977	2007	-0.26mm	7.8mm	0.00	1%
Max Temp	1977	2007	0.02°C	0.60°C	0.11	3%
Min Temp	1977	2007	0.00°C	0.00°C	0.00	0%
Pan Evap	1977	2007	-0.02mm/24hr	-0.45mm/24hr	0.16	-11%
Humidity (9am)	1977	2006	-0.04%	-1.02%	0.02	-1%
Humidity (3pm)	1977	2006	-0.09%	-2.61%	0.10	-5%

Table 5.6. Statistics for interannual linear trends.

In addition to assessing the fit of the trends to the linear trend lines, a regression analysis

was conducted for each climate variable. Regression analysis provides a measure of the statistical significance of the linear trend known as a "p-value". Where the p-value is found to be less than 0.05, the linear trend is considered to be statistically significant. Linear trends found to be significant are reported in the text.

Average annual precipitation for the region varies between 550mm and 1700mm (Figure 5.26). The linear trend line shown in Figure 5.26 indicates a decrease in average precipitation over the January 1948 to December 2007 time period of 3.3mm per annum, or 200mm in total. Regression analysis suggests that this trend is statistically significant (p=0.03). Considering the interdecadal variability (Figure 5.27), a slight decrease in average rainfall is evident for the 1948-1976 time period, however no decrease is evident in the 1977-2007 time period.

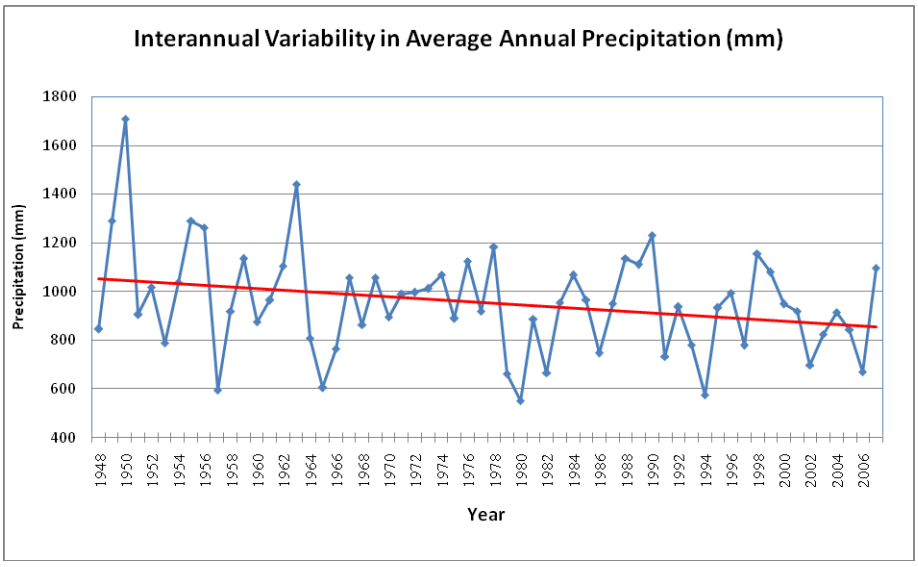

Figure 5.26. Interannual variability in average total annual precipitation (mm) showing linear trend.

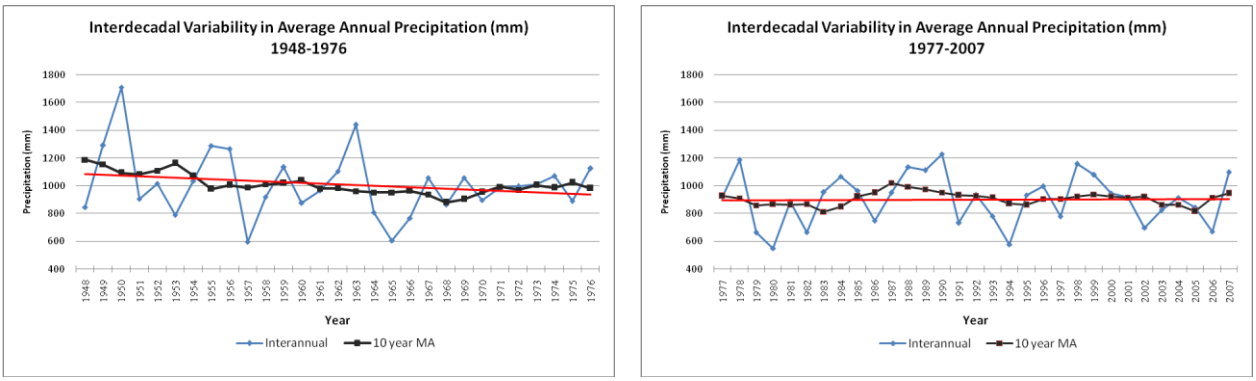

Figure 5.27. Comparison of average annual precipitation (mm) recorded by stations in the Hunter, Lower North Coast and Central Coast Region for the 1948-1976 and 1977-2007 time periods.

Figure 5.28 shows an increase in average annual maximum temperature during the period from 1970 to 2007. Average annual maximum temperatures for the region range between 22.2°C and 24.5°C. Limited data for the time period prior to 1977 makes interdecadal comparision difficult, however variability of average maximum temperatures post 1976 do appear to increase (Figure 5.29). Based on the available data for the time period from 1970 to 2007, an approximate 1°C increase in maximum average annual temperature has occurred in the region. This increase is statistically significant (p=0.0).

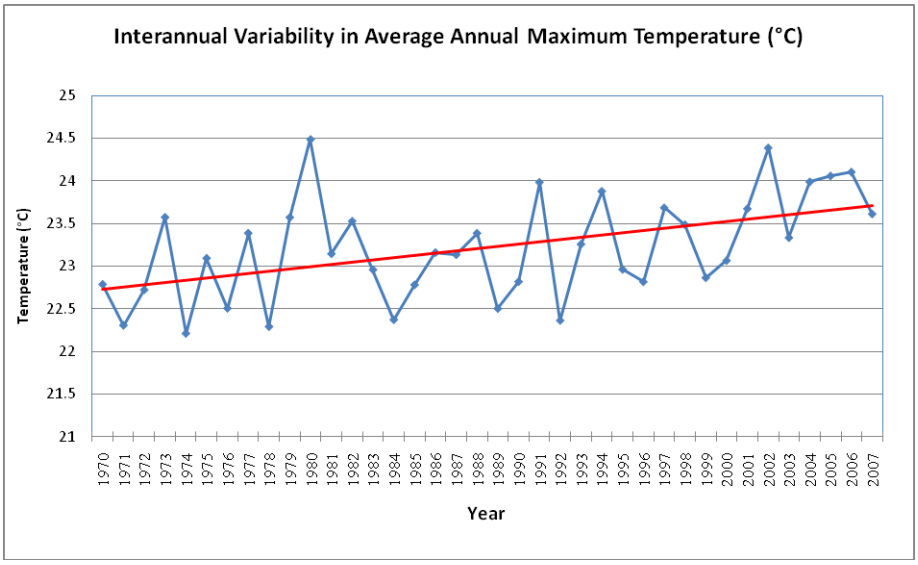

Figure 5.28. Interannual variability in average annual maximum temperature (°C) showing linear trend.

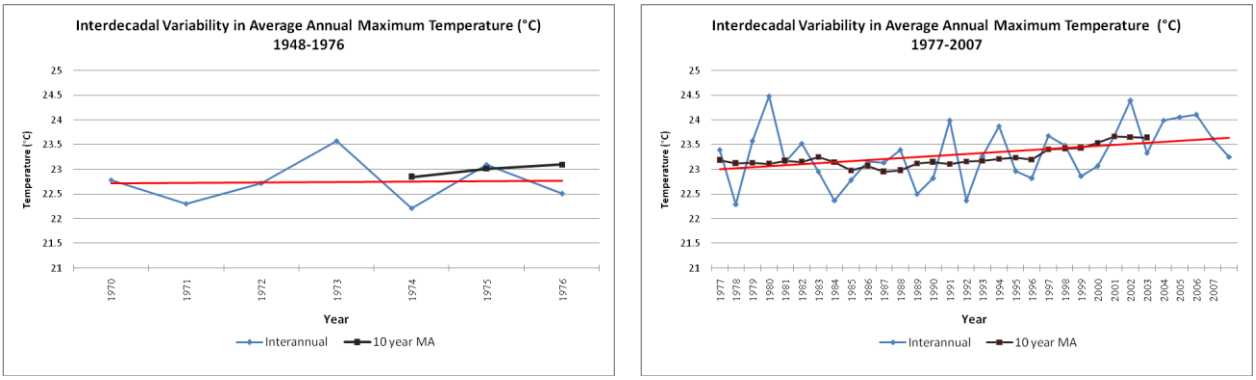

Figure 5.29. Comparison of in average annual maximum temperature (°C) recorded by stations in the Hunter, Lower North Coast and Central Coast Region for the 1970-1976 and 1977-2007 time periods.

Average annual minimum temperatures for the region range between 10.3°C and 12.1°C. Despite a similar range to annual maximum temperatures, average annual minimum temperatures show only a slight increase over the period from 1970 to 2007 (Figure 5.30). Based on the available data for the time period from 1970 to 2007, an approximate 0.2°C increase in minimum average annual temperature has occurred in the region. However, the 30 year period from 1977 to 2007 has seen no change to annual average minimum

temperatures (Figure 5.31).

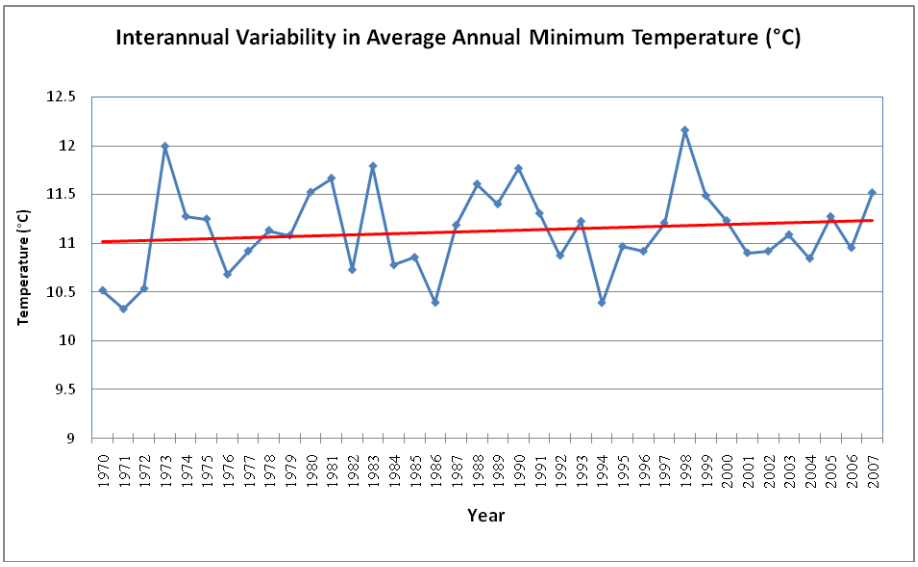

Figure 5.30. Interannual variability in average annual minimum temperature (°C) showing linear trend.

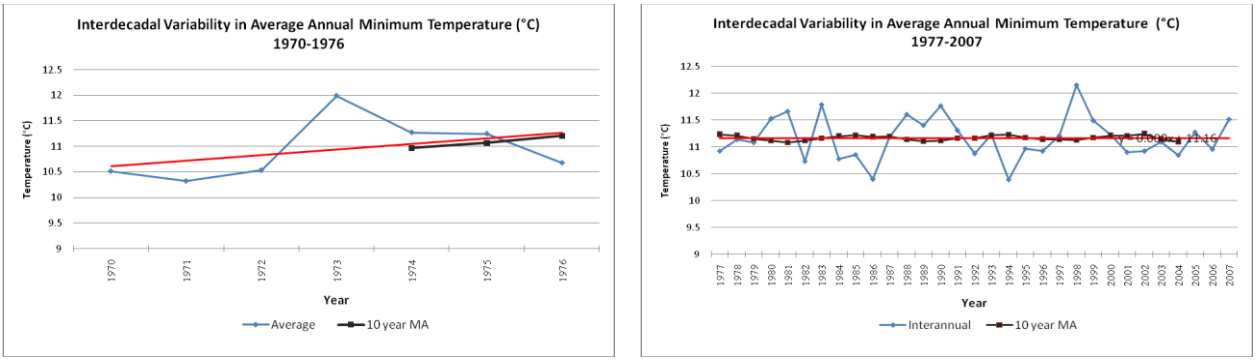

Figure 5.31. Comparison of in average annual minimum temperature (°C) recorded by stations in the Hunter, Lower North Coast and Central Coast Region for the 1970-1976 and 1977-2007 time periods.

Average annual pan evaporation for the region ranges between 3.2mm/24hr and 5.25mm/24hr. Analysis of average annual pan evaporation in the region from 1969 to 2007 shows a slight decrease of approximately 0.3mm/24hr (Figures 5.32 and 5.33). This decrease is consistent with other studies, although less than has been reported. For example, a 4mm/24hr decrease was reported in a study of pan evaporation trends across Australia for the period from 1970 to 2002 (Roderick & Farquhar, 2004). This figure is obtained as an average across Australia; figures reported for the east coast of Australia are significantly lower and more in line with the findings presented in this report.

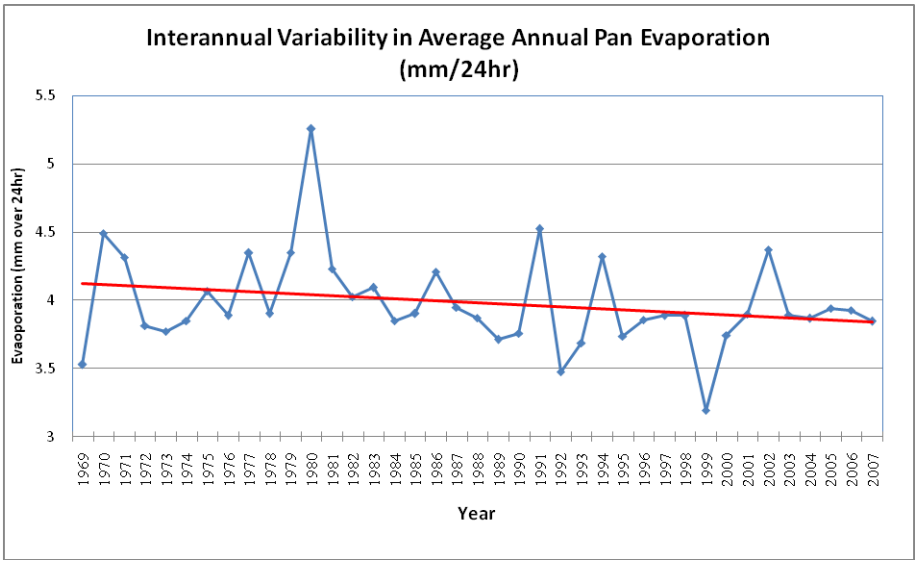

Figure 5.32. Interannual variability in average pan evaporation (mm/24hr) showing linear trend.

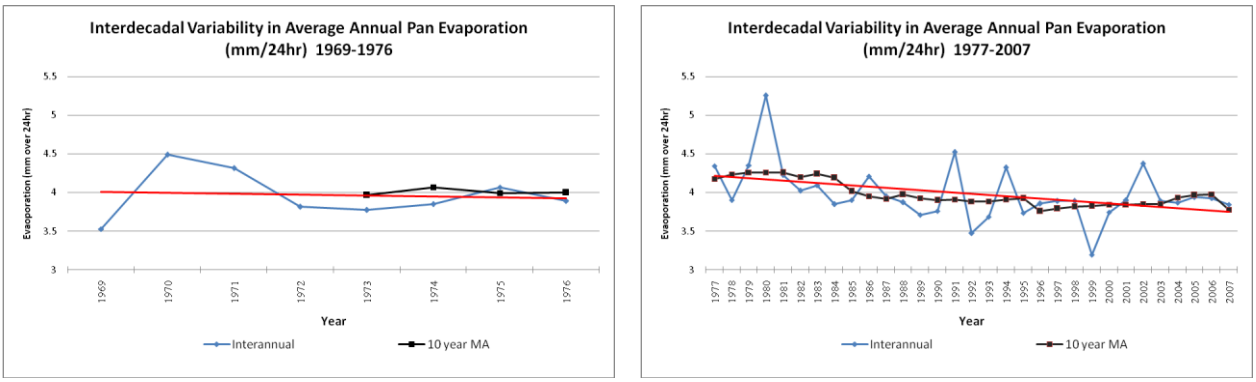

Figure 5.33. Comparison of average pan evaporation (mm/24hr) recorded by stations in the Hunter, Lower North Coast and Central Coast Region for the 1969-1976 and 1977-2007 time periods.

Water balance was calculated by subtracting the average daily pan evaporation (mm/24hr) from the average daily precipitation for each season. Data from three individual pan evaporation stations (Williamtown, Lostock Dam and Scone) are compared against the coastal, central and western zone averages respectively, and shown in Fig 5.34.

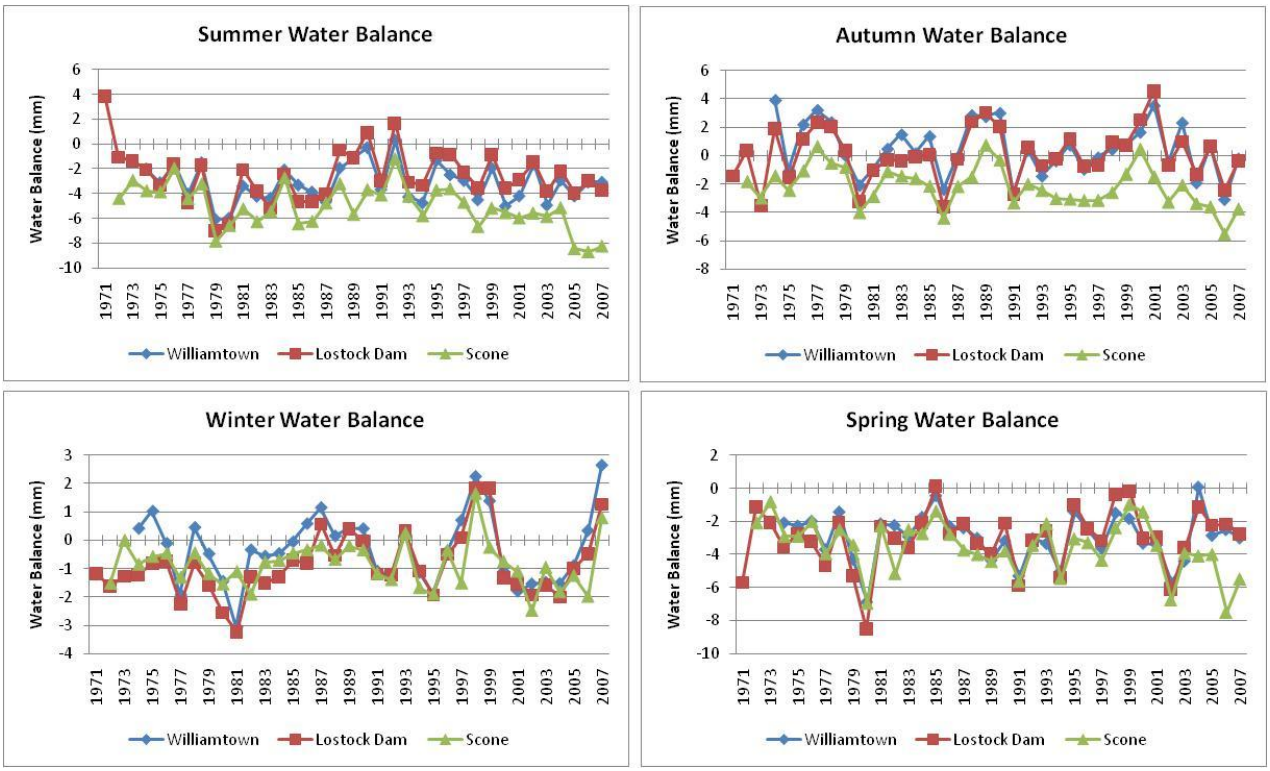

Figure 5.34. Comparison of seasonal average water balance (precipitation minus evaporation) for Williamtown, Lostock dam and Scone.

The analysis of interannual variability in average annual temperature recorded at 9am and 3pm follows the findings for maximum temperature. A statistically significant increasing trend in temperature recorded at 3pm ~1.1°C (p=0.00) occurs over the period from 1970 to 2007 (Figure 5.35). A slight increase over this time period is evident for temperature recorded at 9am.

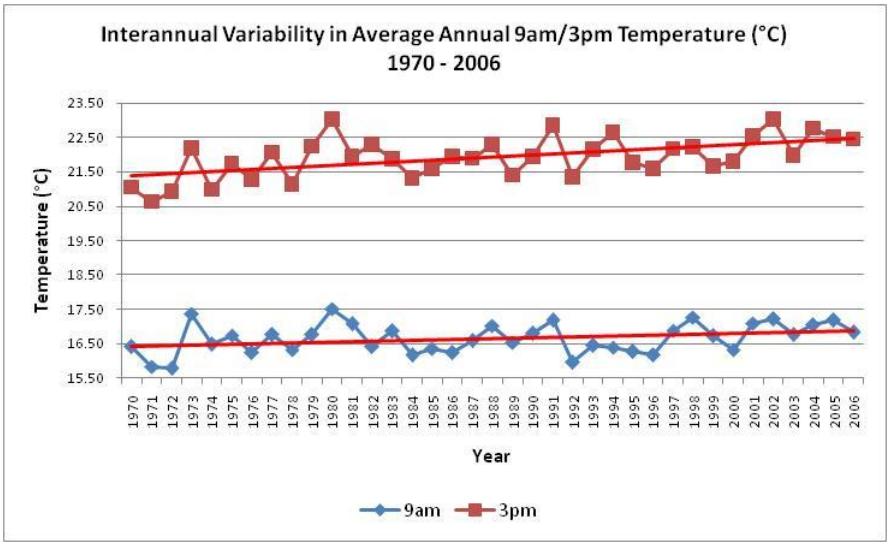

Figure 5.35. Interannual variability in average annual temperature (°C) recorded at 9am and 3pm.

No trends in humidity recorded at 9am and 3pm occur in the region. A slight decrease in average annual humidity recorded at 3pm is evident, however this trend is not statistically significant.

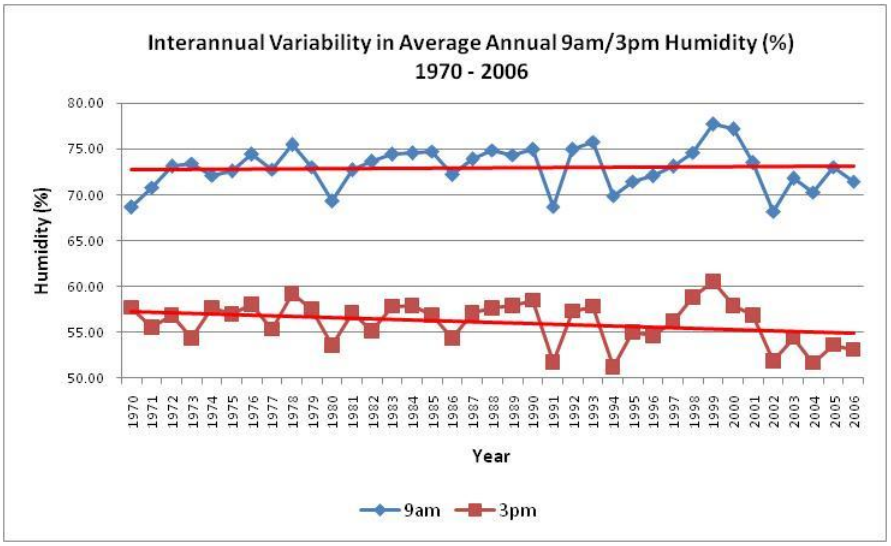

Figure 5.36. Interannual variability in average annual relative humidity (%) recorded at 9am and 3pm.

Trends in the key climate variables of precipitation, maximum/minimum temperature, pan evaporation and 3 hourly (9am and 3pm) temperature and relative humidity have been reported in this section. Care should be taken in interpreting these trends due to the natural variability in the key climate variables and the time period of analysis. That is, trends are valid for the time periods considered only; longer or shorter time periods are likely to produce different results.

5.3 Extreme Events

There are a number of ways in which extreme weather events may be defined, such as through extreme daily readings (i.e. precipitation or maximum temperature), extended periods of higher than average records, or through economic indicators of loss or damage (Easterling et al., 2000). In this section extreme events are considered in terms of:

- daily precipitation readings occurring in the 90th percentile, the 99.9th percentile and daily precipitation events above 50mm;
- daily maximum temperatures above 37 (number of extreme heat days); and
- daily minimum temperature below 0 (number of frost days).

In the case of precipitation, the percentiles are calculated from daily records with precipitation recorded (i.e. above 0mm).

Additionally, variables with high spatial variability such as precipitation may result in only localised extreme events. Thus analysis on a regional level distorts results; extreme localised events may be missed. For this reason, five (5) representative stations within the study boundary are selected for this analysis (Figure 5.37). Three of the five selected stations record both precipitation and minimum/maximum temperature (i.e. Murrurundi, Jerry's Plains and Newcastle). A single station recording both variables was not available in the north of the region, thus Wingham and Taree stations are selected for precipitation and minimum/maximum temperature respectively. All of the selected stations provide reasonable spatial coverage of the region and have been recording data for the maximum available time period.

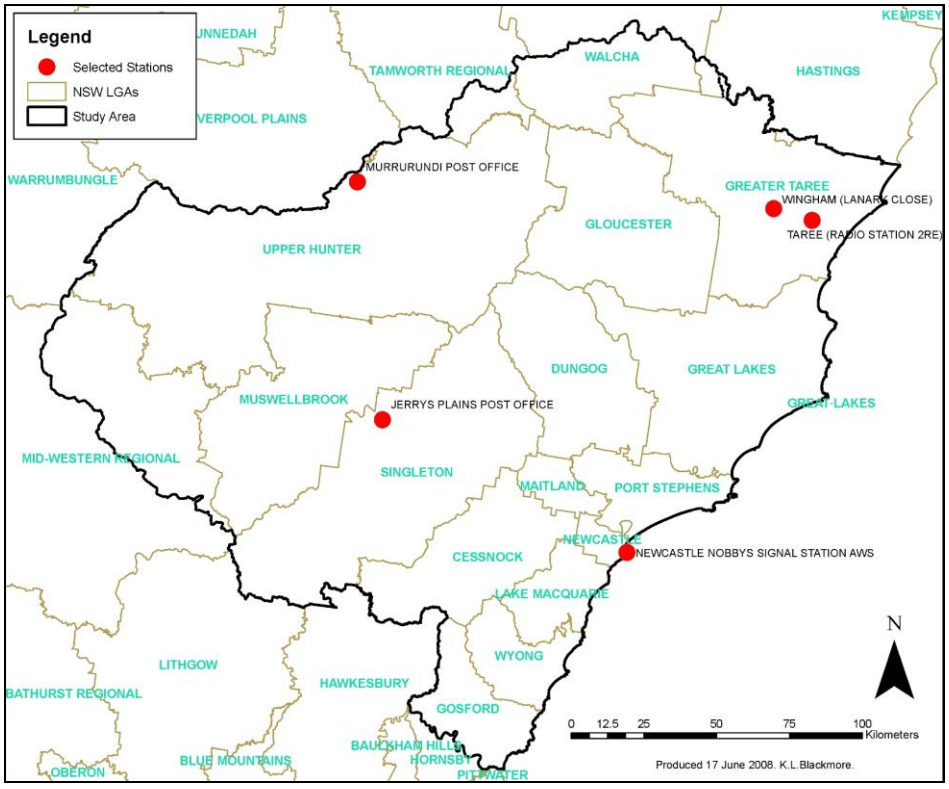

Figure 5.37. Selected stations for analysis of extreme events.

5.3.1 Precipitation

The spatial variability of precipitation events is evident when comparing the top ten recorded precipitation events for the selected stations (Table 5.7). For example, the June 2007 storm which caused severe flooding and damage in Newcastle resulted in the highest recorded daily precipitation at Jerry's Plains and the second highest on record at Newcastle. The event did not however extend through the region as far north as Wingham (15.8mm recorded) or west as Murrurundi (34.3mm recorded).

Date	Murrurundi	Date	Wingham	Date	Newcastle	Date	Jerry's Plains
14/05/1968	156	29/03/1963	259.3	3/02/1990	251.6	**9/06/2007**	**134**
26/02/1955	132.1	21/10/1967	256.5	**9/06/2007**	**209.8**	24/02/1955	123.2
9/02/1992	129.8	29/04/1963	238.3	21/06/1975	190.3	6/02/1950	103.9
24/02/1955	125.7	2/03/1976	224.6	15/06/1951	147.8	10/06/1964	97.5
24/01/1976	122.8	25/03/1978	198	28/04/1963	142.7	23/05/1981	89.2
20/11/2000	117.6	22/02/1954	197.6	4/02/1990	140.4	13/05/1968	87.1
6/02/1950	110.5	20/03/1978	187	18/02/1962	124.7	22/04/1964	86.6
11/12/2002	106.8	18/02/1959	167.6	28/07/1952	118.6	18/06/1949	82.3
23/01/1976	106	13/01/1968	161.3	6/02/1950	109.2	30/11/2007	82
1/02/1971	102.4	26/04/1966	151.4	2/08/1990	107.9	5/01/1968	81.5

Table 5.7. Top ten precipitation events on record.

Table 5.7 also highlights some apparent seasonal trends in extreme precipitation events in the region. Both Newcastle and Jerry's Plains stations record top ten precipitation events during the winter months whereas no such events occur at Murrurundi or Wingham. This is further evident by considering the frequency of occurrence of precipitation in the 99^{th} and 90^{th} percentiles (Figures 5.38 and 5.39 respectively). The 99^{th}%ile includes the top 61-82 precipitation events recorded at each of the four stations; note that the number of records and level (mm) of precipitation recorded varies relative to the average annual rainfall recorded at these stations. The cutoff value in millimetres for these stations are: Jerry's Plains - >51.2mm; Newcastle - >66.4mm; Murrurundi - >61mm; and, Wingham - >87mm. In Newcastle, extreme precipitation events are most likely to occur in June and February, whereas these event peak in Wingham during March, Murrurundi during January and Jerry's Plains in February. Regionally, extreme precipitation events are less likely to occur during late winter to early spring.

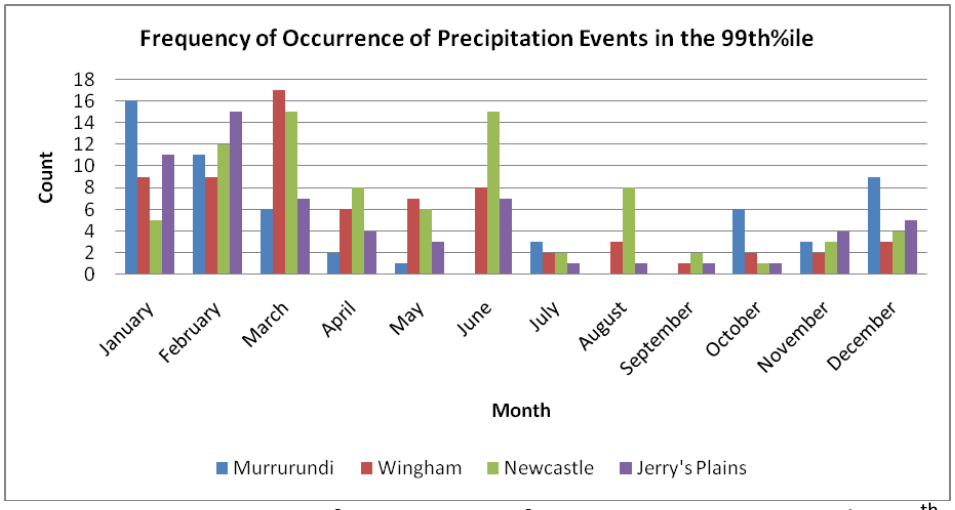

Figure 5.38. Frequency of Occurrence of Precipitation Events in the 99th%ile

A similar pattern is evident when considering precipitation events in the 90th%ile. Precipitation events in the 90thile are most likely to occur in Newcastle from January through to June whereas the other three stations see a general increase in likelihood from October, peaking in January and February. As with the 90th%ile, different cutoffs exist for each station as follows: Murrurundi - >23.3mm (590 records); Newcastle - >22.6mm (811 records); Jerry's Plains - >18.5mm (597 records); and, Wingham - >25.5mm (681 records).

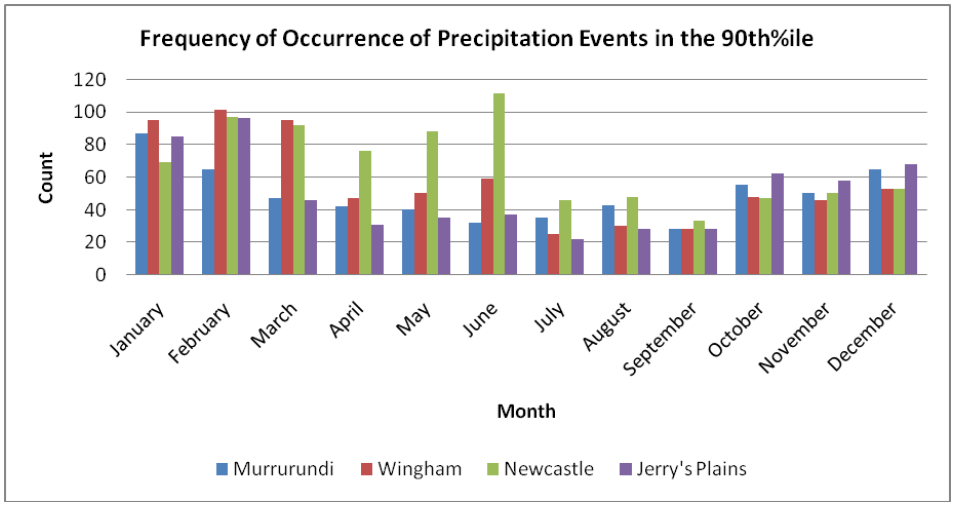

Figure 5.39. Frequency of Occurrence of Precipitation Events in the 90th%ile

Both seasonal and spatial patterns in extreme precipitation events are evident in the region. Figure 5.40 shows the distribution of all daily precipitation events >=50mm as a proportion of all precipitation events (i.e. >=0.1mm). This surface is derived from all 80 rainfall stations in the study area and buffer zone (see Section 2.1.1). Daily precipitation events 50mm or greater occur most frequently along the coast, with the centres of Gosford and Buladelah, and the area north of Taree, most susceptible. Future analysis utilising projected data to 2100AD from global climate models will allow consideration of how these extreme rainfall patterns are likely to change in the future.

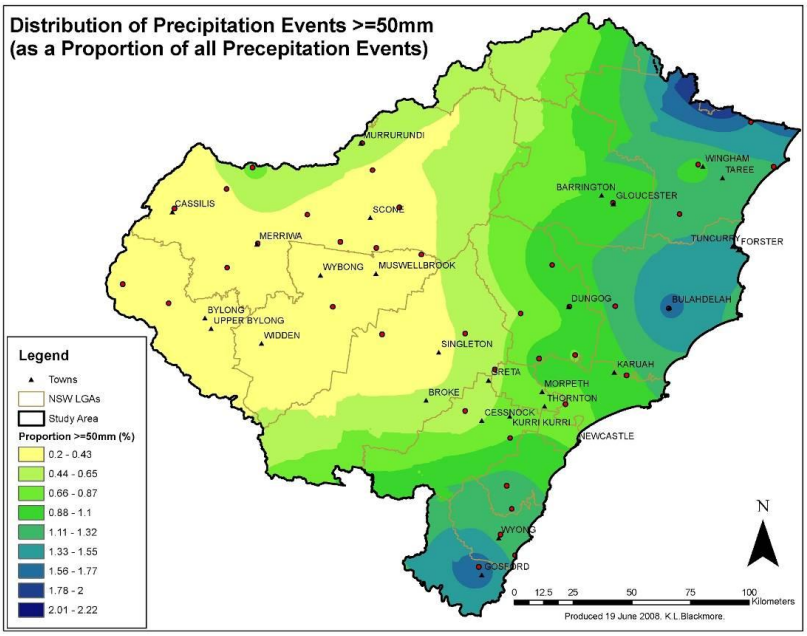

Figure 5.40. Distribution of precipitation events >= 50mm as a proportion of all precipitation events.

A slight decreasing trend in the number of days per annum with precipitation >= 50mm is evident at Wingham, Murrurundi and Newcastle (Figure 5.41). On average, these centres receive 50mm or more daily rainfall between 2-3 days per annum. During the period from 1948 to 2007, the number of days has varied between 12 (recorded in 1950 at Newcastle) and 0. A period of increased variability is evident between 1948 and 1964.

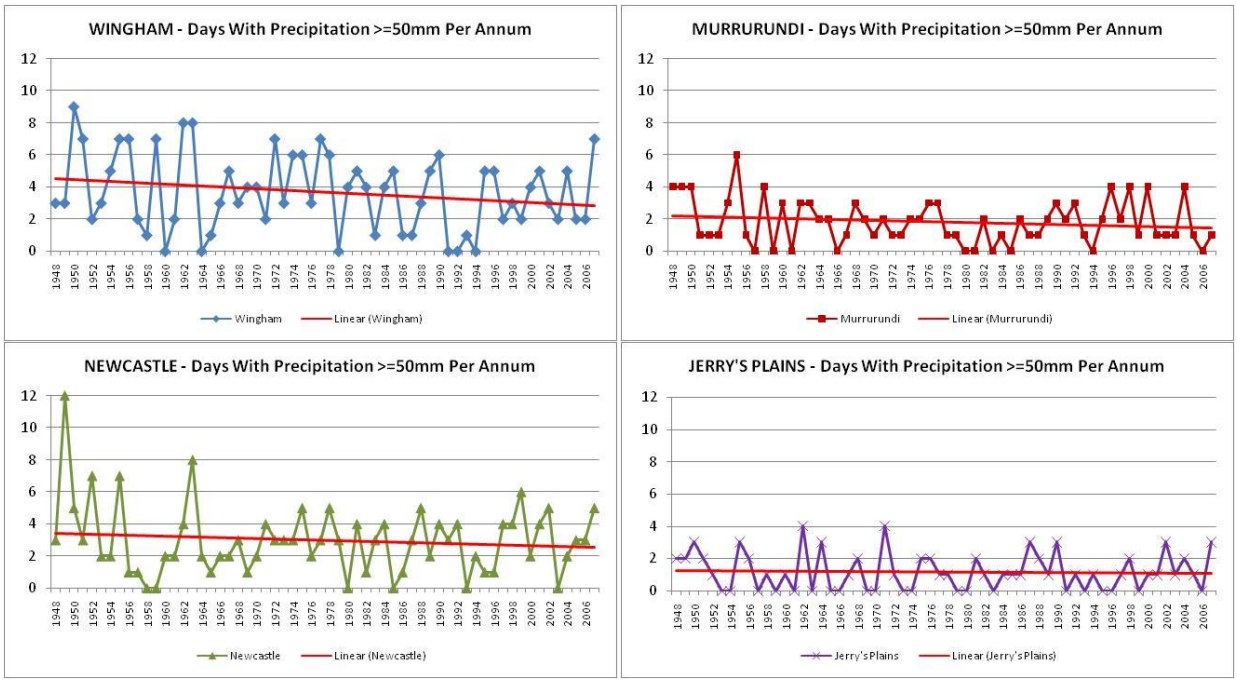

Figure 5.41. Frequency of days per annum with daily precipitation >=50mm for Wingham, Murrurundi, Newcastle and Jerry's Plains showing linear trend lines.

Extreme precipitation events have been mapped to each ST (Figure 5.42). Extreme events at Newcastle occur predominantly during ST's 1, 4, 7, 10 and 11. Extreme events at Jerrys Plains and Wingham occur during ST's 10 and 11, whilst extreme events at Murrurundi occur primarily during ST's 10 and 11 from inland low depressions associated with the northern Australian trough.

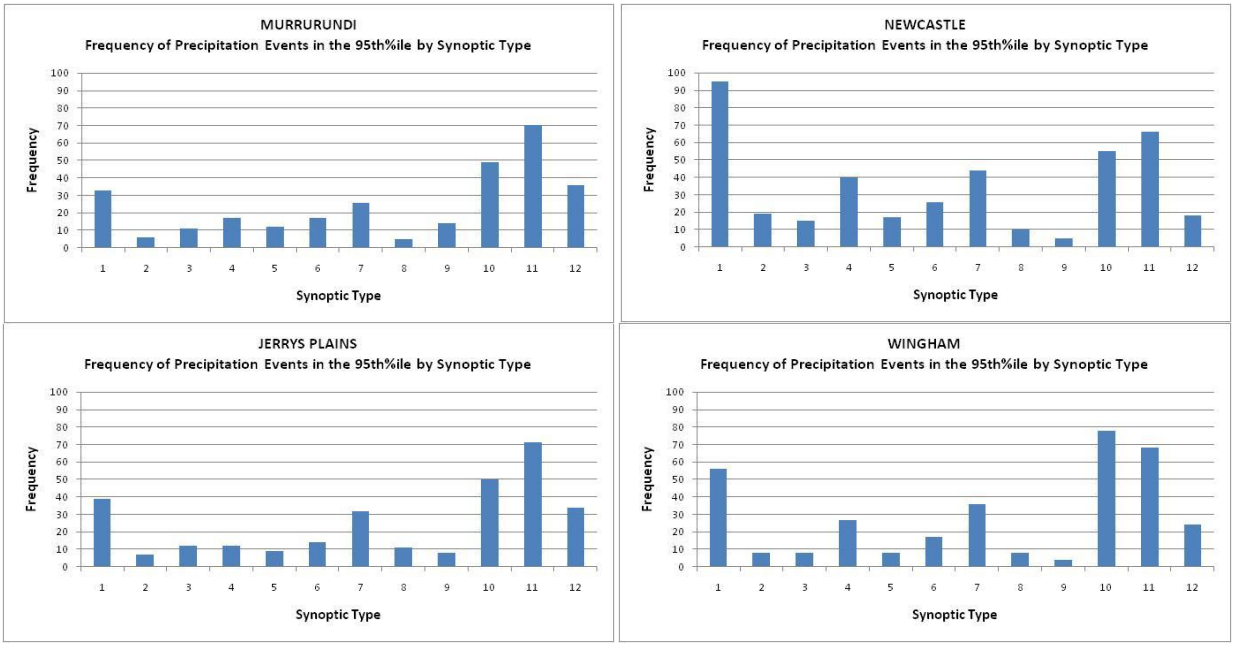

Figure 5.42. Frequency of precipitation events in the 95th%ile by synoptic type for Murrurundi, Newcastle, Jerry's Plains, Wingham.

5.3.2 Maximum Temperature

The frequency with which maximum temperatures greater or equal to 37°C are experienced within the region varies significantly according to the spatial location of the recording station. Using the four selected sites, a comparative histogram of the number of days with maximum temperature >=37°C shows clear differentiation between Jerry's Plains and the other three stations (Figure 5.43). (Note that temperature records for the north of the region are obtained from Taree rather than Wingham, which was used for precipitation. Taree station lies approximately 14km east/south east of Wingham). Peaks in frequency occur in 1979-1980, 1983 and also in 2002 and 2004.

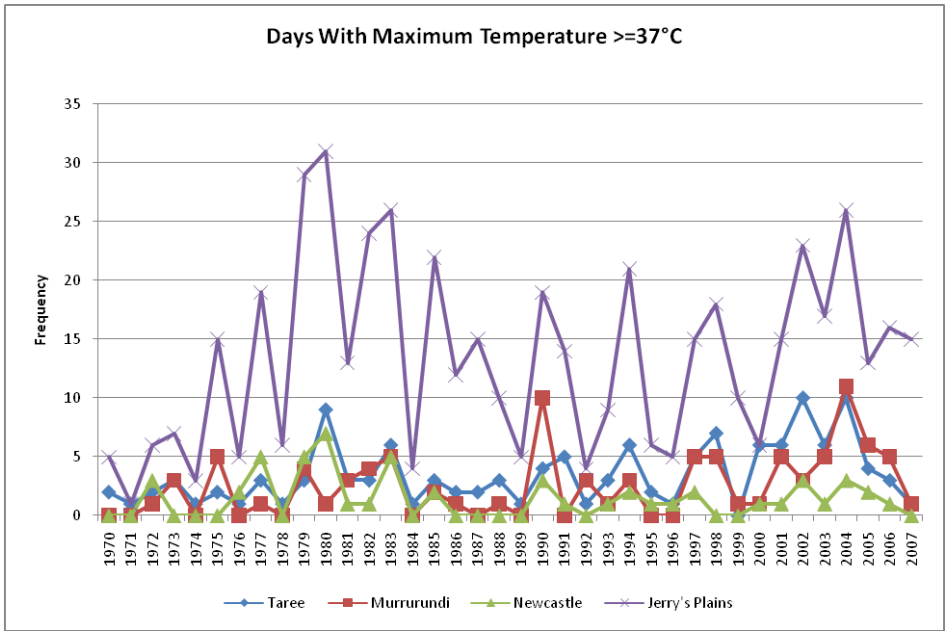

Figure 5.43. Frequency of days per annum with maximum temperature >=37°C.

An increasing trend in the frequency of days with maximum temperatures greater than or equal to 37°C is evident at Taree, Murrurundi and Jerry's Plains (Figure 5.44). However Newcastle shows little trend, although a slight decrease may be inferred.

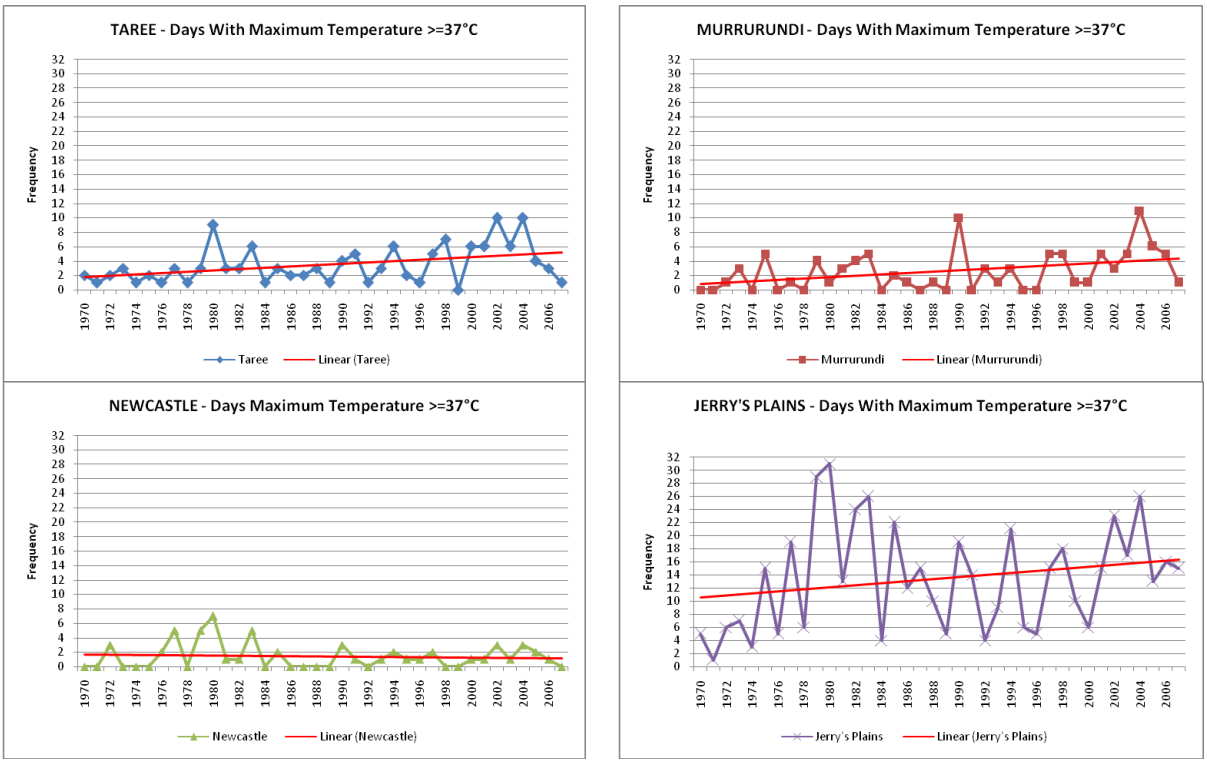

Figure 5.44. Frequency of days per annum with maximum temperature >=37°C for Taree, Murrurundi, Newcastle and Jerry's Plains showing linear trend lines.

Extreme temperature events greater than or equal to 37°C have been mapped to each ST (Figure 5.45). Extreme high temperature events at Newcastle occur primarily during ST's 10 and 11. Extreme events at Taree, Murrurundi and Jerry's Plains occur primarily during ST's 10, 11 and 12.

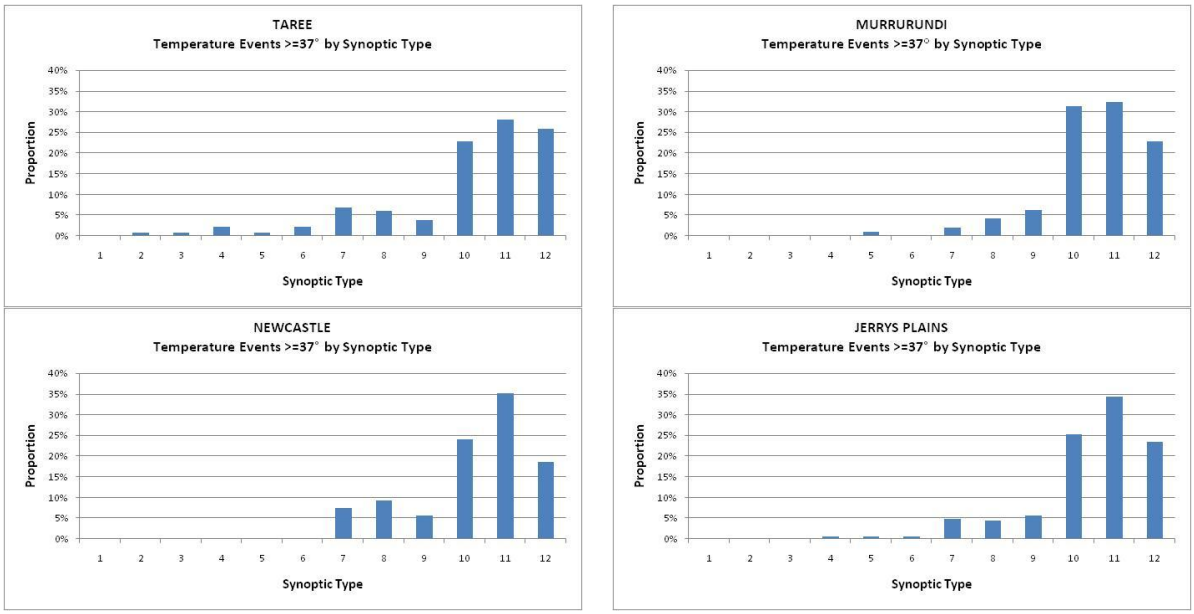

Figure 5.45. Temperature events >=37°C by synoptic type for Taree, Murrurundi, Newcastle and Jerry's Plains.

5.3.3 Minimum Temperature

Murrurundi, the most westerly of the selected stations, records significantly more days with minimum temperatures below 0°C, with Taree recording comparatively less and no instances recorded between 1970 and 2007 at Newcastle (Figure 5.46). The variability in frequency during the 1970 to 2007 time period is substantial, ranging from 16 recorded days (1974) to 71 recorded days (1994) at Murrurundi.

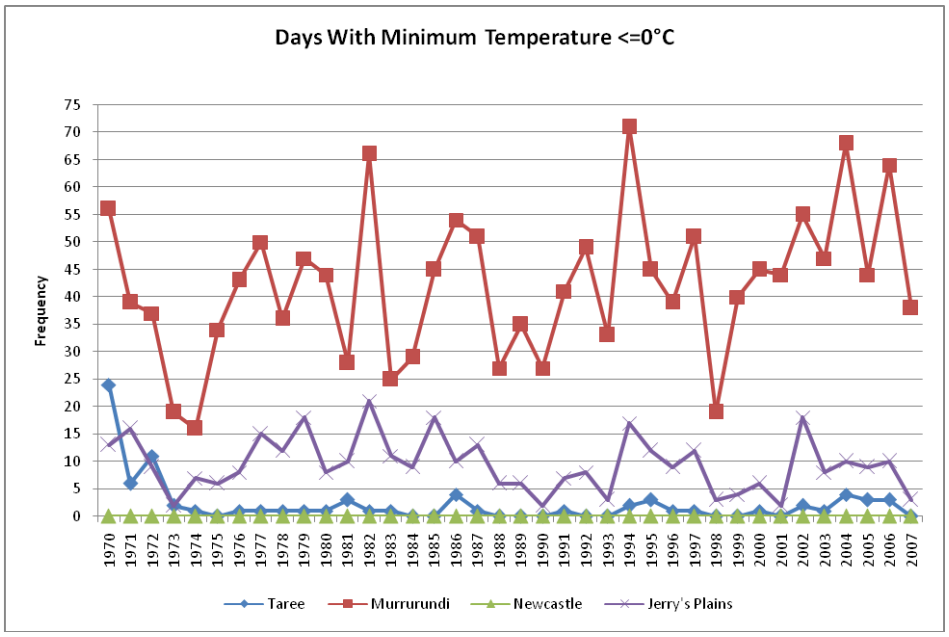

Figure 5.46. Frequency of days per annum with minimum temperature <=0°C.

Figure 5.47 shows the frequency of days with minimum temperatures <=0°C and linear trend lines for each of the selected stations. Both Taree and Jerry's Plains show a negligible decrease in frequency over the period from 1970 to 2007. A linear increase of 39%, or 13 more days, over this time period is evident for Murrurundi. While substantial, this increase is not statistically significant.

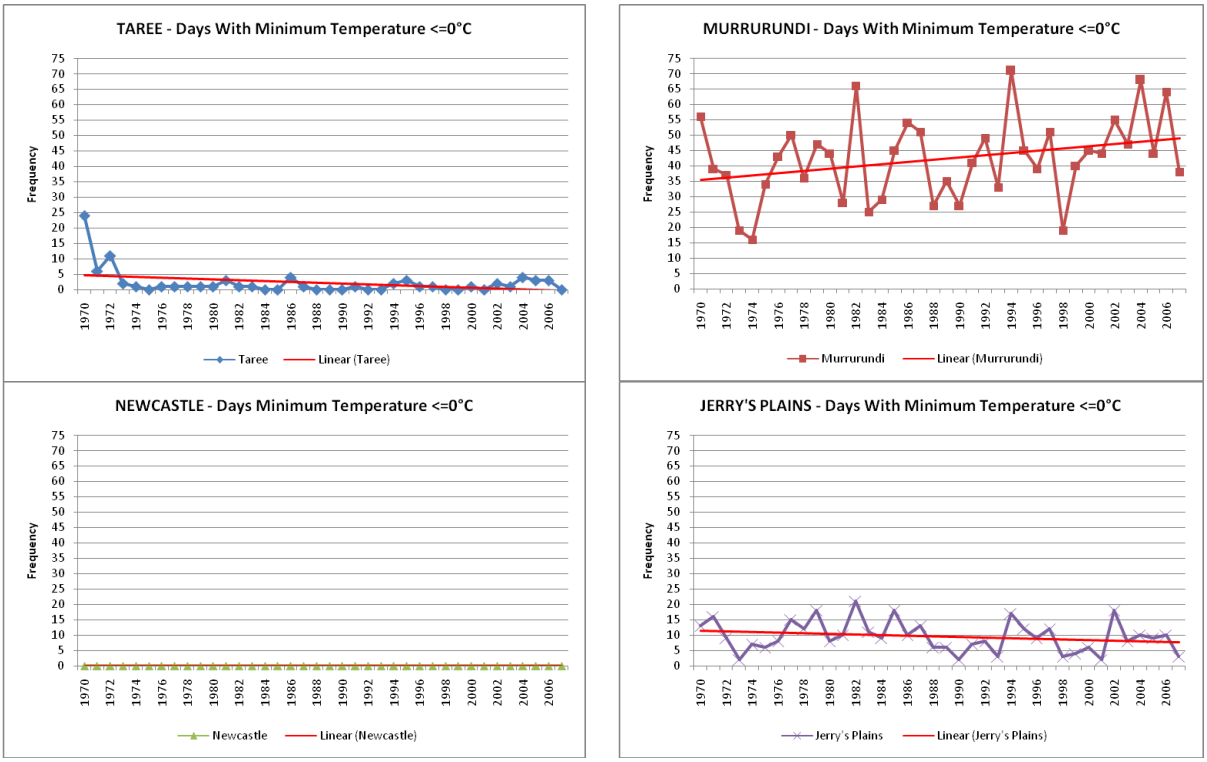

Figure 5.47. Frequency of days per annum with minimum temperature <=0°C for Taree, Murrurundi, Newcastle and Jerry's Plains showing linear trend lines.

The frequency of occurrence of temperature events where the recorded temperature is less than or equal to 0°C have been mapped to each ST (Figure 5.48). These extreme events at Taree occur primarily during ST 3, and to a lesser extent during ST 1. This trend is reversed at Murrurundi and Jerry's Plains, which are both more westerly locations. Extreme events occur primarily during ST 1, and less frequently ST 3 at these centres.

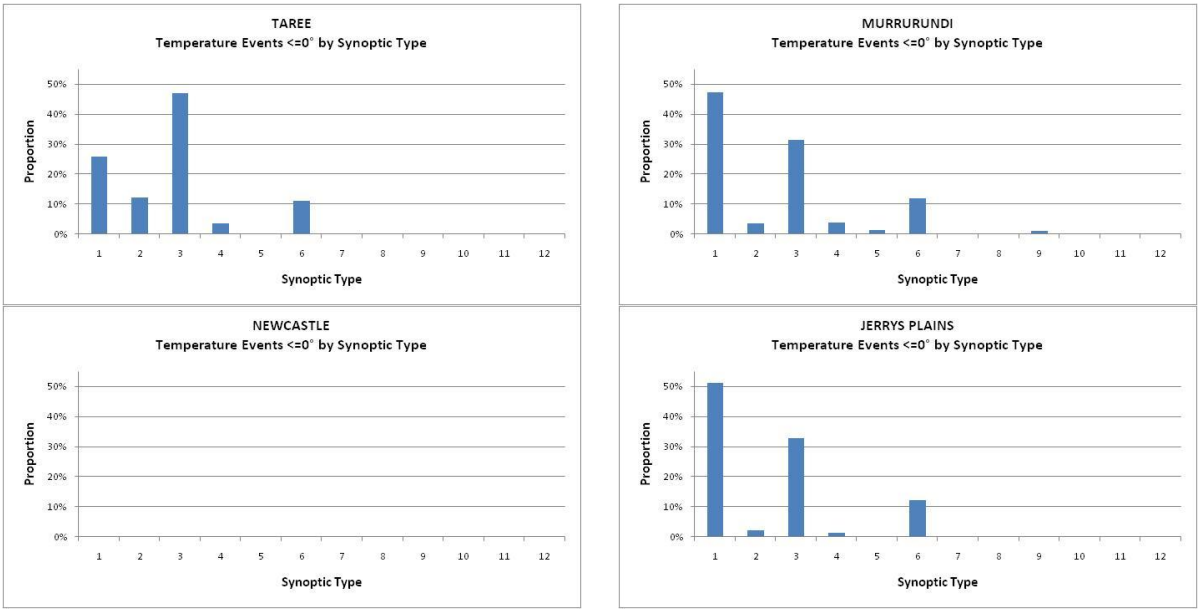

Figure 5.48. Temperature events <=0°C by synoptic type for Taree, Murrurundi, Newcastle and Jerry's Plains.

Summary of Extreme Events

Regionally, extreme precipitation events are less likely to occur during late winter to early spring. Extreme precipitation events occur more frequently along the coast during January, February and March. In Newcastle, this period extends through April and May, and peaks in June. These events are most likely to occur under the influence of ST's 1, 10 and 11.

Of the stations analysed, high temperature events occur most frequently at Jerry's Plains, which is in the central sub-region. A slight increase in the frequency of high temperature events from 1970 to 2007 is evident at Taree, Jerry's Plains and Murrurundi. Regionally, high temperature events are most likely to occur under the influence of ST's 10 and 11.

Trends in the frequency of temperature events below or equal to 0°C have also been analysed. Coastal influences result no recorded events at Newcastle from 1970 to 2007. Murrurundi, the most westerly of the recording stations analysed, shows an increasing trend. Regionally, low temperature events are most likely to occur under the influence of synoptic types 1 and 3.

6 Summary of Sub-Regional Climate Variability

6.1 Synoptic Types and Mean and Extreme Climate

The relationship between the Synoptic Types (ST's) and the Southern Hemisphere climate drivers was outlined in section 4. In addition, the variability in the frequency of the ST's was discussed as a function of the El Nino-Southern Oscillation (ENSO) and the Interdecadal Pacific Oscillation (IPO). Whilst there was no statistically significant relationship between the ST's and the Southern Oscillation Index (SOI), a statistically significant relationship between the ST's and the IPO was determined. The shifts in ST from the 1946 to 1976 (IPO-ve) period to the 1977 to 2007 (IPO+ve) period describe a trend in increasing high pressure in the Subtropical Anticyclone over eastern and southern Australia. The most variable ST's that are statistically significant between the two IPO periods are: ST 1, 2, 3, 4, 6, 10 and 12. During the IPO +ve phase (1977 to 2007) the dominant ST's change to the following:

(v) Summer: ST 10 decrease in frequency, and ST 7, 8 and 12 have a small increase;
(vi) Autumn: ST 6, 9 and 10 decreases in frequency whilst, ST 1 and 4 increase;
(vii) Winter: ST 2 and 6 decrease in frequency whilst, ST 1 and 3 increase;
(viii) Spring: ST 4 and 12 decrease in frequency whilst, ST 1 and 6 increase.

The changes in ST's are shown by the arrows in Fig 6.1 below.

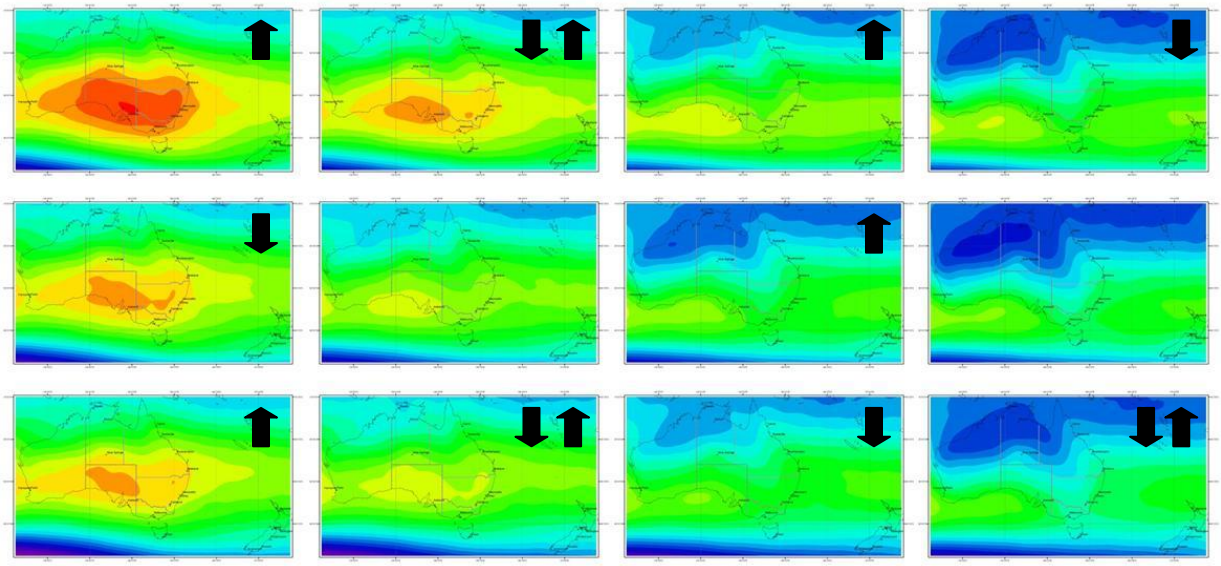

Figure 6.1. IPO related shifts in the 12 key synoptic types derived using the SOM methodology

The analysis of ST's has provided the baseline data to assess the projected changes in atmospheric circulation at 2030, 2050, 2070 and 2100 AD during Stage 3 of the study. The annual to decadal frequency of the ST's provide a framework to assess changes in the spatial distributions of the key clime variables and the frequency of extreme events.

6.2 Air Temperature

Despite the shifts in ST's there were no statistically significant trends in annual temperature across the region for the period of available temperature data within the region (since ~1950) (Figures 6.2 and 6.3). However, the annual and seasonal average temperature record at Newcastle, Murrurundi, Gloucester reveal some significant trends. Summer average maximum temperatures at Williamtown have risen ~0.04°C/yr since 1950 (p=0.00). Similar statistically significant increasing trends for Autumn (~0.01°C/yr), Winter (~0.02°C/yr) and Spring (~0.03°C/yr) are evident at Williamtown. Average maximum temperatures in Winter and Spring at Lostock Dam show an increasing trend of ~0.03°C/yr (p=0.01) and ~0.04°C/yr (p=0.02) respectively. No significant trends in average maximum temperature are evident at Murrurundi. Generally, minimum average temperatures show no trends. Only Williamtown summer average minimum temperature shows a slight increasing trend of ~0.01°C/yr (p=0.02).

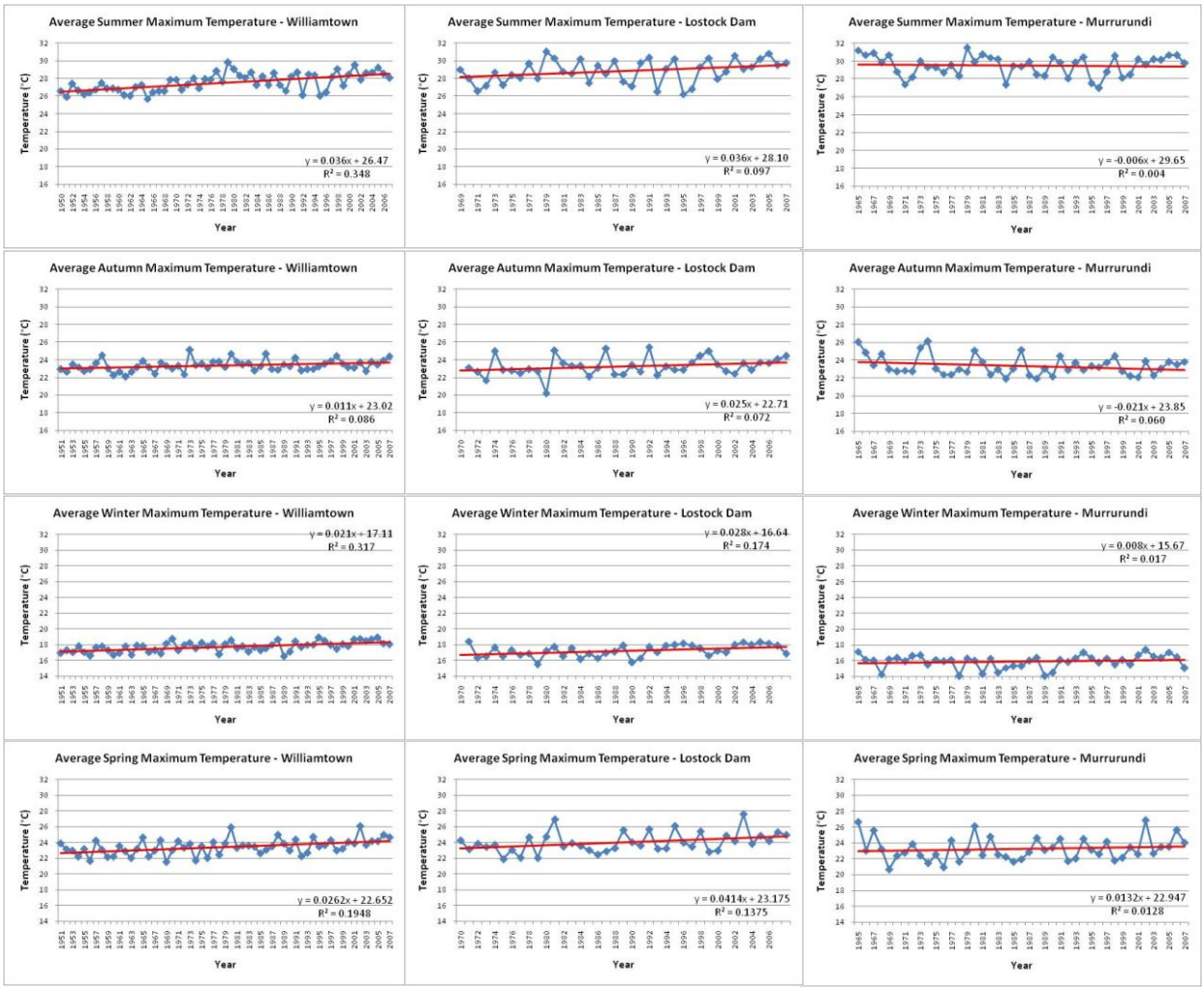

Figure 6.2. Average seasonal maximum temperature records for Williamtown, Lostock Dam and Murrurundi.

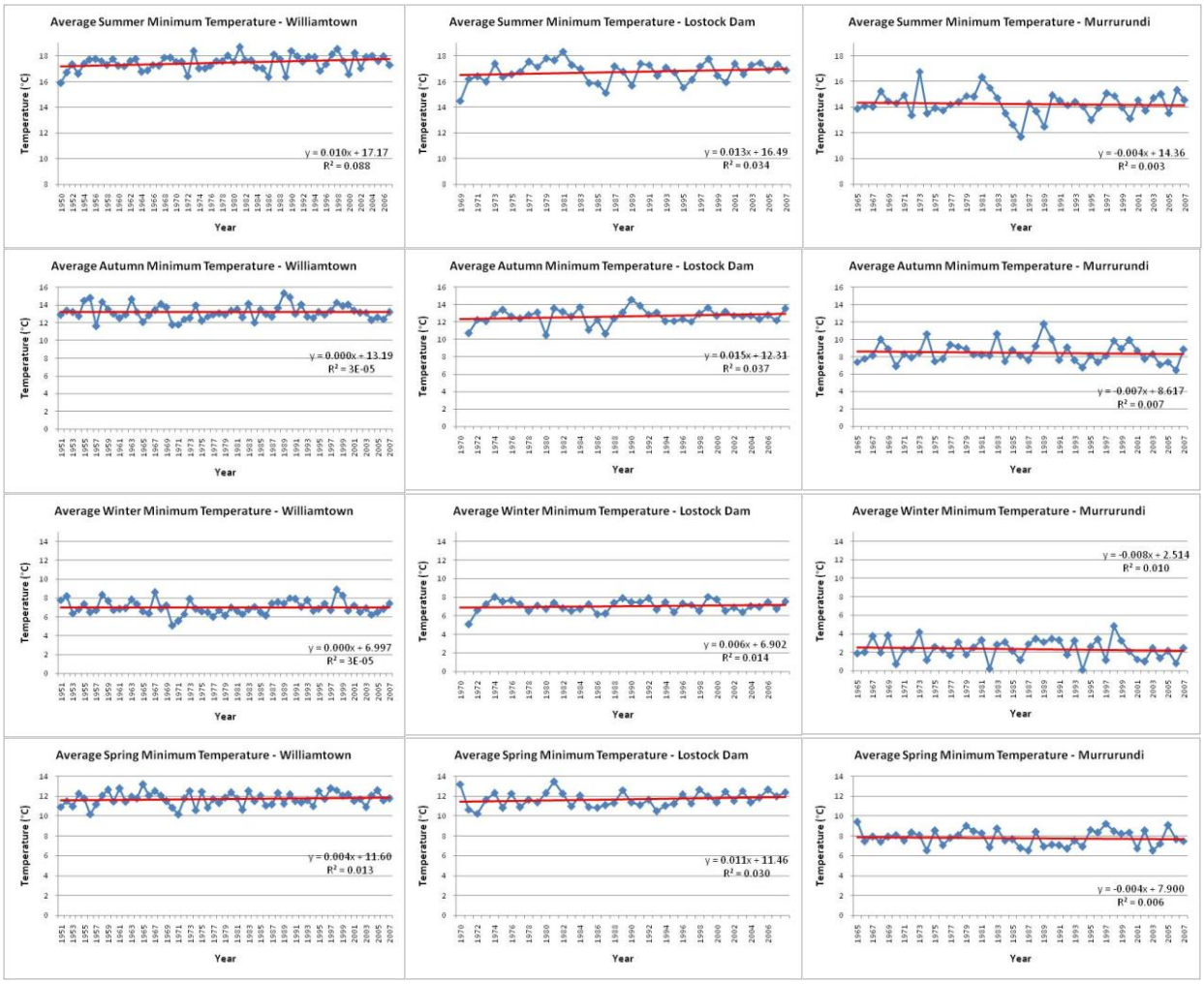

Figure 6.3. Average seasonal minimum temperature records for Williamtown, Lostock Dam and Murrurundi.

Regionally, extreme maximum temperatures above 37°C occur primarily during ST's 10, 11 and 12. Extreme minimum temperatures below 0° C occur primarily during ST's 1, 3 and 6. A statistically significant trend of increasing frequency of temperature below 0° C is evident at Murrurundi. Analysis of hot spells (i.e. events with three consecutive days of temperatures above or equal to 37°C) shows an increasing trend in the frequency of occurrence of these events at Jerry's Plains.

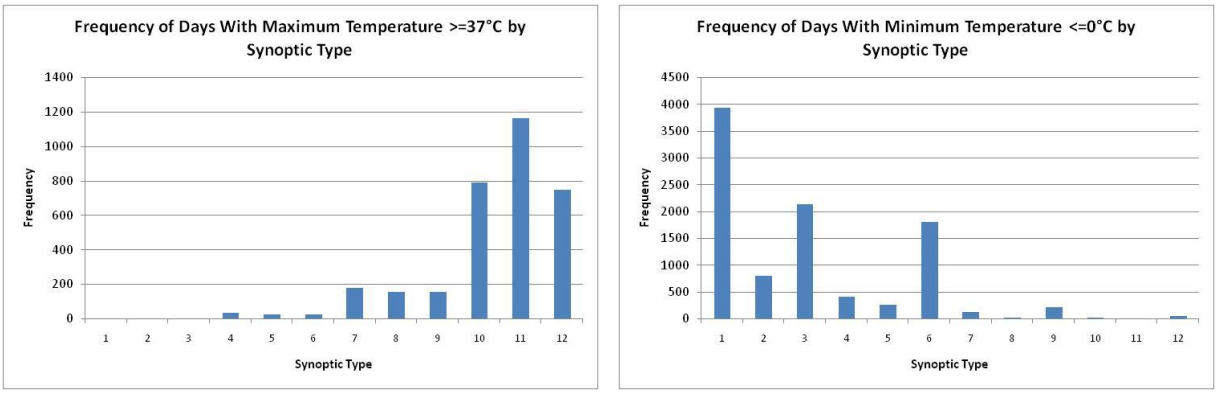

Figure 6.4. Frequency of days with maximum temperatures >=37°C and minimum temperatures <=0°C by synoptic type.

6.3 Precipitation, Evaporation, Relative Humidity and Water Balance

The annual average precipitation records for Newcastle, Murrurundi and Gloucester are shown in Figure 6.5. No significant trends are recorded due to the large interannual variability. Trend analysis was also conducted on the seasonal average precipitation records that are shown in Figure 6.6. Newcastle and Gloucester contain no significant trends, but Murrurundi in the western zone has experienced an increase in summer and spring precipitation of 106 mm, with a trend of 0.78 mm/yr (p=0.01), and 74 mm, with a trend of 0.544 mm/yr (p=0.00) respectively over the 136 year period since 1871. The summer increase is stepwise with an abrupt increase after 1950. A trend in decreasing (more negative) water balance for summer and autumn is detected at Scone since the beginning of the records in 1971.

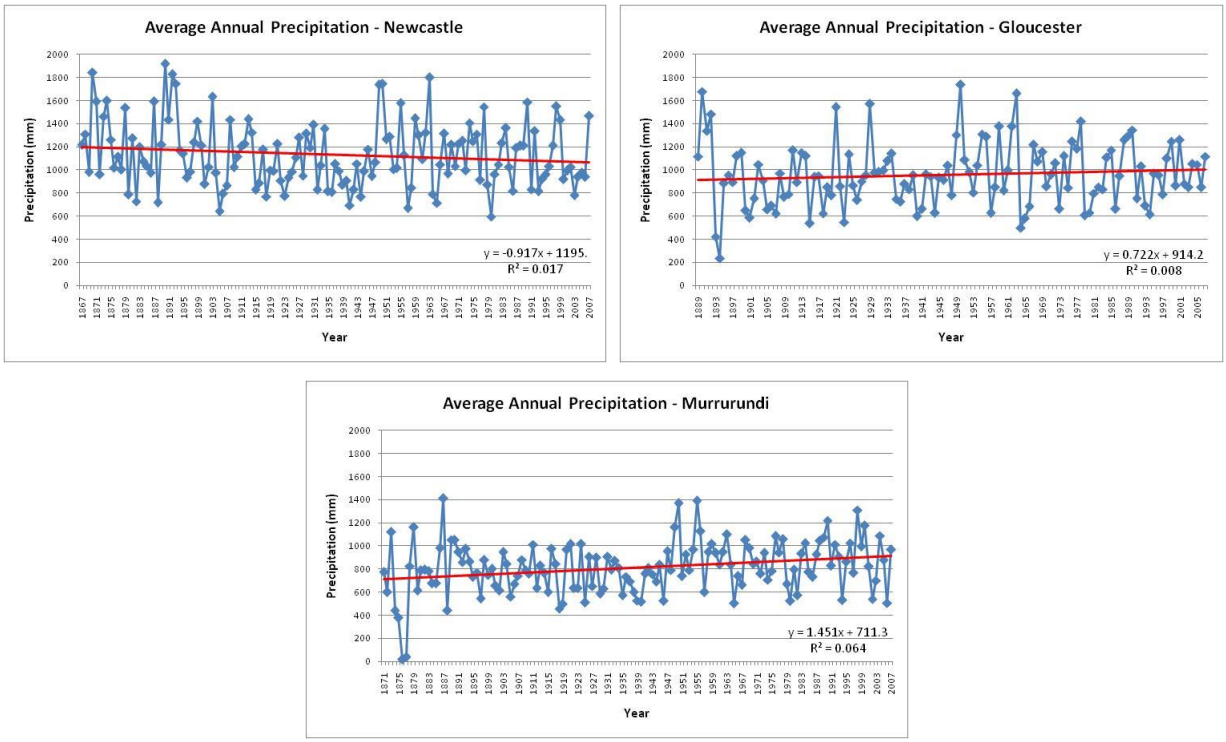

Figure 6.5. Annual average precipitation records for Newcastle, Gloucester and Murrurundi.

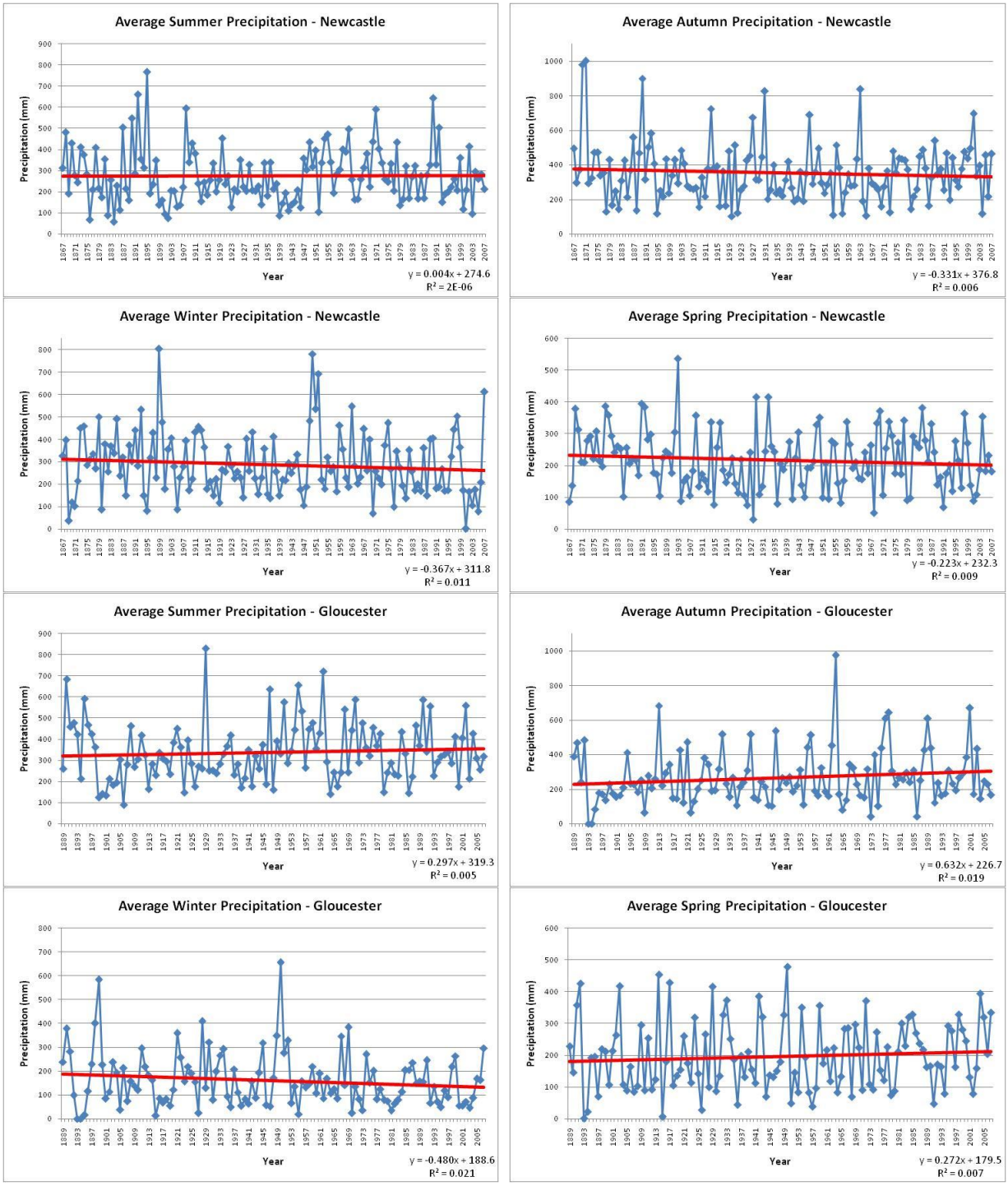

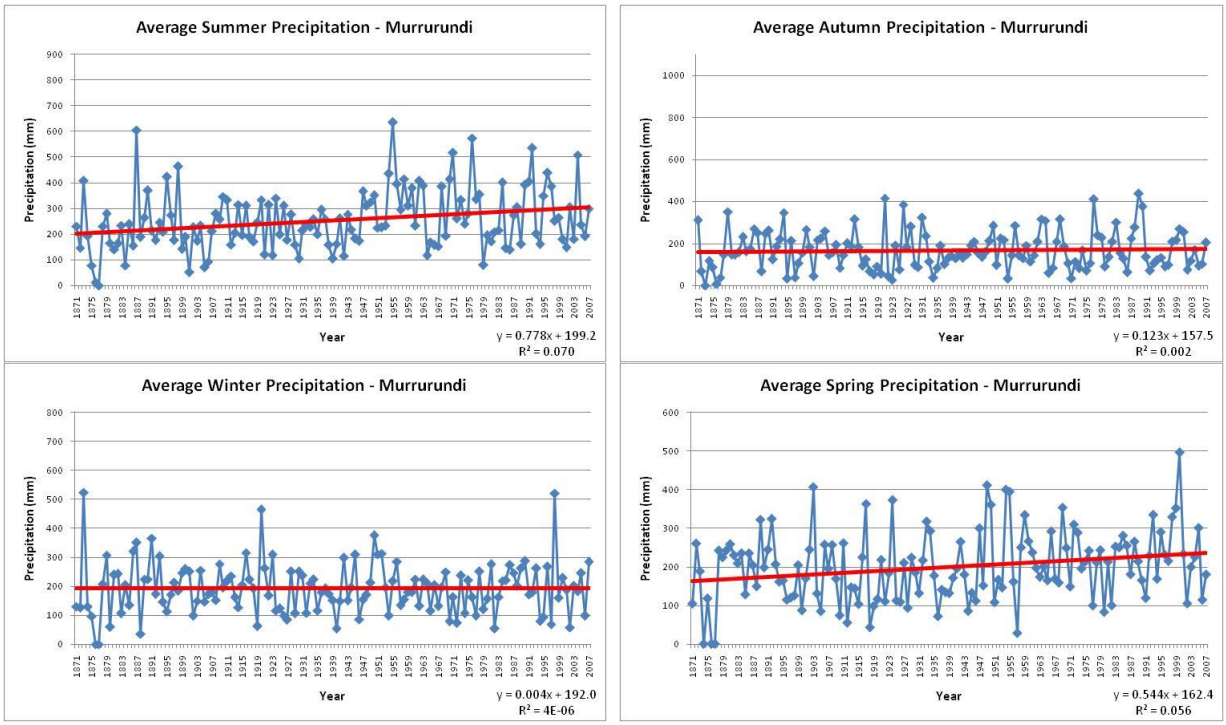

Figure 6.6. Seasonal average precipitation records for Newcastle, Gloucester and Murrurundi.

Persistent dry and wet spells have been analysed by calculating the deviation from average annual precipitation for Newcastle, Gloucester and Murrurundi. Although not statistically significant, all stations show a slight decrease; that is, the occurrence of dry periods is becoming more frequent (Figure 6.7). Notable dry periods occur between 1964 – 1974, from 1978 – 1984 and more recently from 1990 to 2006, broken only by a wet period between 1995 – 1998. The period between 1949 – 1963 is characterised by extreme wet periods, with another notable wet period occurring between 1985 – 1990.

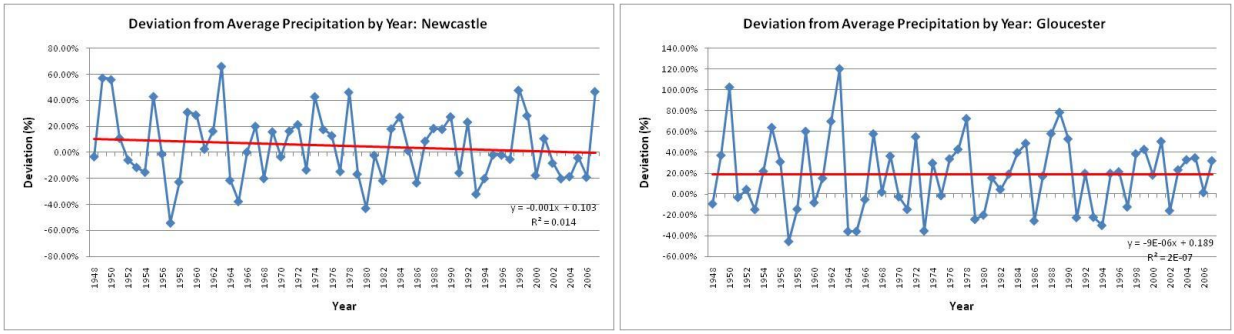

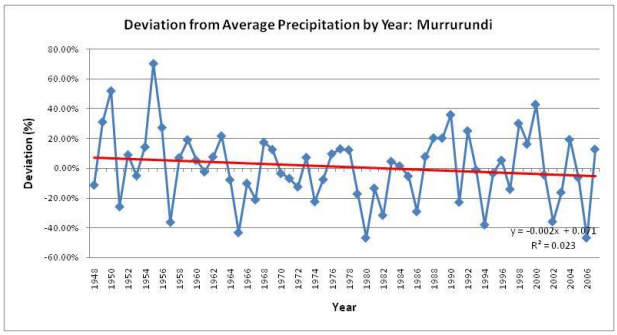

Figure 6.7. Deviation (%) from average annual precipitation for Newcastle, Gloucester and Murrurundi.

Deviations from average monthly precipitation have been mapped to each ST for Newcastle, Gloucester, Wingham and Murrurundi. Thus rather than indicating the wettest/driest STs, the graphs in Figure 6.8 show average percentage above or below the expected or average monthly precipitation value for each ST. At Newcastle, STs 4 and 7 produce an average of 40% or higher than the expected precipitation. ST 3 results in precipitation that is on average almost 60% lower than anticipated. Murrurundi station, located in the western sub-region, shows a pattern of deviations which is markedly different to that of the coast (i.e. Newcastle). ST 9 produces an average almost 50% or higher than anticipated precipitation at Murrurundi, whereas types 1 and 3 produce lower than anticipated precipitation. The most significant deviations occur at Gloucester. Here, ST's 4 and 7 produce precipitation over 100% more than anticipated. At Wingham, ST's 3 and 9 produce significantly lower than average precipitation.

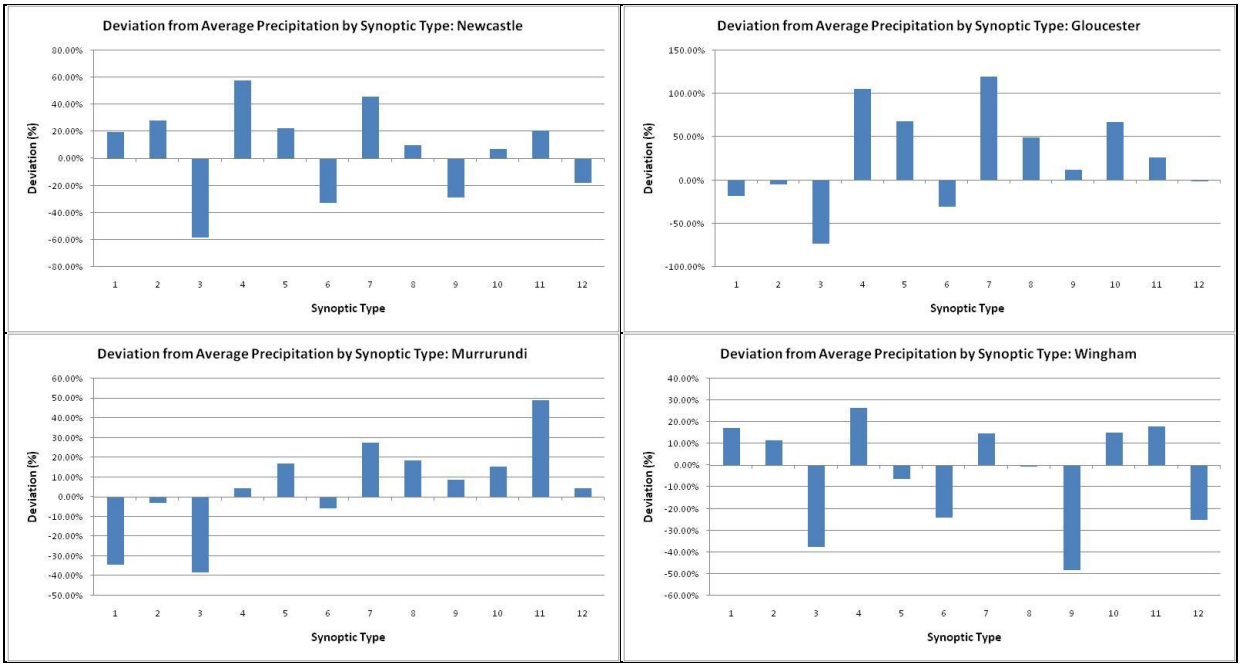

Figure 6.8. Deviations from average monthly precipitation mapped to each ST for Newcastle, Gloucester and Murrurundi.

Extreme precipitation events have been mapped to each ST. Extreme events (i.e. daily rainfall events in the 95th%ile) at Newcastle occur primarily during ST's 1, 4, 7, 10 and 11. Extreme events at Wingham occur during ST's 1, 7, 10 and 11, whilst extreme events at Murrurundi occur primarily during ST's 10 and 11 from inland low depressions associated with the northern Australian trough.

6.4 Wind

Average wind speed shows a slight decrease across the region of 2.4km/hr for the period from Jan 1970 to Dec 2007. While not large, this decrease is statistically significant (p=0.00). Sub-regional analysis of trends shows a decrease in average wind speed in the central and western parts of the region. Only the decrease in the central part of the region of 6.5km/hr over the 38 year time period is statistically significant (p=0.00).

Maximum wind gust data for the region is only available for an extended time period from Williamtown. Analysis reveals no trend, significant or otherwise, in average maximum wind gusts for this station.

6.5 Sea Surface Temperature, Sea Level and Wave Climate

Annual average sea surface temperatures off the study region have increased by ~0.5° C in the past few decades. Tide gauge measurements at Fort Denison in Sydney indicate that relative sea-level has risen by 1.2 mm/year over the past century (White et al., 2005), with an acceleration to ~3 mm/yr in the past decade. Mean annual sea level along the Central, Hunter and Lower North Coast NSW can vary by as much as 0.150 m between years, without any long-term trend in sea level Extreme water levels have been found to have increased in frequency by a factor of 2-3 since 1950.

Monthly mean wave climate parameters (Significant Wave Height, Maximum Wave Height, Peak Period, and Wave Direction) have been analysed for each ST to provide a typology of monthly wave conditions since 1948. These data will be used to assess the projected changes in wave climate out to the 2100 AD time horizon in Stage 3 of the study.

7 Acknowledgements

The following acknowledgements are made in respect to assistance and/or data provided to compile this report:

- Danielle Verdon for the initial analysis of the suitability of station data.
- Howard Bridgman, the University of Newcastle, for assistance and provision of the climatic atlas of the Hunter Region.
- *NOAA_ERSST_V3 data provided by the NOAA/OAR/ESRL PSD, Boulder, Colorado, USA, from their web site at* http://www.cdc.noaa.gov/.
- *NCEP Reanalysis data provided by the NOAA/OAR/ESRL PSD, Boulder, Colorado, USA, from their web site at* http://www.cdc.noaa.gov/ .
- Bureau of Meteorology (BOM).

8 References

Alexander, L.V., Zhang, X., Peterson, T.C., Caesar, J., Gleason, B., Klein Tank, A.M.G., Haylock, M., Collins, D., Trewin, B., Rahimzadeh, F., Tagipour, A., Kumar, K. R., Ravedekar, J., Griffiths, G., Vincent, L., Stephenson, D.B., Burn, J., Aguilar, E., Brunet, M., Taylor, M., New, M., Zhai, P., Rusticucci, M. & Vazquez-Aguirre, J.L. (2006). Global observed changes in daily climate extremes of temperature and precipitation, *Jn. Geophys Res.*, 111 (DO5109).

Australian Bureau of Meteorology (2007). Australian Daily Rainfall Data. IDCJDC03. http://www.bom.gov.au/climate/how/newproducts/products.shtml

Australian Bureau of Meteorology (2007). Australian Daily Maximum and Minimum Temperature Data. IDCJDC04. http://www.bom.gov.au/climate/how/newproducts/products.shtml

Australian Bureau of Meteorology (2007). Australian Daily Wind Data. IDCJDC06. http://www.bom.gov.au/climate/how/newproducts/products.shtml

Bridgman, H. A. (1984). Climatic atlas of the Hunter Region. Board of Environmental Studies Research Paper No.9, The University of Newcastle.

Cai, W., G. Shi, T. Cowan, D. Bi, and J. Ribbe, (2005). The response of the Southern Annular Mode, the East Australian Current, and the southern mid-latitude ocean circulation to global warming. *Geophys. Res. Lett*., 32, L23706, doi: 0.1029/2005GL024701.

Childs, C. (2004). Interpolating surfaces in arcgis spatial analyst. *ArcUser. July-September.* [online]. Retrieved 12 February, 2008. http://www.esri.com/news/arcuser/0704/files/interpolating.pdf.

Church, J. A., and White, N.J. 2006. A 20th century acceleration in global sea-level rise. *Geophysical Research Letters*, 33, L01602, doi:10.1029/2005GL024826.

Crane, R. G. & Hewitson, B. C. (2003). Clustering and upscaling of station precipitation records to regional patterns using self-organizing maps (SOMs). *Clim. Res*. *25*, 95–107.

Earls, J. & Dixon, B. (2007). Spatial interpolation of rainfall data using arcgis. ESRI Users Group Conference. [online]. Retrieved 12 February, 2008. http://www10.giscafe.com/link/display_detail.php?link_id=22230.

Easterling, D.R., Evans, J.L., Groisman, P.Ya., Karl, T.R., Kunkel, K.E. & Ambenje, P. (2000). Observed variability and trends in extreme climate events: a brief review, *BAMS*, *81(3),* 417-425.

Ghil, M. and Mo, K. (1991). Intraseasonal oscillations in the global atmosphere, Part II: Southern Hemisphere. Journal of Atmospheric Sciences, 48 (5), 780-790.

Goodwin, in prep.

Goodwin, I. D. (2005). A mid-shelf, mean wave direction climatology for southeastern Australia, and its relationship to the El Niño – Southern Oscillation since 1878 A.D. *International Journal of Climatology*, 25, 1715-1729.

Goodwin, I. D., van Ommen, T. D., Curran, M. A. J. and Mayewski, P. A. (2004). Mid latitude winter climate variability in the south Indian and south-west Pacific regions since 1300 AD. *Climate Dynamics* 22, 783-794, DOI:10.1007/S00382-004-0403-3.

Hewitson, B. C. & Crane, R. G. (1994). *Neural Nets: Applications in Geography*. London : Kluwer Academic.

Hewitson, B. C. & Crane, R. G. (2002). Self-organizing maps: applications to synoptic climatology. *Climate Res.*, *22*, 13–26.

Hope, P.K., Drosdowsky, W. & Nicholls, N., (2006). Shifts in the synoptic systems influencing southwest Western Australia, *Clim. Dyn., 26*, 751-764.

Kalnay, E., Kanamitsu, M., Kistler, R., Collins, W., Deaven, D., Gandin, L., Iredell, M., Saha, S., White, G., Woolen, J., Zhu,Y., Chelliah, M., Ebisuzaki, W., Higgins, W., Janowiak, J., Mo, K. C., Ropelewski, C., Wang, J., Leetma, A., Reynolds, R., Jenne, R., & Joseph, D. (1996). The NCEP/NCAR 40-year reanalysis project. *Bulletin of American Meteorology Society*, *77*, 437-471.

Kistler R, E Kalny and W Collins. (2001). The NCEP-NCAR 50-year reanalysis; Monthly means CD-ROM and documentation, *Bulletin of American Meteorology Society,* 82(2): 247–267.

Kohonen, T. (1997). *Self-Organizing Maps*. Berlin : Springer.

Kulmar, M. Pers. Comm., 2005, Manly Hydraulics Laboratory, NSW Department of Commerce)

Lord, D. and Kulmar, M. (2000). The 1974 storms revisited: 25 years experience in ocean wave measurement along the south-east Australian coast. In, *Proceedings of the 27th International Conference on Coastal Engineering*, ASCE, Sydney, 559-572.

Malmgren, B. A. and Winter, A. (1999). Climate zonation in Puerto Rico based on principal components analysis and an artificial neural network. *Journal of Climate,* 12: 977-985.

Matlab Version 7.4.0.287 (R2007a). The Mathworks, Inc [Computer software].

Pook, M.J., McIntosh, P. C., and Meyers, G. A. (2006). The synoptic decomposition of cool-season rainfall in the southeastern Australian cropping region. *Journal of Applied Meteorology and Climatology*, 45, 1156-1170.

Ridgway, K. R., (2007). Long-term trend and decadal variability of the southward penetration of the East Australian Current. *Geophys. Res. Lett*., 34, L13613, doi: 10.1029/2007GL030393.

Roderick, M.L. & Farquhar, G.D. (2004). Changes in Australian pan evaporation from 1970–2002. *International Journal of Climatology, 24*, 1077–1090.

Smith, T.M., & Reynolds, R.W. (2003). Extended reconstruction of global sea surface temperatures based on COADS data (1854-1997). *Journal of Climate*, *16*, 1495-1510.

Smith, T.M., and Reynolds, R.W. (2004). Improved Extended Reconstruction of SST (1854-1997). *Journal of Climate*, *17*, 2466-2477.

Smith, T.M., Reynolds, R.W., Peterson, T.C., & Lawrimore, J. (2007). Improvements to NOAA's Historical Merged Land-Ocean Surface Temperature Analysis (1880-2006). *Journal of Climate, 21(10)*, 2283-2296.

Sturman, A. and Tapper, N. (2006).The weather and climate of Australia and New Zealand. Second Edition. Oxford University Press, Melbourne, 541pp.

Vesanto, J., Himberg, J., Alhoniemi, E., & Parhankangas, J. (1999). *SOM Toolbox for Matlab*. [Computer software]. Available from http://www.cis.hut.fi/projects/somtoolbox/.

Visbeck, M and Hall, A. (2004). Reply. Journal of Climate, 17, 2255-2258.

White, N.J., Church, J.A., and Gregory, J.M. 2005. Coastal and global averages sea level rise for 1950 to 2000. Geophysical Research Letters, 32, L01601, doi:10.1029/2004GL021391.

Wright, W.J. (1989). A synoptic climatological classification of winter precipitation in Victoria. *Australian Meteorological Magazine*, 37, 217-229.

Xue, Y., Smith, T.M., & Reynolds, R.W. (2003). Interdecadal changes of 30-yr SST normals during 1871-2000. *Journal of Climate, 16*, 1601-1612.

You Z.J., Lord D. (2008). Influence of the El Niño–Southern Oscillation on NSW Coastal Storm Severity. Journal of Coastal Research: Vol. 24, No. sp2 pp. 203–207.

Appendix A – Discontinuous Station Data Analysis

In some instances weather gauges have been decommissioned and relocated within a short distance from the original position and in most cases the BOM assigns a new station number for this temperature gauge. Therefore, in order to maximise spatial coverage, stations that have been discontinued and replaced by a secondary gauge at a nearby location were also considered for inclusion in the final data sets. This Appendix contains a comparison of meteorological data (during a 6 month period of overlap) for stations within the region that have been relocated. While a number of sites were considered, only those which were found to be suitable for this study (i.e. correlations greater than 0.7 and a similar timeseries during the period of overlap) are shown in the following sections.

A1: Temperature

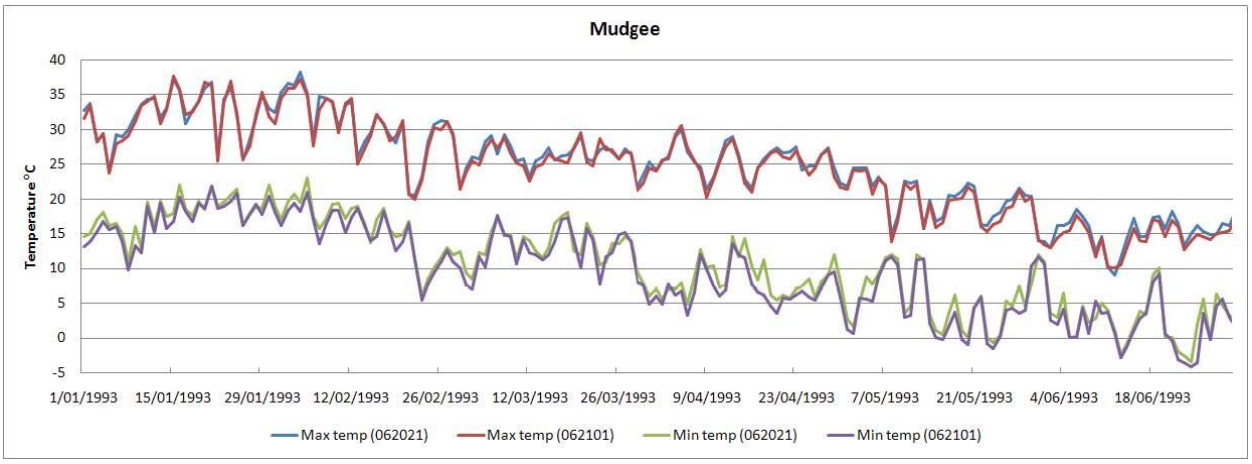

Figure A1-1: Comparison of temperature timeseries for Mudgee stations 062021 and 062101, exhibiting a correlation of 0.98 for max temp and 0.99 for min temp.

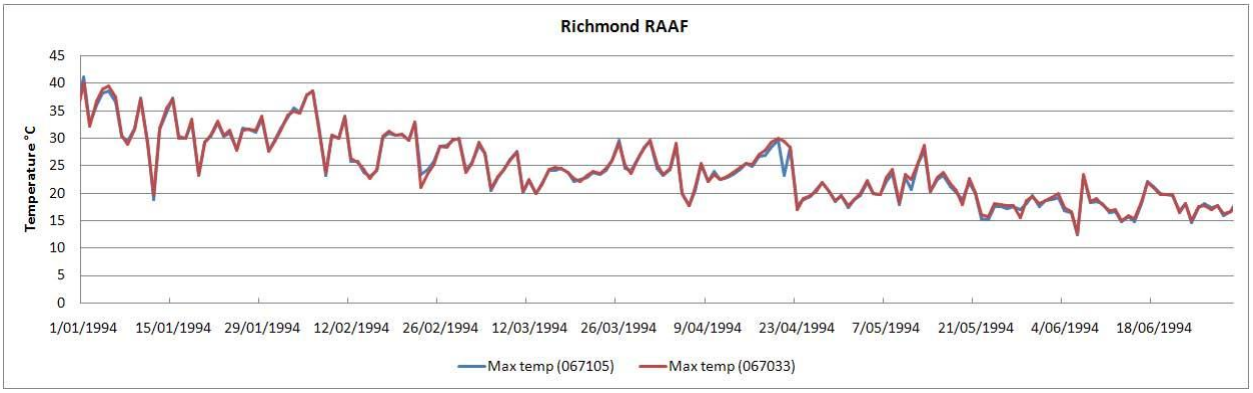

Figure A1-2: Comparison of temperature timeseries for Richmond RAAF stations 067105 and 067033, exhibiting a correlation of 0.99 for max temp (note that period of overlap unavailable for min temp).

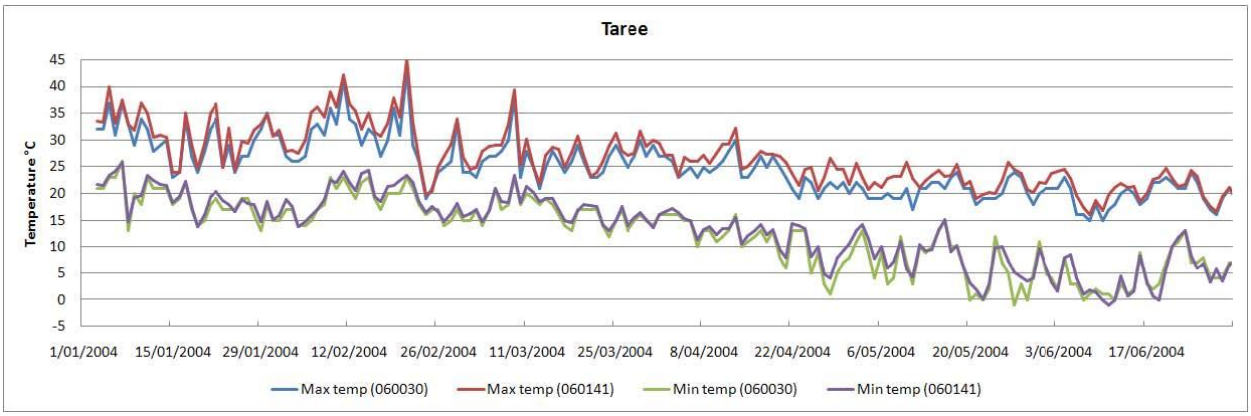

Figure A1-3: Comparison of temperature timeseries for Taree stations 060030 and 060141, exhibiting a correlation of 0.98 for both max and min temperatures.

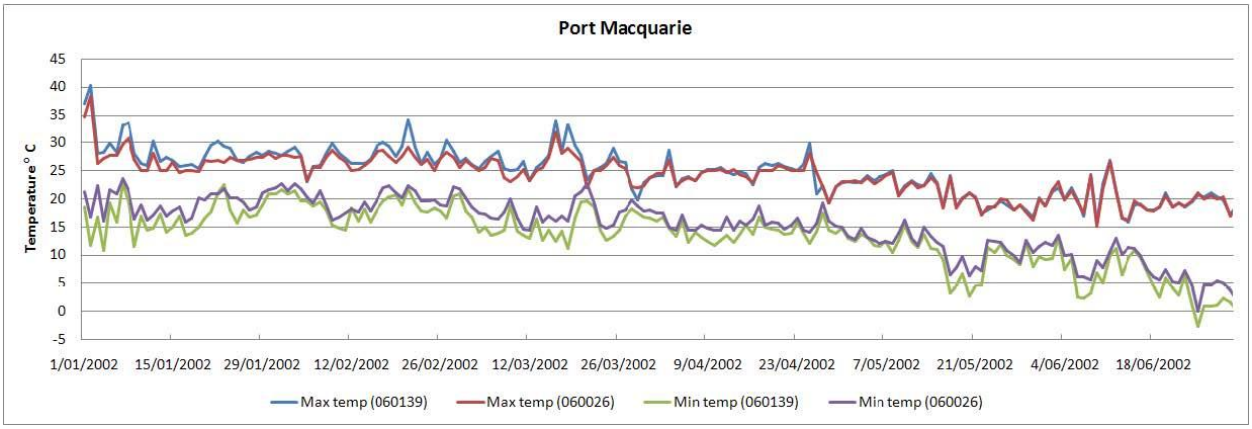

Figure A1-4: Comparison of temperature timeseries for Port Macquarie stations 060139 and 060026, exhibiting a correlation of 0.96 for max temp and 0.97 for min temp.

A2: Relative Humidity

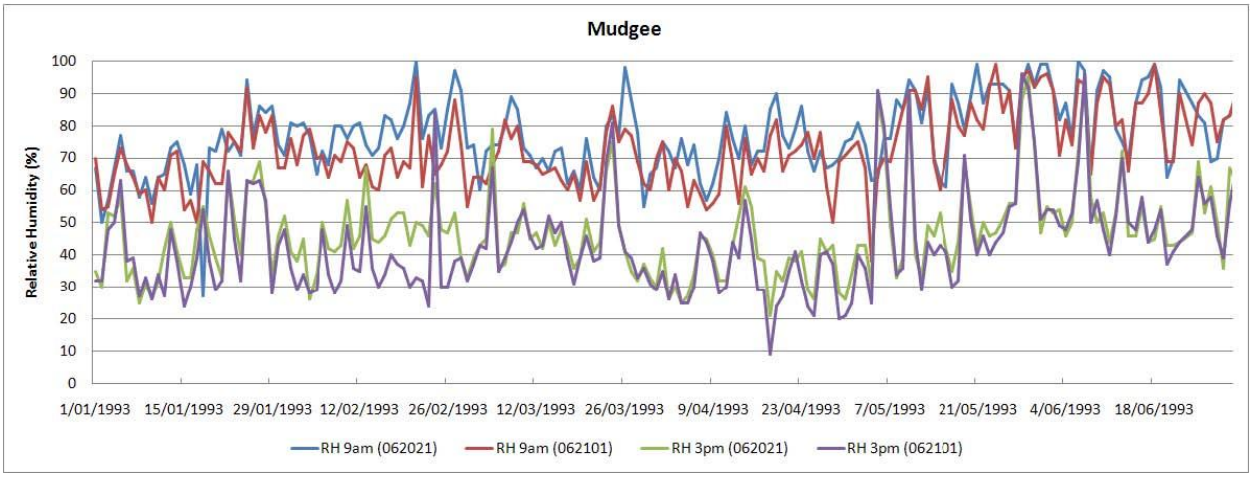

Figure A2-1: Comparison of relative humidity (RH) timeseries for Mudgee stations 062021 and 062101, exhibiting a correlation of 0.84 for 9am RH and 0.92 for 3pm RH.

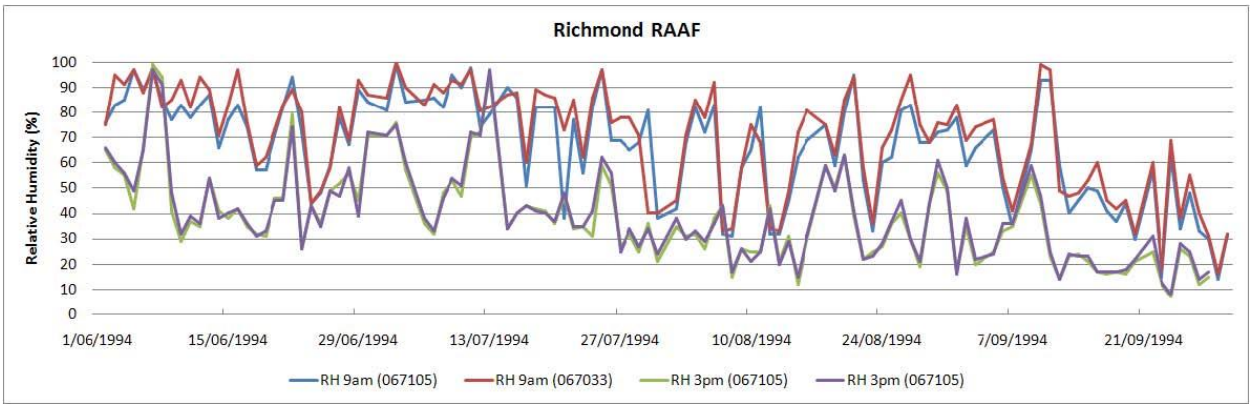

Figure A2-2: Comparison of relative humidity (RH) timeseries for Richmond RAAF stations 067105 and 067033, exhibiting a correlation of 0.95 for 9am RH and 0.99 for 3pm RH.

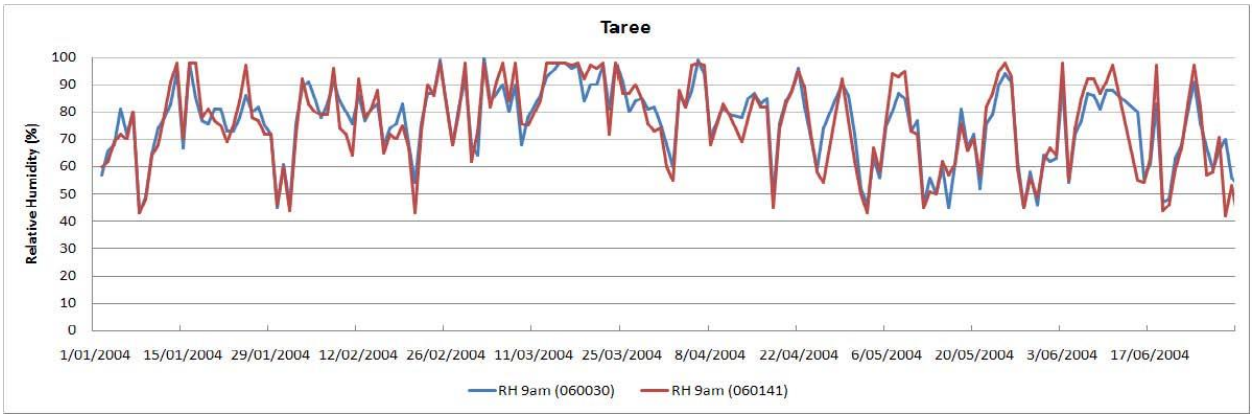

Figure A2-3a: Comparison of relative humidity (RH) timeseries for Taree stations 060030 and 060141, exhibiting a correlation of 0.88 for 9am RH.

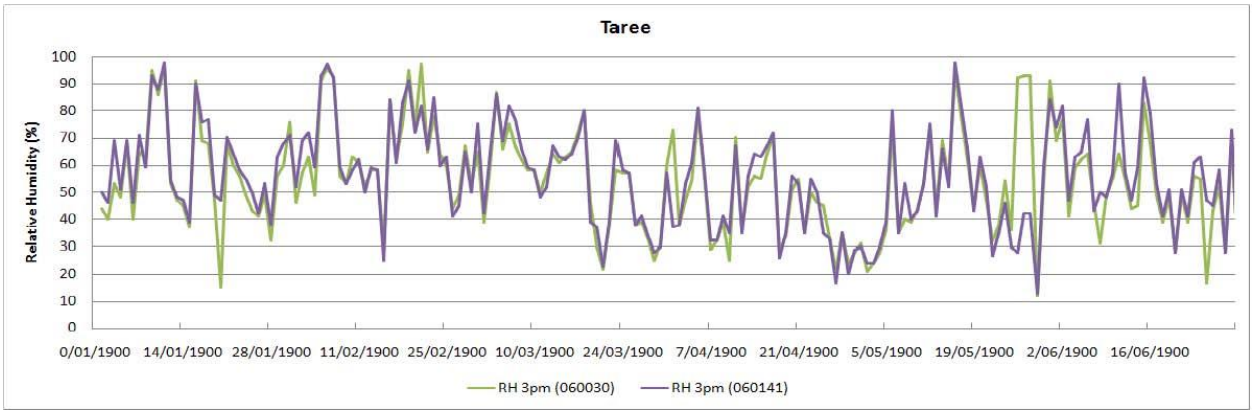

Figure A2-3b: Comparison of relative humidity (RH) timeseries for Taree stations 060030 and 060141, exhibiting a correlation of 0.88 for 3pm RH.

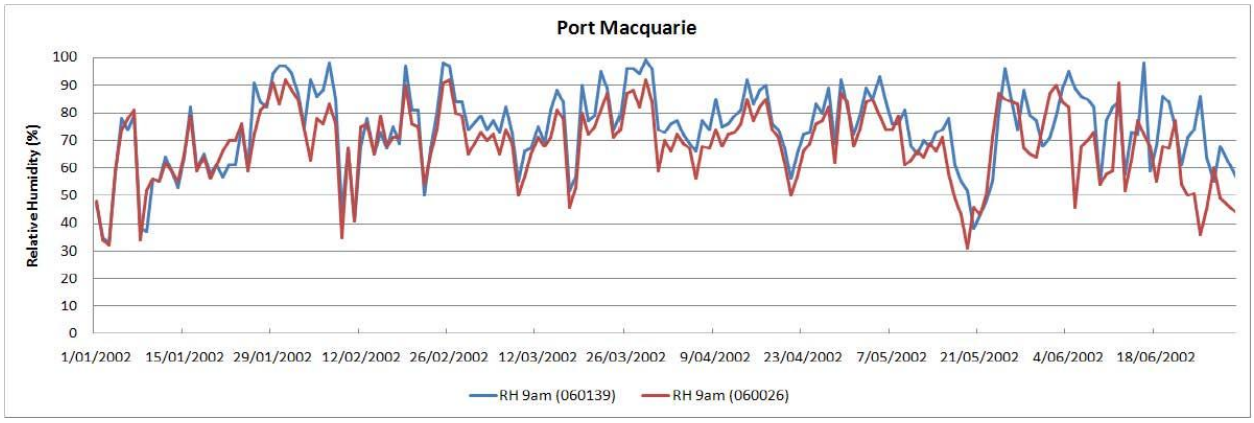

Figure A2-4a: Comparison of relative humidity (RH) timeseries for Port Macquarie stations 060139 and 060026, exhibiting a correlation of 0.84 for 9am RH.

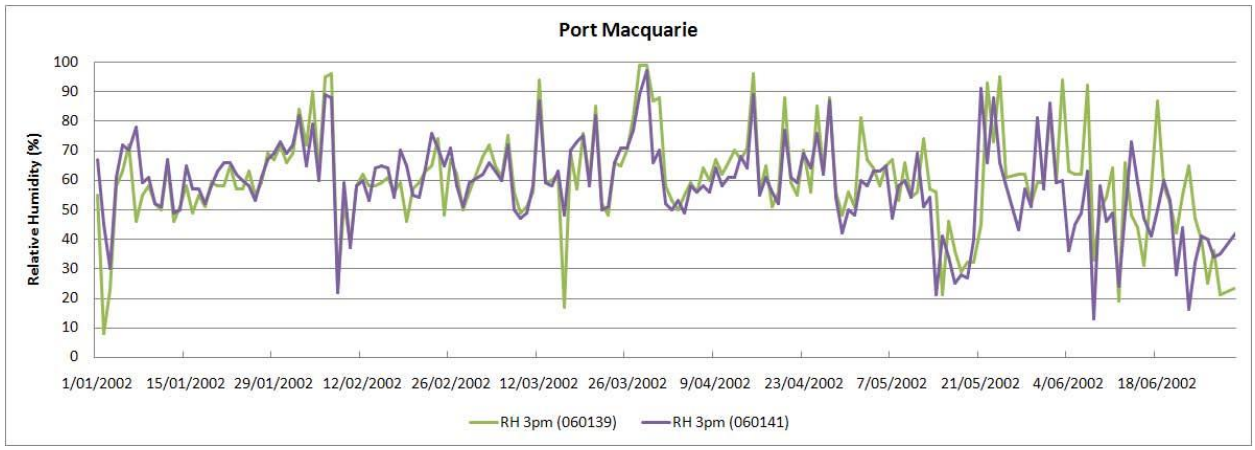

Figure A2-4b: Comparison of relative humidity (RH) timeseries for Port Macquarie stations 060139 and 060026, exhibiting a correlation of 0.73 for 3pm RH.

A3: Windspeed

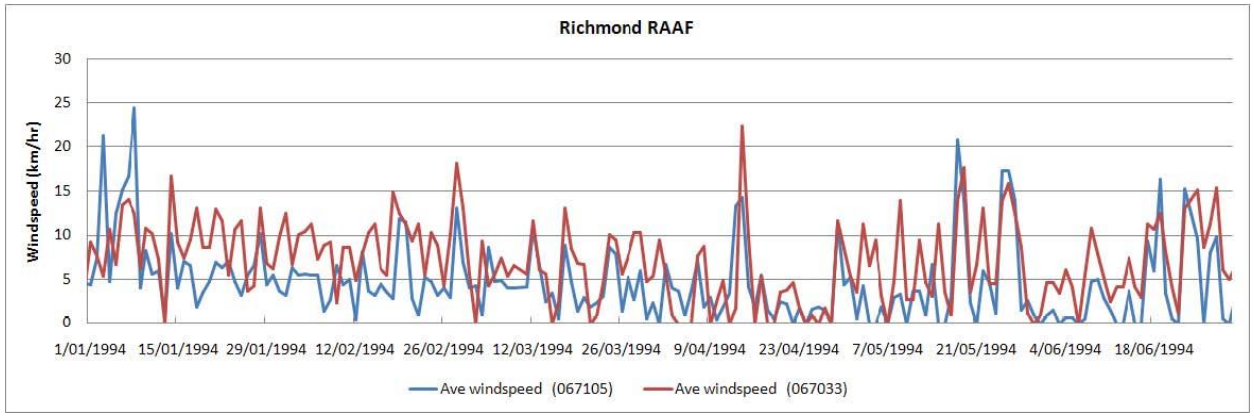

Figure A3-1: Comparison of windspeed timeseries for Richmond RAAF stations 067105 and 067033, exhibiting a correlation of 0.73.

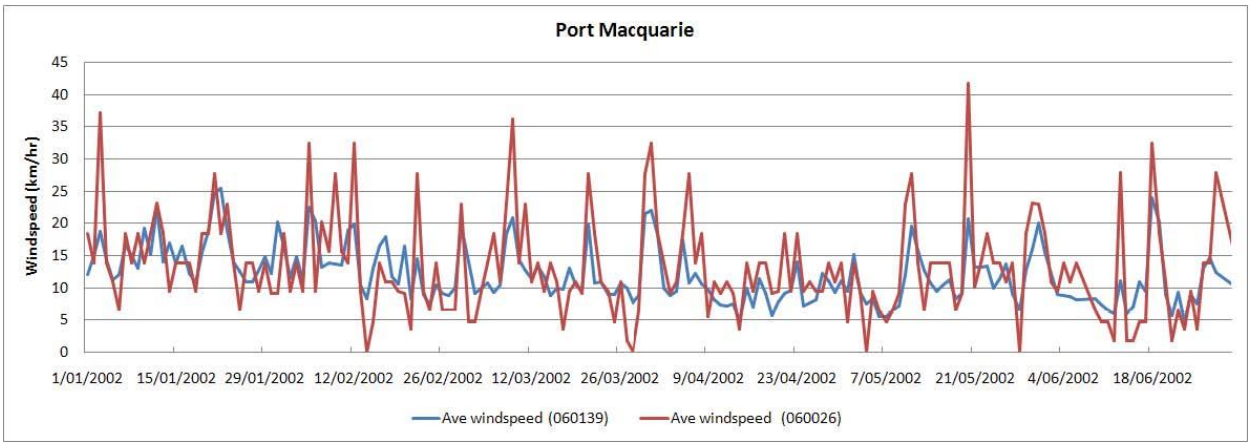

Figure A3-2: Comparison of windspeed timeseries for Port Macquarie stations 060139 and 060026, exhibiting a correlation of 0.74.

Appendix B – Colour Grid Representation of Synoptic Types for Each of the IPO Periods

Summer Types - 1948-1976			
0.0%	0.0%	0.0%	31.0%
0.0%	0.0%	2.3%	41.4%
0.0%	0.0%	1.1%	24.1%

Summer Types - 1977-2007			
0.0%	0.0%	5.4%	20.4%
0.0%	0.0%	7.5%	37.6%
0.0%	0.0%	0.0%	29.0%

Autumn Types - 1948-1976			
12.6%	17.2%	19.5%	20.7%
1.1%	5.7%	2.3%	0.0%
2.3%	9.2%	5.7%	3.4%

Autumn Types - 1977-2007			
29.0%	20.4%	20.4%	11.8%
3.2%	6.5%	1.1%	1.1%
4.3%	1.1%	1.1%	0.0%

Winter Types - 1948-1976			
44.8%	1.1%	0.0%	0.0%
12.6%	0.0%	0.0%	0.0%
20.7%	19.5%	1.1%	0.0%

Winter Types - 1977-2007			
51.6%	1.1%	0.0%	0.0%
2.2%	1.1%	0.0%	0.0%
33.3%	10.8%	0.0%	0.0%

Spring Types - 1948-1976			
4.6%	14.9%	9.2%	2.3%
3.4%	8.0%	3.4%	2.3%
4.6%	11.5%	17.2%	18.4%

Spring Types - 1977-2007			
9.7%	3.2%	8.6%	4.3%
4.3%	9.7%	5.4%	1.1%
7.5%	21.5%	20.4%	4.3%

Appendix C – Synoptic Type Profiles

Synoptic Type 1

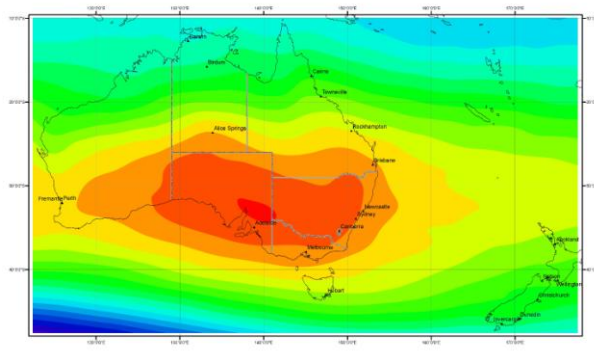

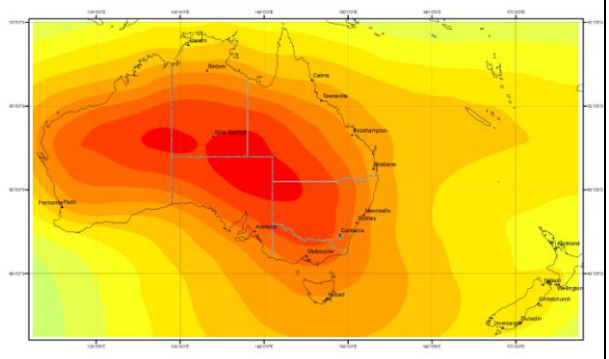

- High pressure over central and south eastern Australia, with a strong long wave ridge over south eastern Australian longitudes
- Most frequently occurring type (19.2% of time)
- Dominant winter and autumn type, also occurs to a lesser degree in spring
- Largest variation in annual average monthly precipitation, averaging 71mm, ranging from 1.4mm to 359mm
- Produces approximately 50% of temperature events where the minimum temperature is <=0°C in western parts of the region (i.e. Jerrys Plains and Murrurundi)
- Responsible for 23% of extreme precipitation events (i.e. in the 95th percentile) in Newcastle; 17% of events regionally

Synoptic Type 2

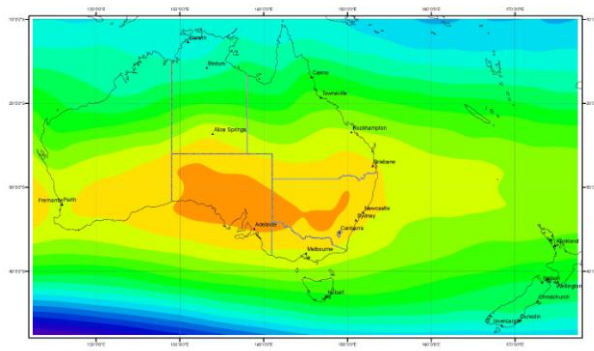

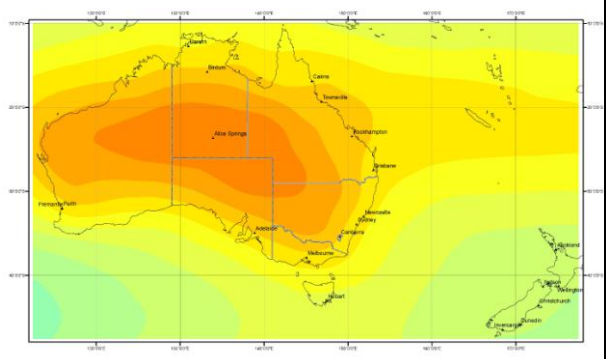

- High pressure over central and south eastern Australia, with a weak long wave ridge over south eastern Australian longitudes
- Occurs infrequently (3.3% of time)
- Predominantly occurs during winter, followed by spring and autumn
- Similar average monthly precipitation to ST1 (74mm) however less variable (i.e. ranging from 9mm to 226mm)

Synoptic Type 3

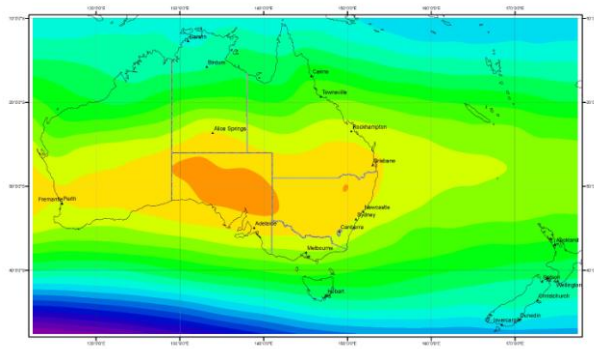

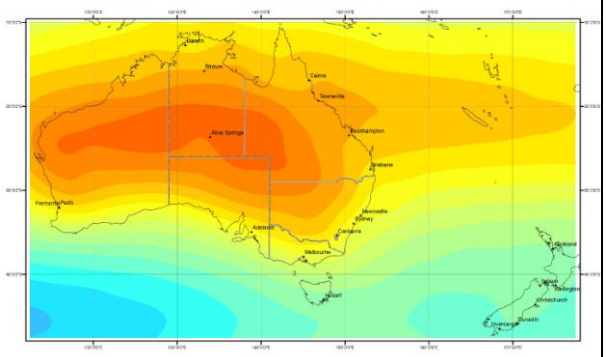

- High pressure over central and northern Australia
- Occurs 9.2% of time, predominantly in winter, followed by spring and autumn
- Comparatively low average monthly precipitation (45mm), ranging from 1.3mm to 132mm
- Produces almost 50% of temperature events where the minimum temperature is <=0°C in northern parts of the region (i.e. Taree)

Synoptic Type 4

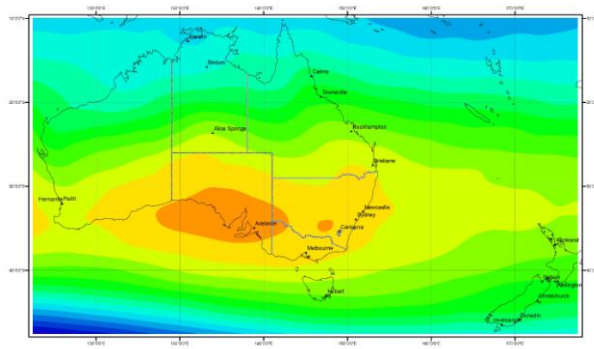

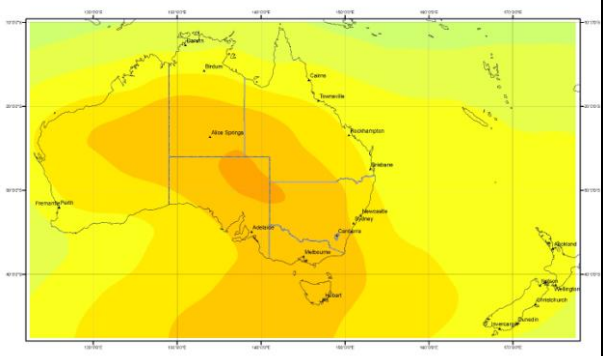

- High pressure through central and southern Australia with a strong long wave ridge over southern Australian longitudes
- Occurs 7.2% of time, predominantly in autumn, followed by spring and winter
- Relatively wet type with average monthly precipitation of 83mm, ranging from 10mm to 245mm

Synoptic Type 5

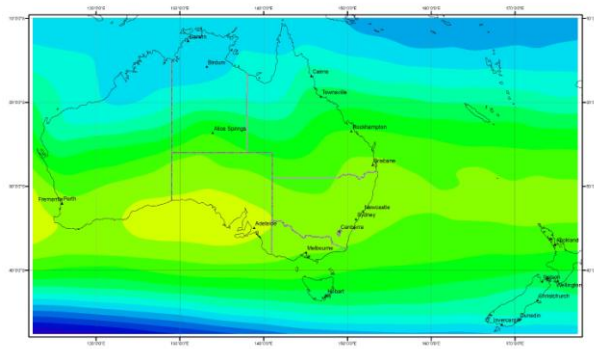

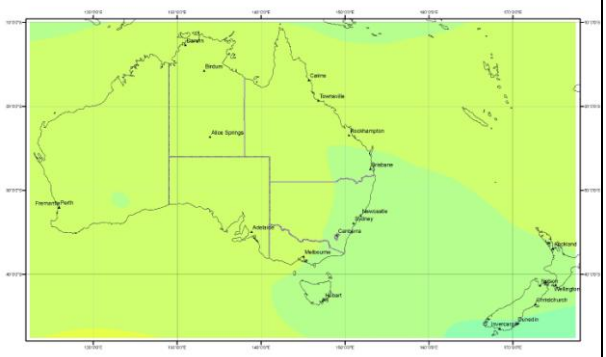

- Stable pressure over Australia
- Occurs infrequently (3.9% of time), predominantly in spring followed by autumn, and rarely in winter

- Associated with average monthly precipitation of 78mm, ranging from 10mm to 207mm

Synoptic Type 6

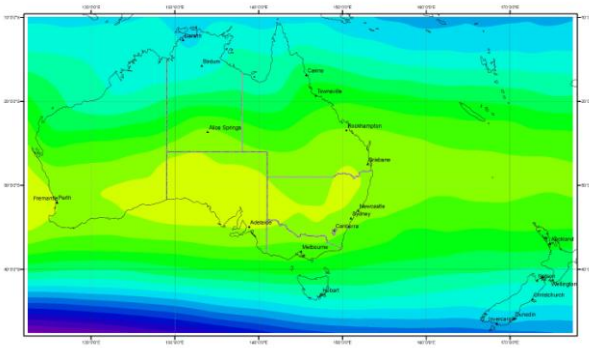
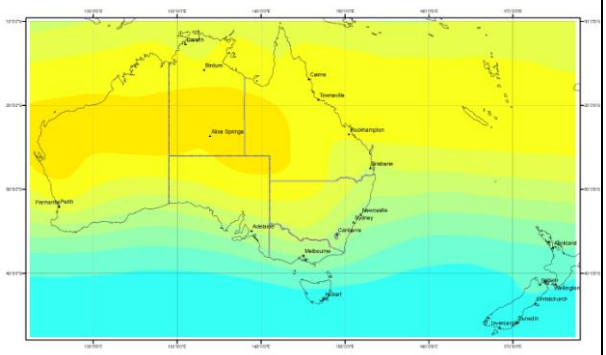

- High pressure over northern Australia with an equator-ward circumpolar trough
- Occurs 9.2% of time, predominantly in spring and winter, less frequently during autumn
- Relatively low average monthly precipitation (53mm), ranging from 2mm to 204mm

Synoptic Type 7

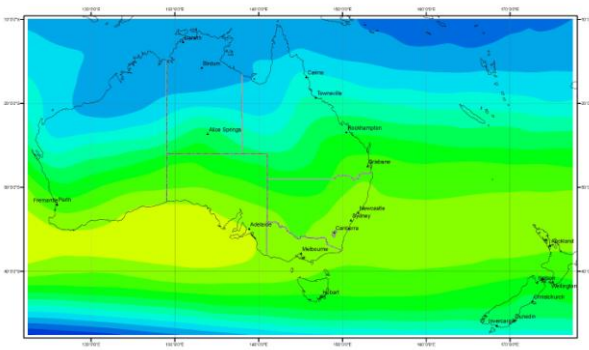
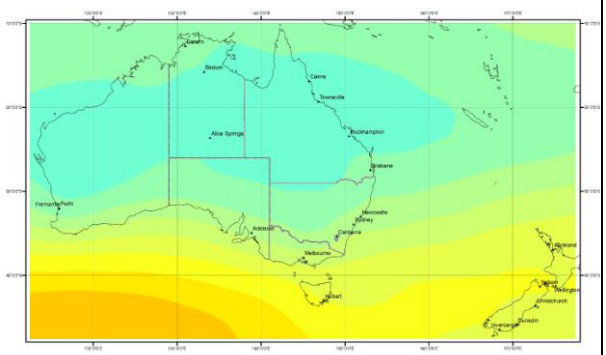

- High pressure band below southern Australia, low pressure over central and northern
- Occurs 7.9% of time, predominantly during spring, followed by autumn and rarely during summer
- ST associated with high average monthly precipitation (101mm), ranging from 11mm to 297mm

Synoptic Type 8

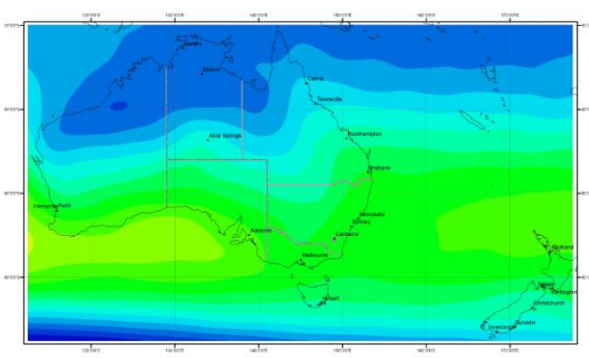
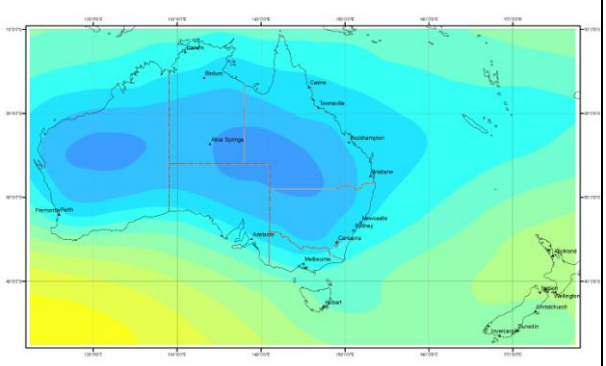

- Low pressure over central and eastern Australia, high pressure south-east of western Australia and a weak long-wave in south eastern Australian longitudes
- Most infrequently occurring type (2.8% of time), occurring predominantly during summer and spring, and rarely during autumn
- Associated with average monthly precipitation of 88mm, ranging from 16mm to 126mm

Synoptic Type 9

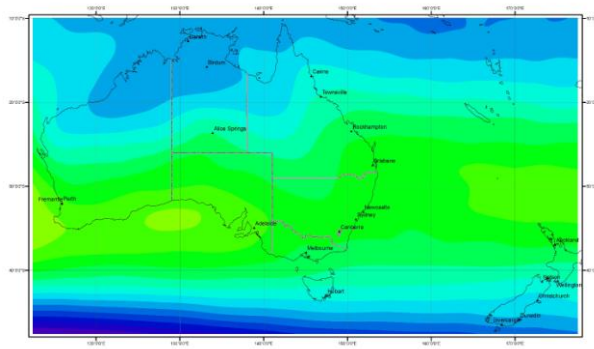

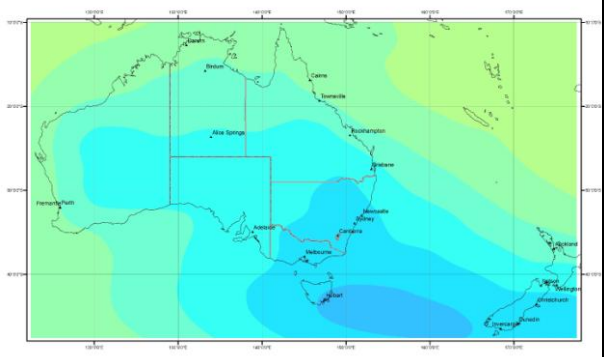

- Low pressure over central and south eastern Australia, southern Tasman Sea low and strong long-wave trough over Tasman Sea longitudes
- Occurs 5.8% of time, dominant spring type which can occur during autumn and very infrequently during summer and winter.
- Low average monthly precipitation (50mm) with the smallest range (i.e. 7mm to 114mm)

Synoptic Type 10

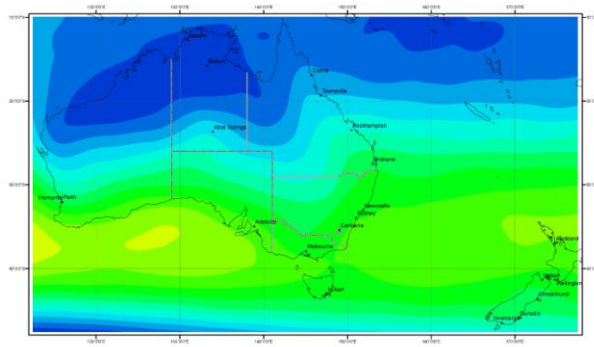

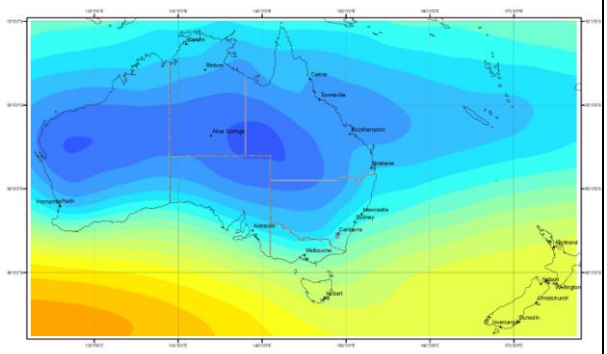

- Low pressure over central and eastern Australia, high pressure below southern Australia
- Occurs 11.2% of time, predominantly in summer, followed by autumn and less frequently in spring
- High average monthly precipitation (122mm) ranging from 14mm to 277mm
- Responsible for 17% of extreme precipitation events (i.e. in the 95th percentile) regionally and up to 23% in the northern parts of the region (i.e. Wingham)
- Produces 26% of extreme heat days (i.e. >=37°C) regionally and up to 31% in the most western parts of the region (i.e. Murrurundi)

Synoptic Type 11

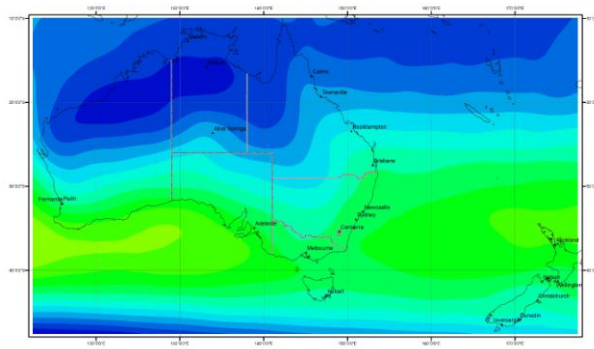

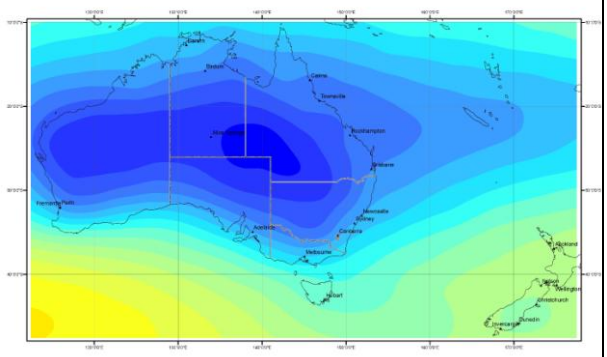

- Strong low pressure over Australia
- Occurs 10.4% of time, dominant summer type which occurs rarely during spring and autumn
- Highest average monthly precipitation of STs (122mm), ranging from 24mm to 343mm
- Responsible for the highest number (20%) of extreme precipitation events (i.e. in the 95th percentile) regionally and up to 24% in the western parts of the region (i.e. Jerrys Plains and Murrurundi)
- Produces 33% of extreme heat days (i.e. >=37°C) regionally and up to 35% in coastal areas (i.e. Newcastle)

Synoptic Type 12

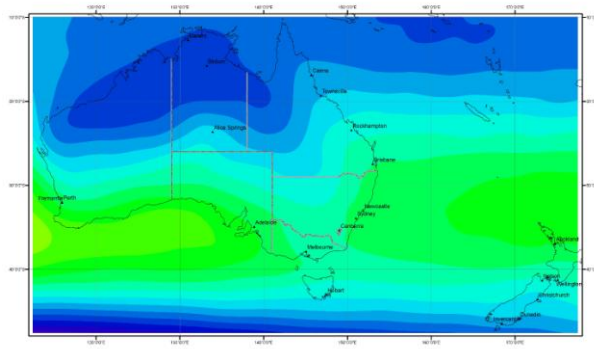

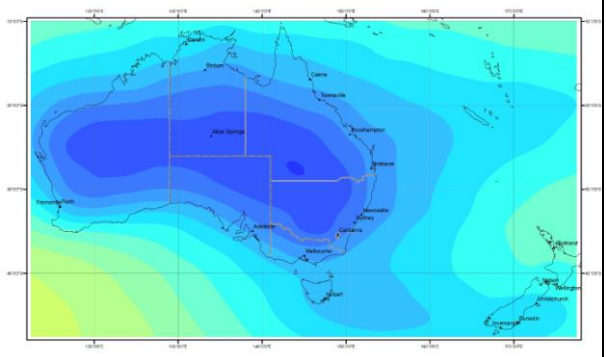

- Strong low pressure over Australia with a moderate long-wave trough in south-eastern Australia and Tasman Sea longitudes
- Occurs 9.9% of time, predominantly in summer, followed by spring and infrequently in autumn
- Produces average monthly precipitation of 70mm with a range of 6mm to 220mm
- Produces 23% of extreme heat days (i.e. >=37°C) regionally and up to 26% in northern areas (i.e. Taree)

HCCREMS (the Hunter and Central Coast Regional Environmental Management Strategy) is a partnership initiative of the 14 local councils of the Hunter, Central and Mid North Coast regions of NSW.

Established in 1996, the HCCREMS team works with urban, rural and costal councils to facilitate a collaborative approach to sustainable planning, development and natural resource management. Our activities include:

- Facilitating local government input to a range of natural resource management and planning processes.
- Providing specialist support and services to member councils on environmental management and planning issues.
- Developing and maintaining a repository of the region's natural resource management data and maps.
- Designing and managing a range of regional environmental projects through the Hunter and Central Coast Regional Environmental Management Strategy (HCCREMS) framework.

At the time of publishing our project areas include:

- Biodiversity
- Aquatic and terrestrial weeds
- Roadside environmental management
- Climate change adaptation
- The urban water cycle
- Environmental compliance
- Sustainability
- Community education, including rural residential living
- Natural resource data management and mapping

For more information visit **www.huntercouncils.com.au/environment/hccrems**

With thanks to our partners:

and our member councils:

An initiative of the Hunter and Central Coast Regional Environmental Management Strategy.